

BEST

AVAILABLE

COPY

DESIGN OF TAPERED MEMBERS

By

G. C. Lee, M. L. Morrell and R. L. Ketter

State University of N. Y. at Buffalo

Reproduced from
best available copy.



Reproduced by
**NATIONAL TECHNICAL
INFORMATION SERVICE**
Springfield, Va. 22151

UNCLASSIFIED

Security Classification

DOCUMENT CONTROL DATA - R & D

Security classification of title, body of abstract and indexing annotation must be entered when the overall report is classified

1. ORIGINATING ACTIVITY (Corporate author) State University of New York At Buffalo		2a. REPORT SECURITY CLASSIFICATION Unclassified	
		2b. GROUP	
3. REPORT TITLE Design of Tapered Members			
4. DESCRIPTIVE NOTES (Type of report and inclusive dates) Final Report Feb 1966 - Dec 1971			
5. AUTHOR(S) (First name, middle initial, last name) George C. Lee; M. L. Morrell; Robert L. Ketter			
6. REPORT DATE December 1971		7a. TOTAL NO. OF PAGES 52	7b. NO. OF REFS 74
8. CONTRACT OR GRANT NO. NAy-63864		9a. ORIGINATOR'S REPORT NUMBER(S) None	
b. PROJECT NO. Y-RO09-03-03-904		9b. OTHER REPORT NO(S) (Any other numbers that may be assigned this report) None	
10. DISTRIBUTION STATEMENT Distribution of this document is unlimited			
11. SUPPLEMENTARY NOTES		12. SPONSORING MILITARY ACTIVITY Naval Facilities Engineering Command Asst. Commander for Research & Development Washington, D. C. 20390	
13. ABSTRACT The report covers all major aspects of the design of tapered frames; from total frame analysis to stress analysis of individual members - to the development of tapered design formulas. The primary objective of the report is to present the rationale behind the development of the design formulas. The design formulas developed describe the gross behavior of isolated members. The normal underlying assumption that members are adequately proportioned against local buckling is made. Also contained in the report is a brief description of several of the frame analysis and stress analysis methods applicable to tapered framing. The problem of effective length of a tapered column in rigid frames is also treated. The basic approach used follows: theoretical solutions are first obtained, then using these solutions - the A.I.S.C. prismatic members design formulas are modified to effect the same solutions by the introduction of appropriate multiplying factors which are dependent only on the tapering geometry. Since these factors reduce to unity when there is no taper, it must be recognized that this approach assumes that the current A.I.S.C. allowable stress formulas for prismatic members are adequate.			

14

KEY WORDS

Steel Structures
Tapered Framing
Stress Analysis
Design Formulas
Proportioning Tapered Members

LINK A

LINK B

LINK C

ROLE

WT

ROLE

WT

ROLE

WT

DESIGN OF TAPERED MEMBERS

(A Summary Report Including Design Recommendations)

By

G. C. Lee; M. I. Morrell; and R. L. Ketter

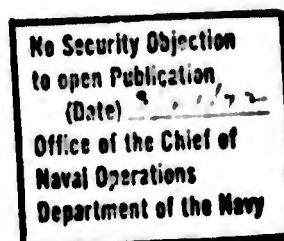


This research study has been carried out as part of an investigation jointly sponsored by the Naval Facilities Engineering Command, American Institute of Steel Construction, American Iron and Steel Institute, and the Metal Building Manufacturer's Association. Reproduction of this report in whole or in part is permitted for any purpose of the United States Government.

December 1971

**Department of Civil Engineering
State University of New York at Buffalo**

**This document has been approved
for public release and sale;
its distribution is unlimited**



*THIS COPY WAS OF POOR QUALITY.
WHILE REPRODUCTION FROM
THIS COPY.*

TABLE OF CONTENT

1.	INTRODUCTION	1
2.	FRAME AND STRESS ANALYSIS	3
	2.1 Frame Analysis	
	Earlier Proposed Methods	
	The Slope-Deflection Method	
	The Finite Element Method	
	2.2 Axial And Flexural Stresses	
	2.3 Torsional Stresses	
3.	STABILITY CONSIDERATIONS	9
	3.1 General Analysis of Single Members	
	3.2 Initial Yield Solutions	
	3.3 Elastic Axial Stability Solutions	
	3.4 Elastic Lateral Stability Solutions	
4.	DEVELOPMENT OF DESIGN FORMULAS	24
	4.1 Compression	
	4.2 Bending	
	4.3 Axial Compression And Bending	
	4.4 Comparison With Experimental Data	
5.	EFFECTIVE LENGTH	40
	5.1 Slope-Deflection Equations	
	5.2 Side-Sway Prevented	
	5.3 Side-Sway Permitted	
	5.4 Comments on The Use of Effective Length	
6.	SUMMARY AND DESIGN EXAMPLE	47
7.	ACKNOWLEDGMENTS	
8.	REFERENCES	
9.	TABLES AND FIGURES	
10.	APPENDIX - A summary of the proposed design specifications	

Reproduced from
best available copy.

1. INTRODUCTION

The use of "tapered structural elements," having tapered depths and/or widths, was first proposed by Amirikian (1) for reasons of economy in 1952. In view of the lack of basic understanding of the behavior of these types of members, in particular the lack of information having to do with design against instability, the Naval Facilities Engineering Command, the American Institute of Steel Construction, the American Iron and Steel Institute, and the Metal Building Manufacturer's Association have jointly sponsored since 1966 a research project at the State University of New York at Buffalo to carry out such studies. As part of those studies, both analytical and experimental investigations were conducted on the behavior of such tapered members and the results were used to develop proposed design formulas. This paper, which summarizes many of the conclusions of those investigations, is concerned primarily with a) the overall analysis of tapered member framing, and b) the development of the design formulas regarding the proportioning of tapered members.

A general treatment for any arbitrarily tapered beam would be very ambitious and, in general, impractical due primarily to the difficulties associated with the coupling of flexural and torsional deformations. For this reason the most common tapered I section now being used was chosen for examination, and design formulas for such members were developed. It is to be recognized, however, that the formulas suggested may also be applied (with caution) to other sections which are "sufficiently braced" to prevent torsional deformation.

Also contained in this paper is a brief description of several of the frame analysis and stress analysis methods applicable to tapered framing. It also is to be noted that a later section of the report is devoted to the problem of effective length of a tapered column in rigid frames.

The basic approach used in the development of design formulas for tapered members was as follows: theoretical solutions are first obtained, then - using these solutions - the A.I.S.C. prismatic member design formulas are modified to effect the same solutions by the introduction of appropriate multiplying factors which are dependent only on the tapering geometry. Since these factors (by definition) reduce to unity when there is no taper in the member, it must be recognized that this approach assumes that the current A.I.S.C. allowable stress formulas for prismatic members are adequate.

2. FRAME AND STRESS ANALYSIS

From the structural analyst's point of view, frames comprised of tapered members possess unique properties which can be utilized in both analysis and design. Consider, for example, the moment diagram of a continuous prismatic beam under arbitrary loading. In general, the moment maxima will occur near the center of each span and at the supports. If the cross-section is decreased at mid-span and increased at the supports, and if the loading is kept constant, the moment diagram changes: greater values are realized near the supports and smaller ones are observed at mid-span. The limiting condition is reached when a real hinge is specified at the mid-span. Thus as the shape of the member is changed from its originally assumed outline of constant cross-section to that of a wedge, the bending moment diagram changes from the initial irregular outline of reversed flexure to that of single flexure corresponding to two simple, articulated cantilever beams.

Tapered beam framing will result in weight saving for many structural and loading situations. The characteristic redistribution of stresses permits better utilization of structural material than does conventional, prismatic framing. It should be recognized, however, that this weight saving does not necessarily mean that the resulting structure will be less expensive, though in many cases this will be true.

2.1 Frame Analysis

The in-plane analysis of certain, particular types of single-story tapered frame assemblies has been shown to be simpler than the analysis of conventional, prismatic rigid frames (1). For example, though each simple

frame shown in Fig. 2.1 is statically indeterminate, only two unknown stress resultants are assumed to be associated with each interconnection. Moreover, these unknowns can be determined from the condition that two adjacent simple frames must have the same deflections at the common link. The standard procedure for the analysis of such statically indeterminate structures would be as follows: a) The framing assembly is subdivided into its component simple frames, each frame subjected to unknown horizontal forces and vertical forces at each of the connections, in addition to its own applied loading. b) The horizontal and vertical deflections of each frame at each of the linkage points are expressed in terms of the applied load and the unknown H and V forces. In general four equations are written for each frame. c) Finally, by equating the joint displacements, a set of simultaneous equations is obtained, the solution of which yields the unknown hinge reactions. It is to be recognized that this method is well suited for solution by hand for small assemblies, consisting of two to four simple frames, or by digital computer for larger assemblies.

Since each member of each simple frame has a rigid joint at one of its ends and a hinged connection at the other end, the bending moment diagram in that member is similar to that of a cantilever beam. Assuming first-order theory, this permits computation of the deflection of a simple frame by summing the deflections of the component members. A number of deflection solutions are presented in Amirikian's paper for tapered cantilever beams of various proportions for typical loading conditions. The reader is referred to the original paper (1) for a number of examples of application of the method of analysis just described.

Other standard methods of analysis, based on either the flexibility or the stiffness approach, such as moment distribution, can be adapted also to tapered frame assemblies. For highly redundant frames, however, a more automated approach is desirable, and the finite element method has distinct advantage. The reader is referred to reference 2 for a discussion of the use of finite element approaches to the solution of frames consisting of both prismatic and tapered members of thin-walled sections.

Once the stress resultants are obtained by any of the frame analysis methods described above, the axial force, bending moment, and shear force variations along the member can be determined as if the members were prismatic.

2.2 Axial and Flexural Stresses

The computation of stresses in tapered members is complicated by the fact that at least one new parameter must be introduced into the solution to describe the variation of cross-sectional properties along the length of the member. Remaining within the normally assumed approximations of structural mechanics, the well-known formulae for axial and flexural stresses still apply -- with the exception that the cross-sectional properties vary (3,4). Assuming that the centroidal axis at each section is also the axis of symmetry at that section, the normal stress, c_a , due to an axial load, P , acting at the centroid of the cross-section, located at a distance along the member, of z , is

$$c_a = \frac{P}{A(z)}$$

2.2-1

The normal stress, σ_b , located at the same distance z from the origin, and at a distance c from the centroidal axis, measured in a perpendicular direction from the longitudinal axis, and due to a bending moment, m , is

$$\sigma_b = \frac{m(z)c}{I(z)} \quad 2.2-2$$

where $I(z)$ is the moment of inertia about the axis of bending at the section in question.

The shear stress, τ_v , also located at a distance z from the origin, at a point (x,y) on the cross-section, and due to a shearing force $V(z)$ is

$$\tau_v = \frac{V(z)Q(z)}{I(z)t} \quad 2.2-3$$

where $Q(z)$ is the first moment of area about the centroidal axis. It is to be understood that the $Q(z)$ will vary with x and y at a particular cross-section.

Because of the variable cross-sectional parameters, the points of maximum stresses will not necessarily occur at points of maximum stress resultants. For a particular case differential calculus may be used to rigorously determine the maxima of Eq. 2.2-1, -2, and -3. Alternatively, a simple trial and error approach may be employed.

2.3 Torsional Stresses

When transverse loads are applied to prismatic elastic beams at points other than the shear center, these loads can be replaced by a statically equivalent load system assumed to act about the shear center. This enables the flexural and torsional stresses to be computed separately and then readily superimposed to obtain the complete stress distribution. However, such a

procedure cannot be directly followed for an arbitrarily tapered beam. For such members the shear center also may be a function of the longitudinal coordinate. As an example, consider a channel section which has a linearly varying depth and a constant flanged width (Fig. 2.2-a). Here the shear center converges toward the web, in the plane of symmetry, as one moves from the smaller to the larger end of the member. If this channel is cantilevered at the large end and a concentrated force is applied parallel to the web at the shear center of the small end, (Fig. 2.2-b), then the channel both bends and twists. (It should be noted that the exact, coupled flexural-torsional solution for such beams is not available). If the force is applied perpendicular to the web at the shear center (Fig. 2.2-c), the channel will bend without twisting.

It is possible to uncouple the flexural-torsional behavior of tapered beams for selected cross-sectional geometries and loadings. In general, in order to uncouple these deformations, a tapered beam must possess a linear centroidal axis (which must also coincide with the longitudinal, coordinate axis) and a locus of shear centers which lie in a plane parallel to the centroidal axis. Furthermore, the loads must lie in a plane parallel to the shear center plane. Some examples of cross-sections which satisfy these conditions are sections which have two axes of symmetry (I-beam and rectangular beams), and sections which have one axis of symmetry and the loads are applied parallel to that axis (channels and T-beams).

Torsional stresses in tapered beams which satisfy the above conditions and have small angles of taper can be computed using the normally recognized prismatic formulas for thin-walled beams. The St. Venant's shearing stress

at a location z along the member is

$$\tau_{st} = Gt \frac{d\theta}{dz} \quad 2.3-1$$

where G is the shear modulus, t is the thickness, and θ is the angle of twist.

The warping shearing stress is

$$\tau_w = -ES_w(z) \frac{d^3\theta}{dz^3} \quad 2.3-2$$

where E is the elastic modulus and $S_w(z)$ is the warping statical moment.

The warping normal stress is

$$\tau_w = EI_w(z) \frac{d^2\theta}{dz^2} \quad 2.3-3$$

where $I_w(z)$ is the warping constant.

The normal and shearing stresses determined in the manner described above can be combined to form the total stress distributions at a given cross-section. The maximum stress and its location along the member can then be determined using differential calculus.

A more accurate torsional analysis has been reported by Lee and Szabo (5). Deformations and stresses can be fully calculated using their theory.

3. STABILITY CONSIDERATIONS

In general, the results reported in this section are concerned with the analysis of linearly tapered beam-columns of doubly symmetric I-section. Both "in-plane" and lateral buckling strengths are determined using the Rayleigh-Ritz procedure. The end-loading conditions examined are those of bending and bending plus axial thrusts. In both cases, the plane of "loading" is presumed to be the plane of the web.

3.1 General Analysis of Simple Members

It is assumed that the tapered cross-section in question has a double symmetric "I" shape so that the shear-center axis coincides with the centroidal axis of the member. The flanges are presumed to be of constant width "b" and thickness "t_f" along the entire length of the member. The web thickness is also presumed to be uniform, having a value of "t_w". For the linearly tapered member, the depth at any distance "z" from the smaller end can be expressed as

$$d_z = d_0 \left(1 + \frac{z}{l} \gamma \right) \quad 3.1-1$$

where "d₀" represents the smallest depth at z = 0, and "γ" represents the "tapering ratio." In terms of the depths at the ends of the member, the tapering ratio is defined by

$$\gamma = \frac{d_1}{d_0} - 1 \quad 3.1-2$$

Thus, for a prismatic member, $\gamma = 0$. For a member whose depth at the large end is three times that of its smaller end, $\gamma = 2$. This geometry is defined in Fig. 3.1.

The deformational parameters for the member in question in the "x" direction (i.e. perpendicular to the web) and in the "y" direction (in the plane of the web) will be denoted as "u" and "v", respectively. Twisting about the longitudinal axis, "z", will be defined as " ϕ ".

From the principle of virtual displacement,

$$\delta U - \delta W = 0 \quad 3.1-3$$

where " δU " represents the first variation in the strain energy, and " δW " is the work done by the externally applied forces moving through the assumed virtual displacements, " δu ", " δv " and " $\delta \phi$ ". It is to be remembered that these virtual displacements must satisfy the prescribed geometrical boundary conditions for the particular problem in question.

Assuming that the bending rigidity of the member about the y-axis is a constant, the bending components of the first variation in the strain energy are (5)

$$\delta U_x = \int_0^L EI_y \left(\frac{d^2 u}{dz^2} \right) \delta \left(\frac{d^2 u}{dz^2} \right) dz$$

and

$$\delta U_y = \int_0^L EI_x(z) \left(\frac{d^2 v}{dz^2} \right) \delta \left(\frac{d^2 v}{dz^2} \right) dz$$

The strain energy for non-uniform torsion may be written as (7)

$$U_\phi = \frac{1}{2} \int_0^L \left\{ \frac{EI_y}{2} \left[\frac{d^2}{dz^2} \left(u + \frac{dz}{2} \cdot \phi \right) \right]^2 + \frac{EI_x}{2} \left[\frac{d^2}{dz^2} \left(u - \frac{dz}{2} \cdot \phi \right) \right]^2 + GK \left(\frac{d\phi}{dz} \right)^2 \right\} dz$$

where the first two terms represent the flange bending strain energies due to warping and the last term is the pure torsional strain energy. Given

the specified linear variation in depth of the member defined in equation 3.1-1, the first variation component of the non-uniform torsional strain energy may be written as

$$\delta U = \frac{EI_y}{2} \int_0^L \left\{ u'^2 + \bar{d}_0^2 \left(\frac{y}{l} \right)^2 \varphi'^2 + \bar{d}_0^2 \left(\frac{y}{l} \right) \left(1 + \nu \frac{z}{l} \right) \varphi' \varphi'' + \frac{\bar{d}_0}{4} \left(1 + \nu \frac{z}{l} \right)^2 \varphi'^2 + \frac{GK}{EI_y} \varphi'^2 \right\} dz$$

where, by definition

$$\bar{d}_0 = d_0 - r_f$$

For the loading condition shown in Fig. 3.2 it is assumed that the applied end-bending moments can be related by a non-dimensional parameter "α", where $M_0 = \alpha M_L$. The primary bending moment at any distance "z" measured from the smaller end of the member is therefore

$$M_x(z) = M_L \left[\alpha + (1 - \alpha) \frac{z}{L} \right] \quad 3.1-4$$

where $-1 \leq \alpha \leq +1$. The external work done by the applied loads during the virtual displacements "δu", "δv" and "δφ" may be written as

$$\delta W = \int_0^L \left\{ P(u' \delta u' + v' \delta v' + r^2 \varphi' \delta \varphi') - M_x(\varphi \delta u'' + u'' \delta \varphi + \delta v'') \right\} dz$$

where

$$r^2 = \left[\frac{I_y + I_x(z)}{A(z)} \right]$$

Substituting these expressions in the appropriate first variational expressions just defined, equation 3.1-3 can be rewritten in the following more usable form:

$$\int_0^L \left\{ EI_y u'' \delta u'' + EI_x(z) v'' \delta v'' + EI_y \left[\frac{d^2}{dz^2} \left(\frac{y}{L} \right)^2 \varphi'' \right] + \frac{d^2}{dz^2} \left(\frac{y}{L} \right) \left(1 + \nu \frac{E}{L} \right) \varphi'' + \frac{GK}{EI_y} \varphi' \delta \varphi' \right. \\ \left. + EI_y \left[\frac{d^2}{dz^2} \left(\frac{y}{L} \right) \left(1 + \nu \frac{E}{L} \right) \varphi' + \frac{d^2}{dz^2} \left(1 + \nu \frac{E}{L} \right)^2 \varphi'' \right] \delta \varphi'' \right\} dz \\ - \int_0^L \left\{ P(u' \delta u' + v' \delta v' + r^2 \varphi' \delta \varphi') - M_x(\varphi \delta u'' + u'' \delta \varphi + \delta v'') \right\} dz = 0$$

3.1-5

To obtain a solution to the in-plane deformational and lateral stability behavior of tapered members, Eq. 3.1-5 could be used to establish the corresponding differential equations and the appropriate boundary conditions. However, due to the complicated non-geometrical (i.e. static) boundary conditions that are required to handle the torsion problem, and also because of the many difficulties that frequently are encountered when attempting to obtain direct solutions to these types of differential equations, this approach was not used (5). Rather Eq. 3.1-5 was solved using the Rayleigh-Ritz procedure, which presumes a series of geometrically appropriate displacement functions. As will be demonstrated later, the following assumed displacement functions yield sufficiently accurate answers with comparatively rapid convergence.

$$u(z) = \sum_{n=0}^{\infty} a_n u_n(z) \\ v(z) = \sum_{n=0}^{\infty} b_n v_n(z) \\ \varphi(z) = \sum_{n=0}^{\infty} c_n \varphi_n(z)$$

3.1-6

where

"u_n", "v_n" and "φ_n" are the following infinite power series:

$$u_n(z) = f(z)z^n$$

$$v_n(z) = g(z)z^n$$

$$\phi_n(z) = h(z)z^n$$

3.1-7

The functions "f(z)", "g(z)" and "h(z)" must satisfy the geometrical boundary conditions for the specified problems. Several obvious algebraic forms that might be presumed are given in Fig. 3.3.

Introducing Eqs. 3.1-6 into Eq. 3.1-5 and noting that "δ_n", "δ_b" and "δ_c" are arbitrary, the following simultaneous, algebraic equations result:

$$\sum_{n=0}^{\infty} a_n(A_{mn} - PB_{mn}) + \sum_{n=0}^{\infty} c_n P_{mn} = 0 \quad 3.1-8$$

$$\sum_{n=0}^{\infty} b_n(B_{mn} - PC_{mn}) = -S_n \quad 3.1-9$$

$$\sum_{n=0}^{\infty} c_n(H_{mn} - PL_{mn}) + \sum_{n=0}^{\infty} d_n L_{mn} = 0 \quad 3.1-10$$

where

$$A_{mn} = \int_0^l EI_y u_m'' u_n'' dz \quad , \quad B_{mn} = \int_0^l u_m' u_n' dz$$

$$D_{mn} = \int_0^l M_x(z) v_m'' u_n'' dz \quad , \quad E_{mn} = \int_0^l EI_x(z) v_m'' v_n'' dz$$

$$F_{mn} = \int_0^l v_m' v_n' dz \quad , \quad S_n = \int_0^l M_x(z) v_n'' dz$$

3.1-11

$$H_{mn} = \int_0^l EI_y \left[\left(\frac{v}{r} \right)^2 + \frac{GK}{EI_y} \right] \phi_m' \phi_n'$$

$$+ \frac{G^2}{2} \left(\frac{v}{r} \right) \left(1 + \nu \frac{E}{G} \right) (\phi_m'' \phi_n' + \phi_m' \phi_n'')$$

$$+ \frac{3^2}{4} (1 + \sqrt{\frac{E}{G}})^2 \omega_m'' \omega_n'' \} dz$$

$$I_{mn} = \int_0^l r^2 \omega_m' \omega_n' dz, \quad K_{mn} = \int_0^l M_x(z) u_{12}'' \omega_n dz$$

For "in-plane" bending, Eq. 3.1-9 provides the complete solution. Equations 3.1-8 and 3.1-10 are simultaneous equations that must be solved to determine the lateral-torsional buckling load.

For simply-supported end-conditions the displacement functions may be taken as

$$u_m(z) = v_m(z) = \omega_m(z) = z(z-l)z^m$$

Or using the non-dimensional, independent parameter $\zeta = \frac{z}{l}$, these functions become

$$u_m(\zeta) = v_m(\zeta) = \omega_m(\zeta) = (\zeta - 1)\zeta^m \tag{3.1-12}$$

In terms of this new parameter, Eqs. 3.1-8, -9, and -10 may be rewritten in the following non-dimensional form:

$$\sum_{n=0}^{\infty} \bar{a}_m \left\{ \frac{EI_y}{l^3} \bar{A}_{mn} - \frac{P}{l} \bar{B}_{mn} \right\} + \sum_{n=0}^{\infty} \bar{c}_m \frac{M_x}{l} \bar{D}_{mn} = 0 \tag{3.1-13}$$

$$\sum_{n=0}^{\infty} \bar{b}_m \left\{ \bar{E}_{mn} - \left(\frac{P}{I_y} \right) \left(\frac{I_{y0}}{I_{x0}} \right) \pi^2 \bar{F}_{mn} \right\} = - \frac{M_x \cdot l}{EI_{x0}} \bar{G}_m \tag{3.1-14}$$

3.1-15

$$\sum_{n=0}^{\infty} \bar{a}_m \frac{M_x}{l} \bar{D}_{mn} + \sum_{n=0}^{\infty} \bar{c}_m \left[\frac{EI_y}{l} \bar{H}_{mn} - \left(\frac{P}{l} \frac{I_{y0}}{I_{x0}} \right) \bar{I}_{mn} \right] = 0$$

where

$$\bar{A}_{mn} = \int_0^l u_m'' u_n'' d\zeta \quad , \quad \bar{B}_{mn} = \int_0^l u_m' u_n' d\zeta$$

$$\bar{D}_{mn} = \int_0^l \alpha m_m u_m'' d\zeta + \int_0^l (1+\alpha) \zeta \omega_m u_n'' d\zeta$$

$$\bar{K}_{mn} = \int_0^l I_x(\zeta) v_m'' v_n'' d\zeta \quad , \quad \bar{F}_{mn} = \int_0^l v_m' v_n' d\zeta$$

3.1-16

$$\bar{S}_n = \int_0^l M_x(\zeta) v_n'' d\zeta \quad , \quad \bar{K}_{nn} = \bar{D}_{nn}$$

$$\begin{aligned} \bar{H}_{mn} = \int_0^l \left\{ [V^2 \left(\frac{d_0}{l}\right)^2 + \left(\frac{GK_0}{EI_y}\right)] \varphi_m' \varphi_n' \right. \\ + \left(\frac{GK_0}{EI_y}\right) \cdot k \cdot \zeta \cdot \varphi_m' \varphi_n' \\ \left. + \frac{1}{2} \left(\frac{d_0}{l}\right)^2 [2\nu(1+\nu\zeta)(\varphi_m' \varphi_n')' + (1+\nu\zeta)^2 \varphi_m' \varphi_n'] \right\} d\zeta \\ \bar{I}_{mn} = \int_0^l R(\zeta) \varphi_m' \varphi_n' d\zeta \end{aligned}$$

and

EI_y = bending rigidity about the y-axis, assumed to be constant.

$$I_x(\zeta) = I_{x0} (1 + \nu\zeta)^2 (1 + \mu\nu\zeta)$$

I_{x0} = moment of inertia about the x-axis, at the smaller end of the member ($\zeta = 0$).

$$\mu = \frac{d_0^2 t_w}{12 I_{x0}}$$

γ = tapering ratio of the member

P_{y0} = axial yield load corresponding to uniform yielding of the member at its smaller end = $\sigma_y \cdot A_0$

σ_y = yield stress level of the material

A_0 = area of cross-section at smaller end of member (at $\zeta = 0$)

$P_{e_{x0}}$ = Euler's buckling load about the x-axis, presuming the cross-sectional properties of the smaller end of the member = $\frac{\pi^2 EI_{x0}}{L^2}$

r_{y0} = weak axis radius of gyration at the smaller end of the member = $\frac{L_{y0}}{A_0}$

" constant

α = end moment ratio = $\frac{M_0}{M_1}$ = end eccentricity ratio for eccentrically loaded members = $\frac{e_2}{e_1}$

$M_x(\zeta)$ = moment about the x-axis at the general location " ζ " = $M_0[\alpha + (1-\alpha)\zeta]$

GK_0 = St. Venant's torsional rigidity at the smaller end of the member ($\zeta = 0$)

$$GK(\zeta) = GK_0(1 + \eta_k \zeta)$$

$$\eta_k = \frac{e_1^2 \bar{e}_0 \gamma}{3I_y}$$

$$R(\zeta) = \frac{(\eta_1)(1+\eta_1\zeta)^2(1+\eta_2\zeta) + 1}{1 + \eta_2 \cdot \eta_1 \zeta}$$

$$\eta_1 = \frac{I_{x0}}{I_{y0}}$$

$$\eta_2 = \frac{A_{y0}}{A_0}$$

A_{w0} = area of web at $\zeta = 0$

Using these definitions as well as those listed in Eqs. 3.1-12 and 3.1-16, it is possible to define from Eqs. 3.1-14 the in-plane, beam-column action. Correspondingly, the lateral-torsional buckling strength is obtained by considering Eqs. 3.1-13 and 3.15.

It is to be recognized that for tapered members the "useful limits" of the end-moment ratio " α " will be different from those values that are meaningful for prismatic beams. In this paper the useful limits will be defined as $\alpha = \pm k$, where "k" corresponds to that particular end-moment ratio where the maximum bending stresses at both ends of the member are equal. "k" values vary with tapering ratios " γ ". Equating the extreme fiber bending stresses yields

$$\frac{C^2 E I_y \alpha_0}{2 I_{x0}} = \frac{M_0 d_1}{2 I_{x1}} \quad 3.1-17$$

or

$$k = \pm \frac{1}{(1+\gamma)(1+\gamma^2)} \quad 3.1-18$$

For prismatic members $\gamma = 0$, and $k = \pm 1$.

In this investigation, digital computer programs were developed to solve Eqs. 3.1-13, -14, and -15. Specific numerical solutions were obtained to Eqs. 3.1-13, -14, and -15 for several typical tapered members.* The cross-sectional properties at the smaller ends of the tapered members and additional geometric and statical properties for these members are given in Fig. 3.4.

* The actual numerical solutions are omitted from this paper due to the voluminous tables concerned. (Over 7500 individual cases were considered.) The solutions may be obtained upon request from the authors.

3.2 Initial Yield Solution

To obtain in-plane displacements and "strengths," Eq. 3.1-14, which is here again repeated, must be solved.

$$\sum_{n=0}^{\infty} \bar{b}_n \left\{ \bar{E}_{nn} - \left(\frac{P}{P_{yo}} \right) \left(\frac{P_{yo}}{P_{exo}} \right) \pi^n \bar{F}_{nn} \right\} = - \frac{M_0 c}{EI_{x0}} \bar{S}_n.$$

For each term in the series the value of \bar{b}_n can be ascertained, providing the determinate of the bracketed term is non-vanishing.

$$\{\bar{b}_n\} = - \frac{M_0 c}{EI_{x0}} \left[\bar{E}_{nn} - \left(\frac{P}{P_{yo}} \right) \left(\frac{P_{yo}}{P_{exo}} \right) \bar{F}_{nn} \right]^{-1} \{\bar{S}_n\} \quad 3.2-1$$

The in-plane displacement "v" is therefore

$$v(c) = - \frac{M_0 c}{EI_{x0}} \sum_{n=0}^{\infty} \left[\bar{E}_{nn} - \left(\frac{P}{P_{yo}} \right) \left(\frac{P_{yo}}{P_{exo}} \right) \bar{F}_{nn} \right]^{-1} \{\bar{S}_n\} (c^{m+2} - c^{n+1}) \quad 3.2-2$$

where \bar{E}_{nn} , \bar{F}_{nn} and \bar{S}_n are defined in Eqs. 3.1-16 and 3.1-17. They represent power series and can be readily integrated and summed, using a digital computer.

Normal stresses in the tapered member are determined from a consideration of the equation

$$\sigma = \frac{P}{A(c)} + \frac{M_x(c) \cdot \frac{1}{2} D(c)}{I_x(c)}$$

where

$$M_x(c) = EI_{x0} (1+\nu c)^2 (1+\nu c) v''(c)$$

To facilitate the solution process, and to more generalize the results, this equation can be nondimensionalized,

$$\left(\frac{\sigma}{\sigma_y}\right) = \left(\frac{P}{P_{y0}}\right) \left(\frac{1}{1 - \eta_2 \gamma \zeta}\right) + \frac{M_{yL}}{M_{yL}} (1 + \gamma \zeta)(1 + \gamma)(1 + \mu \gamma) \cdot \sum_{n=0}^{\infty} \left[\bar{E}_{mn} - \left(\frac{P}{P_{y0}}\right) \left(\frac{P_{y0}}{P_{axp}}\right) \bar{F}_{mn} \right]^2 \{S_n\} ((n+2) - (n+1)\zeta^n - n(n+1)\zeta^{n+1}) \quad 3.2-3$$

where M_{yL} denotes the initial yield moment at the larger end of the member ($\zeta = 1.0$) with $P = 0$.

Initial yield solutions can be obtained by equating to "1.0" the ratio (σ/σ_y) in equation 3.2-3. The corresponding relationships between (P/P_{y0}) and (M_L/M_{yL}) define the "interaction" at initial yielding. For each cross-section (see Fig. 3.4(a)), the interaction values were obtained for $(P_y/P_{ax})_0 = 0, 0.5, 1.0, 1.5$ and 2.0 ; $\alpha = k, +1, +0.1, 0, -0.1$ and $-k$; and values of γ from zero to six. It is to be noted that for this selection of variables ("P" referenced to the smaller end of the member, and "M" referenced to the larger end), the hereinafter defined, computed non-dimensional "design parameters" were found to be essentially equal for all of the four cross-sections (see footnote on p. 17).

Ten terms in the power series were used in the calculations leading to the interaction solutions. The accuracy of the results was examined by comparing values associated with nine terms, and then with ten. In all cases the deviations were less than 0.1%.

Finally, it must be reemphasized that the maximum stress in tapered members of the type considered herein does not necessarily occur at the ends of the member, even when lateral and axial loads are absent. This is due to the non-uniform section modulus properties of such tapered members.

3.3 Axial Stability (Elastic) Solutions

When the determinant of the bracketed term in Eq. 3.1-14 vanishes, the result is a set of homogeneous equations, and \bar{b}_m cannot be uniquely defined. The particular axial load, P, which makes the determinant vanish is the critical Euler (x-axis) type buckling load, P_{xcr} . That is,

$$\left| \bar{I}_{mn} - \left(\frac{P}{P_{y0}} \right) \left(\frac{P_{y0}}{P_{x0}} \right) \pi^2 \bar{I}_{mn} \right| = 0 \quad 3.3-1$$

For the case of no end eccentricities, Eq. 3.3-1 is valid when $P_{xcr} \leq P_{y0}$. The critical ratios P/P_{y0} were calculated for the first four cross-sections in Fig. 3.4(a) and various values of ν . (See footnote on page 17).

3.4 Lateral Stability (Elastic) Solutions

As was noted earlier, lateral-torsional buckling strength can be determined by solving the homogeneous, simultaneous Eqs. 3.1-13 and 3.1-15. For convenience in calculation, these can be rewritten in the following form:

$$\sum_{n=0}^{\infty} \left\{ (AI_{mn} - \lambda BI_{mn}) \bar{a}_n - \lambda DI_{mn} (\bar{c}_n(i)) \right\} = 0 \quad 3.4-1$$

$$\sum_{n=0}^{\infty} \left\{ -\lambda DI_{mn} \bar{a}_n + (HI_{mn} - \lambda I_{mn}) (\bar{c}_n(i)) \right\} = 0$$

where

$$AI_{mn} = \bar{I}_{mn}$$

$$BI_{mn} = \pi^2 \bar{I}_{mn}$$

$$DI_{mn} = \pi^2 \mu_c \mu_s \bar{D}_{mn}$$

$$HI_{mn} = \bar{H}_{mn}$$

$$I_{mn} = \pi^2 \mu_{xz} l_{mn}$$

$$\lambda = \frac{P}{P_{ey0}} = \text{The Eigenvalue}$$

$$P_{ey0} = \frac{\pi^2 EI_{y0}}{l^2}$$

$$\mu_{zd} = \frac{d_0}{l}$$

$$\mu_{de} = \frac{e_1}{d_0}$$

$$\mu_{zx} = \left(\frac{r_{y0}}{l}\right)^2$$

Reproduced from
best available copy.

The eigenvalue (i.e. the lateral-torsional buckling solution) is obtained by solving the characteristic equation corresponding to

$$\begin{vmatrix} \left[\begin{array}{cc} \Delta I_{mn} & 0 \\ 0 & H I_{mn} \end{array} \right] - \lambda \begin{bmatrix} B I_{mn} & D I_{mn} \\ D I_{mn} & F I_{mn} \end{bmatrix} & = 0 \end{vmatrix} \quad 3.4-2$$

where $n, n = 1, 2, 3 \dots$. The critical value of the axial thrust is given by

$$P_{cr} = \lambda_{cr} P_{ey0}$$

The corresponding "critical end-moment," at the larger end of the member, is

$$(M_z)_{cr} = P_{cr} e_1$$

For the special case where no end eccentricities exist, and the member is subjected to pure axial thrust, Eqn. 3.4-1 can be uncoupled, yielding

$$(AI_{mn} - \lambda BI_{mn}) \bar{a}_m = 0 \quad 3.4-3$$

and

$$(HI_{mn} - \lambda II_{mn})(\bar{C}_m l) = 0 \quad 3.4-4$$

Equation 3.4-3 gives $\lambda_{cr} = +1.0$, or $P_{cr} = P_{e_{y_0}}$. Equation 3.4-4 yields the torsional buckling load for axially loaded, tapered columns.

In the eigenvalue calculations for lateral-torsional buckling, six terms of the power series were used for all cases where $\alpha > 0$. Seven terms were included for those cases where $\alpha \leq 0$. These resulted in a more-or-less uniform convergence criterion of $99\% < \lambda_{n+1} / \lambda_n < 100\%$. Two sub-sets of solutions (pure bending and bending plus axial thrust) for Section I are given in Fig. 3.5 to illustrate the rate of convergence of the solutions. For all cases listed in the figure, the length of the member was presumed equal to 144 inches. Solutions to the other cases and for the other sections are comparable to those illustrated.

For all of the beam-column cases considered in this report it has been presumed that the end-conditions at both ends of the tapered members are "simply-supported." This was true for both bending and for warping torsion. It must be understood, however, that other cases could have been equally well examined, using appropriate algebraic form; for example, those given in Fig. 3.3. The case chosen should give the more conservative solutions and hence is more desirable for design purposes.

Lateral-torsional buckling solutions were obtained for the four selected sections previously defined. For each, four lengths of members, various γ values and four values of α (+1.0, +k, 0 and -k) were considered. In addition, five values of e/d_0 were examined (0.5, 1.0, 2.0, 5.0 and ∞). Solutions for $(P/P_y)_0$ and $(M/M_y)_l$ were obtained using the heretofore described procedure. Unlike the in-plane cases the extreme variations in the solutions tend to suggest that these selected parameters, in and of themselves, do not constitute a unique invariant set insofar as lateral-torsional buckling is concerned. (For the detailed numerical results, see footnote on p. 17).

Reproduced from
best available copy.



4. DEVELOPMENT OF DESIGN FORMULAS

Several avenues of approach are available for the development of design approximations to the solution referred to in Section 3. First, using multi-variable curve fitting techniques, and essentially starting from "scratch", polynomial expressions containing all the variables could be developed. A second, basically different, approach could start from the assumption that adequate design allowable stresses are now available for prismatic members, and these could be modified to handle the tapered problem by the introduction of certain "to be determined" factors into the prismatic formulas. These factors could be calculated from the general condition that

$$\frac{\text{Strength of tapered member}}{\text{Strength of prismatic member based on the smaller cross-section}} = f(V, d_o, b, t, w) \quad 4.0-1$$

with the restriction that when $\gamma = 0$ (prismatic), $f = 1.0$.

Although both approaches require curve fitting techniques, the second approach, the one adopted in this study, offers two advantages to the designer: first, he still will be using the familiar AISC code formulas for prismatic beams -- though modification factors will be introduced; and, secondly, these factors should give the designer an intuitive feeling of the increase in strength of the tapered member over its prismatic counterpart. This increase in strength may help in deciding the potential economy of the structure using such tapered members. It is important to recognize that in the subsequent discussion and development of the tapered beam formulas there is contained as a multiplier the same factor of safety that is incorporated in the prismatic formulas. Furthermore, it must be understood that they are applicable to members with small tapering angles.

Boley (4), using a series solution for tapered rectangular beams and the Bernoulli-Euler theory, found that for tapered angles less than 15° the error in normal stress computed by the general methods hereinbefore described was less than a few per cent. Thus, for

$$\tan \theta = \frac{d_L - d_0}{l} = \gamma \frac{d_0}{l} \quad 4.0-2$$

and θ restricted to less than 15° , γ should be less than

$$\gamma = 0.268 \frac{l}{d_0} \quad 4.0-3$$

Reference to "small taper angles" will refer to tapered beams which satisfy equation 4.0-3. From practical consideration equation 4.0-3 has been further limited to 6. Therefore, when considering the design of tapered members using the information contained in this report

$$\gamma \leq 0.268 \frac{l}{d_0} \leq 6 \quad 4.0-4$$

4.1 Compression (A.I.S.C. 1.5.1.3)

In this Section the maximum allowable stress due to an applied axial load is defined. There are several failure modes of concern: (1) yielding at the smaller end, (2) strong axis buckling, (3) weak axis buckling, and (4) torsional buckling.* Since the effective length, KyL , will be treated separately in Section 5, the formulas in this Section are based on pin-ended members.

* Pure torsional buckling generally does not govern the design of I-shaped columns. Based on the procedures defined in Section 3, one may readily compute the torsional buckling load of a tapered column when necessary.

Considering the elastic case first, a function f (equation 4.0-1) is sought such that

$$\sigma_{\text{taper}} = \sigma_{\text{prismatic}} f(\gamma, d_o, b, t, w, l) \quad 4.1-1$$

where

$$\sigma_{\text{prismatic}} = \frac{\pi^2 E}{(l/r_o)^2}$$

Since buckling can occur about either the strong or weak axis of the member, the function f will be different for each case. Observing that the variation of the weak axis radius of gyration along the length of a tapered member with constant flange width and thickness is small, no modification factor is considered to be necessary. Thus

$$\sigma_{\text{taper}} = \frac{\pi^2 E}{(l/r_{yo})^2} \quad (\text{weak axis}) \quad 4.1-2$$

If the member is braced against weak axis buckling, then the buckling strength about the strong axis must be determined. For this case, it will be assumed that $f = \frac{1}{8}$ so that

$$\sigma_{\text{taper}} = \frac{\pi^2 E}{(gl/r_o)^2} \quad 4.1-3$$

Equation 4.1-3 implies that the buckling stress for a tapered column of length l is equivalent to that for a prismatic column of length gl having a cross-section equal to that of the smaller end of the tapered column. See Fig. 4.1.

Seeking a "g" function of simple form with comparatively small error,

$$g = \frac{\frac{\pi B}{(L/r_0)^2}}{\sigma_{taper}}$$

theoretical solutions for the first four sections defined in Fig.3.4(a) and for various lengths were substituted into the equation for "g". After examining several possible approximating functions, the following was chosen:

$$g = 1.000 - 0.327 \gamma + 0.0649 \gamma^2 (1.00 - 0.0752 \gamma) \quad 4.1-4$$

This function is tabulated in Fig. 4.2. To indicate the degree of error involved, Fig. 4.3 contains values calculated by the "Exact" stress method described in Section 3 divided by equation 4.1-3. It is to be recognized that equation 4.1-3 is conservative for values greater than unity.

In general, elastic formulas are applicable for slenderness ratio greater than a certain limiting ratio. For inelastic buckling, that is, for slenderness ratios less than that limiting value, a transition curve between the elastic curve and the fully yielded cross-section (zero slenderness) has been used in A.I.S.C. prismatic column design. This curve has the form

$$\sigma'_{taper} = \sigma_y - \frac{\beta}{\sigma_{taper}} \quad 4.1-5$$

where

β = arbitrary constant

Accounting for a maximum residual stress equal to one-half the yield stress ($\frac{\sigma_y}{2}$),

as is the case for prismatic members, the limiting slenderness ratio, C_c , is determined by

$$\sigma'_{taper} = \frac{1}{2} F_y = \frac{\pi^2 E}{(C_c)^2}$$

Solving for C_c gives

$$C_c = \sqrt{\frac{2\pi^2 E}{F_y}} \quad 4.1-6$$

Returning to equation 4.1-5, the arbitrary constant " β " is determined by requiring that $(\frac{gl}{r_0}) = C_c$ when $\sigma'_{taper} = \frac{1}{2} \sigma_y$. Thus, substituting these values in equation 4.1-5 gives

$$\beta = \frac{\pi^2 E \sigma_y}{2 C_c^3}$$

The transition curve, therefore, is given by

$$\sigma'_{taper} = \left(1.0 - \frac{(gl/r_0)^2}{2C_c^2} \right) \sigma_y \quad 4.1-7$$

Inclusion of the factor of safety for axial compression in equations 4.1-7 and 4.1-3 yields:

For $(gl/r_0) < C_c$

$$F_{a_y} = \frac{\left[1.0 - \frac{(gl/r_0)^2}{2C_c^2} \right] F_y}{\frac{5}{3} + \frac{3(gl/r_0)}{8C_c} - \frac{(gl/r_0)^2}{8C_c^2}} \quad 4.1-8$$

For $(gl/r_0) > C_c$

$$F_{a_y} = \frac{12\pi^2 E}{23(gl/r_0)^2} \quad 4.1-9$$

where

$$C_c = \sqrt{\frac{2\pi^2 E}{F_y}}$$

and

weak axis: $g = 1.0$

strong axis: $g = \text{equation 4.1-4}$

Equations 4.1-8 and 4.1-9 are plotted in Fig. 4.4 for $F_y = 36, 42, \text{ and } 50 \text{ ksi.}$

4.2 Bending (A.I.S.C. 1.5.1.4)

Often a designer attempts to select a particular tapered member such that the maximum stress is nearly constant along the length of the beam. In the case of a simply-supported beam subjected to end-moments alone, one possible optimum design would require equal extreme fiber bending stresses at both ends, i.e. $(M/S_x)_0 = (M/S_x)_l$. This implies that $M_0/M_l = S_{x0}/S_{xl}$, which is the "limiting" moment gradient $\alpha = +k$ discussed in Section 3.1 (Equation 3.1-18). However, due to the variable moment of inertia, it must be recognized that the maximum stress under this "limiting" moment gradient does not necessarily occur at the ends of the beam. Nonetheless, for the ranges of variables being considered, this condition $M_0/M_l = S_{x0}/S_{xl}$ is an adequate design estimation for tapered beams subjected to end-moments at both ends producing single curvative deformations.

In most common practice a structure is designed such that negligibly small amounts of bending moment exists at the smaller end of a tapered member. To accommodate this, a moment gradient function has been incorporated in the design formulas for $\alpha = 0$. A modification factor to the A.I.S.C. formulas is first sought for the limiting moment gradient case $\alpha = +k$; and then a moment gradient function is developed to relate that critical stress to one corresponding to $\alpha = 0$.

Proceeding as outlined at the beginning of this Section, the critical lateral buckling stress for a prismatic beam subjected to bending moments is given by

$$\sigma_{cr} = \frac{1}{S_x} \sqrt{\frac{\pi^2 E I_y G K}{l^2} + \frac{\pi^4 E I_y E I_w}{l^4}} \quad 4.2-1$$

Instead of using equation 4.2-1 directly, a modifying factor can be developed which can be applied to the length of the member as was done for the pure axial load case in Section 4.1. Thus, the critical buckling stress for a tapered beam can be expressed by

$$(\sigma_{cr})_y = \frac{M_o}{S_{x_o}} = \frac{1}{S_{x_o}} \sqrt{\frac{\pi^2 E I_y G K_o}{(hl)^2} + \frac{\pi^4 E I_y E I_w o}{(hl)^4}} \quad 4.2-2$$

where $h = h(y, d_o, b, t, w, l)$.

Equation 4.2-2 presumes a prismatic beam of length hl , whose cross-sectional properties are those of the smaller end of the tapered beam (Fig. 4.5).

Solving for h^2 yields

$$h^2 = \frac{\pi^2 E I_y G K_o}{l^2 (\sigma_{cr})_y^2 S_{x_o}^2} \left[1 + \sqrt{1 + \frac{[(\sigma_{cr})_y S_{x_o} d_o]^2}{(G K_o)^2}} \right] \quad 4.2-3$$

The above equation was used to calculate value of h for the first four cross-sections defined in Fig. 3.4(a). Various values of length were presumed. In total 128 such points were calculated. While the resulting

values, plotted as a function of the tapering ratio, were quite scattered, there was indicated a strong dependence on the tapering ratio.

Since a modification factor to the A.I.S.C. prismatic beam formulas is desired, it is useful to first examine the basic assumptions of the current A.I.S.C. formulas.

$$\text{For } (L/r_T) \cong \frac{510 \times 10^3 C_b}{F_y} \quad (\text{A.I.S.C. 1.5-6b})$$

$$F_b = \frac{170 \times 10^3 C_b}{(L/r_T)^2}$$

or

$$F_b = \frac{12 \times 10^3 C_b}{L^2/A_f} \quad (\text{A.I.S.C. 1.5-7})$$

These two equations were arrived at by considering the two limiting cases of equation 4.2-1: either complete St. Venant resistance, or total warping resistance. For sections which are thin and deep (i.e. those having high warping resistance) the first formula will generally govern. On the other hand, for sections which are thick and shallow, the second formula is presumed to hold. Thus, in developing a modification factor to these equations, it is reasonable to presume two distinctly different factors: one for those cases where the smaller end is thin and deep, and a second one when the smaller end is thick and shallow.

For the four sections presumed in Section 3.0, it turns out that all of the sections are basically thick and shallow, and therefore the second formula governs. This is true, even though sections I and III are basically beams, and sections II and VI are basically columns. Because of the general nature of the problem being studied, sections I and III were used to find the

modification factor to be used with the A.I.S.C. formula 1.5-7. An entirely different thin, deep section was selected for use in developing a modification to A.I.S.C. formula 1.5-6b. This specially selected section (section V) is also defined in Fig. 3.4(a). Typical results of critical elastic lateral buckling stresses for each of the three sections are given in Fig. 4.6.

For thin, deep sections, substituting the data determined for section V into equation 4.2-3 and curve fitting the resulting points as a function of tapering ratio and (l/r_{T_0}) gives

$$h_w = 1.00 + 0.00385 \gamma \sqrt{l/r_{T_0}} \quad 4.2-4$$

For thick, shallow sections, using the data corresponding to sections I and III and fitting the points as a function of tapering ratio and (ld_0/A_f) gives

$$h_s = 1.00 + 0.0230 \gamma \sqrt{\frac{ld_0}{A_f}} \quad 4.2-5$$

The allowable elastic stress in a tapered member for $\alpha = +k$ is therefore the larger of the two numbers calculated from

$$F_{by} = \frac{170 \times 10^3}{(h_w l/r_{T_0})^2} \quad 4.2-6$$

and

$$F_{by} = \frac{12 \times 10^3}{(h_s ld_0/A_f)} \quad 4.2-7$$

To arrive at a moment gradient coefficient for the $\alpha = 0$ case, the following is assumed:

$$C_{by} = \frac{\sigma_{taper} \Big|_{\alpha = 0}}{\sigma_{taper} \Big|_{\alpha = +k}}$$

Using the particular critical stresses defined in Fig. 4.6 and relating these to comparable values for $\alpha = 0$ yields values for C_{by} which, generally, are inversely proportional to length and tapering ratio. Also it is to be noted that C_{by} is slightly greater for section V (thin and deep) than it is for section III (thick and shallow). Noting that A.I.S.C. specifies a constant ($C_b = 1.75$) multiplies for prismatic beams with $M_0/M_2 = 0$, and attempting to keep the curve fit simple and the same for both ranges, a moment gradient coefficient was obtained with γ as the only variable. The resulting expressions are

$$F_{by} = \frac{170 \times 10^3 C_{by}}{(h_w l / r_{T_0})^2} \quad 4.2-8$$

or

$$F_{by} = \frac{12 \times 10^3 C_{by}}{h_w l d_o / A_f} \quad 4.2-9$$

where

$$C_{by} = \begin{cases} 1.0; & \alpha = +k \\ \frac{1.75}{1.0 + 0.25 \sqrt{\gamma}}; & \alpha = 0 \end{cases}$$

For several different ranges of parameters the ratio of the "exact" stress to the values predicted by the larger of equations 4.2-8 or 4.2-9 (after removing the factor of safety) is tabulated in Fig. 4.7. In reviewing

the errors listed, comparison should be made between the errors for $\gamma = 0$ (which the current A.I.S.C. specification contains), and that for other taper ratios.

Since, as was pointed out in the preceding section, there is always in design, especially design involving welded members, a possibility that inelastic lateral buckling will occur, a "transition curve" is necessary. Thus, equation 4.2-8 is applicable for values greater than some limiting $(h_w l / r_{T_0})$. This limiting value, C_T , occurs when the critical stress is equal to $\frac{1}{2} F_y$. Removing the factor of safety from equation 4.2-8 and imposing the condition that $\sigma_{taper} = \frac{1}{2} F_y$ at $(h_w l / r_{T_0}) = C_T$ yields

$$C_T = \sqrt{\frac{510 \times 10^3 C_{by}}{F_y}} \quad 4.2-10$$

Observing the similarity between equations 4.2-8 and 4.1-9 (column buckling), a transition curve for the allowable inelastic lateral buckling stress may be written as:

$$\text{for } (h_w l / r_{T_0}) \leq C_T \quad 4.2-11$$

$$F_{by} = \frac{2}{3} \left[1.0 - \frac{(h_w l / r_{T_0})^2}{2C_T^2} \right] F_y$$

Equations 4.2-8 and -11 are plotted in Fig. 4.8 for $F_y = 33, 42,$ and 50 ksi. Equation 4.2-9 is plotted in Fig. 4.9. The horizontal parts of the curves in Figs. 4.8 and 4.9 represent $0.6 F_y$, the presumed limiting values of normal stress contained in the current A.I.S.C. formulas.

The tapering ratio has a much smaller effect on the allowable stress for thin, deep beams than it does for thick, shallow beams. This can be seen from equations 4.2-4 and 4.2-5. It is important to keep in mind that there has been presumed throughout all of these derivations a limiting moment gradient $\alpha = +k$ which is a function of the tapering ratio γ (equation 3.1-18).

4.3 Axial Compression and Bending (A.I.S.C. 1.5.1)

The methods for determining "exact" solutions for axial compression and bending necessary to cause initial yield (neglecting residual stresses) were discussed in Section 3.2. The purpose of this section is to fit to the data referred to in Section 3 an interaction curve of the form,

$$\left(\frac{P}{P_y}\right)_0 + C_E \left(\frac{M}{M_y}\right)_L = 1.0 \quad 4.3-1$$

where

$$P_{y0} = A_o F_y$$

$$M_{yL} = S_x F_y$$

$$(P_{x0})_v = \frac{\pi^2 E I_x C}{(L')^2}$$

$$C_E = \text{function to be determined}$$

The particular function C_E finally selected - after a number of trials - has the form

$$C_E = \frac{C_{in}}{\left[1 - \frac{P}{(P_{x0})_v}\right]}$$

where

$$C_{in} = 1.0 + a \frac{P}{(P_{x0})_v} + b \left[\frac{P}{(P_{x0})_v}\right]^2 \quad 4.3-2$$

where

$$e = 0.10 \left[-9.0 + 5.5 \left(\frac{\alpha}{k} \right) + 4.5 \left(\frac{\alpha}{k} \right)^2 \right]$$

$$b = 0.15 \left[4.0 + \left(\frac{\alpha}{k} \right) - 3.0 \left(\frac{\alpha}{k} \right)^2 \right]$$

g is defined in equation 4.1-4, k is defined in equation 3.1-18 and $\alpha = M_0/M_L$

is the moment gradient. Fig. 4.10 contains tabulated values of C_m as a function of $P/(P_{X_0})_Y$ and α/k . As an indication of the error involved when using equation 4.3-1, tabulated values of the "exact" large end moment divided by the large end moment predicted from equation 4.3-1 are given in Fig. 4.11 for $\alpha = +k$.

Equation 4.3-1 is only valid when the maximum axial load is P_{y_0} and the maximum bending moment is M_{y_0} . These maxima are the initial yield limits of the loads. However, a beam-column's strength may be governed by in-plane instability or by lateral buckling either of which may occur before the initial yield stress is reached. Thus, following the A.I.S.C. interaction pattern, equation 4.3-1 can be written more generally in terms of the maximum axial load and maximum bending moment that a beam-column can carry without failure. Equally true, for even greater consistency, equation 4.3-1 can be written in terms of stresses instead of loads. Making these adjustments gives

$$\left(\frac{f_x}{F_{x_0}} \right)_0 + \frac{C_m}{\left[1 - \frac{f_x}{(F_{x_0})_Y} \right]} \left(\frac{f_b}{F_{b_0}} \right)_L = 1.0 \quad 4.3-3$$

where

C_m = equation 4.3-2

f_{a0} = computed axial compressive stress at smaller end

f_{b0} = computed bending stress at larger end

F_{a0} = allowable axial stress (Section 4.1)

F_{b0} = allowable bending stress (Section 4.2)

$$F'_{b0} = \frac{12\pi^2 E}{23(gt_b/r_{sc})^2}$$

As noted above the form of equation 4.3-3 is similar to A.I.S.C. formula (1.6-1 a) except for the introduction of the modification term C_m . For a prismatic beam-column with equal end moments C_m should be unity. However, the A.I.S.C. amplification factor $(1 - f_a/F'_a)$ is an approximation and is good for small f_a/F'_a . If f_a/F'_a is small, and therefore C_m is close to unity, the interaction equation can be approximated by the expression

$$\left(\frac{f_a}{F_{a0}}\right)_0 + \left(\frac{f_b}{F_{b0}}\right)_L \cong 1.0 ; \text{ if } \left(\frac{f_a}{F_{a0}}\right)_0 \cong 0.15 \quad 4.3-4$$

4.4 Comparison with Experimental Data

Two major experimental programs have been carried out on welded, steel tapered sections: an earlier one at Columbia University and a more recent one at State University of New York at Buffalo.

Initially, interest was in the determination of the elastic stability of linear tapered I-beams and channels. The tests were carried out at Columbia (9, 10, 11). In general, the test members were cantilevered and were subjected to axial and transverse (at single and multiple points) loads. The tension flange was braced at the free end, which was always the smaller end for the non-prismatic members. (See Fig. 4.12). The tests were conducted so that several members with the same nominal dimensions were loaded differently, ranging from pure axial load - to axial load plus bending - to bending alone. However, due to the variety of loading and specimens tested, only a few actually corresponded to the assumptions made in the analytic studies.

Results of two test series are plotted in Fig. 4.12: one corresponding to a taper ratio of zero (prismatic) and the other corresponding to a taper ratio of four. It is most important to note that the factors of safety have been removed to afford a truer comparison of the results. Even though this has been done the interaction curve underpredicts the load carrying capacity two-to-threefold. This is due primarily to the end support conditions, and the fact that λ_y is very difficult to predict. The important observation to be made from Fig. 4.12 is that the interaction curve equally underpredicts the strength of the prismatic member. The tests should not really be compared with the developed design formulas, since the formulas are based on simply-supported members. The test results clearly reflect the effect of end restraints.

Later, a second program of testing was initiated at SIMY at Buffalo (12) with the emphasis directed toward the inelastic lateral stability of tapered beams. Recognizing that tapered members are inefficient axial load carriers,

the test program was set up to simulate high bending stress and low axial stress. Thus the test results do not cover the entire range of variables. Also of interest, the specimens were loaded and supported similar to gable roof beams: the axial force component varies as the beam deflects. Results from three specimens are plotted in Fig. 4.13 along with their corresponding interaction curves. The specimens are essentially the same except for their taper ratio.

In contrast to Fig. 4.12, Fig. 4.13 suggests that there is more (consecutive) error in the design formulas as the taper increases. This is because all three specimens failed by lateral buckling very near the coupon yield stress. Equation 4.3-3, it should be remembered, was derived from initial yield considerations.

5. EFFECTIVE LENGTH

The solutions obtained in Section 3.2 were for pin-ended members. If the column in question is restrained at either one or at both of its ends, then the buckling load will be different and a different solution must be found. A restrained column of height l can be considered as a pin-ended column of height $K_y l$, where K_y is the so-called effective length factor. In Section 4.2 a somewhat similar approach was used to obtain a function g which related the buckling load of a pin-ended prismatic column to that of a pin-ended tapered column. Due to the particular analytic procedure used in the development, this function g has been absorbed into the effective length factor K_y derived in this Section. Thus K_y , as will be herein derived, is interpreted as relating a restrained tapered column of height l to a pin-ended prismatic column of height $K_y l$.

The effective length is determined by considering a rectangular rigid frame (Fig. 5.1) composed of prismatic beams and tapered columns. The top beam has a moment of inertia I_T and the bottom beam has a moment of inertia I_B . The loads are presumed to act at the centroids of the columns. The frame has two support conditions in the plane of the frame: (1) vertical support at A and B (side-sway prevented by a horizontal support at C) and (2) vertical support at A and B (side-sway permitted). Finally, it is to be emphasized that only buckling in the plane of the frame is considered in these developments.

5.1 Slope-Deflection Equations

The frame is analyzed by using slope-deflection equation for tapered

members of the following form (13), (see Fig. 5.2).

$$\theta_{AB} = \frac{M_{AB}l}{EI_0} C_{AA} - \frac{M_{BA}l}{EI_0} C_{AB} + \frac{\Delta_{AB}}{l} + \bar{\theta}_{AB} \quad 5.1-1$$

$$\theta_{BA} = \frac{-M_{AB}l}{EI_0} C_{BA} + \frac{M_{BA}l}{EI_0} C_{BB} + \frac{\Delta_{AB}}{l} - \bar{\theta}_{BA} \quad 5.1-2$$

The coefficients C_{AA} , C_{BB} , and $C_{AB} = C_{BA}$ are determined by considering the differential equation for a tapered column, presuming all of the material in the cross-section is concentrated in the flanges. These coefficients have different forms depending on the quantity q/γ^2 , where

$$q = n^2 \frac{P}{P_{e_0}} \quad 5.1-3$$

$$P_{e_0} = \frac{\pi^2 EI_0}{l^2}$$

and

$$\gamma = \frac{d_f - d_0}{d_0}$$

for the range $\frac{q}{\gamma^2} \leq \frac{1}{2}$

$$C_{AA} = \frac{1}{q} - \frac{\gamma}{q} \left[\rho \left(\frac{m+n}{m-n} \right) - \frac{1}{2} \right] \quad 5.1-4(a)$$

$$C_{AB} = C_{BA} = \frac{2\gamma}{q \sqrt{1+\gamma}} \frac{1}{(m-n)} - \frac{1}{q} \quad 5.1-5(a)$$

$$C_{BB} = \frac{1}{q} - \frac{\gamma}{q(1+\gamma)} \left[\rho \left(\frac{m+n}{m-n} \right) + \frac{1}{2} \right] \quad 5.1-6(a)$$

where

$$\rho = \sqrt{\frac{k}{\gamma^2} - \frac{q}{\gamma^3}}$$

$$m = (1 + \gamma)^\rho \quad 5.1-7(a)$$

$$n = (1 + \gamma)^{-\rho}$$

For $\frac{q}{\gamma^2} = k$

$$C_{AA} = \frac{1}{q} - \frac{\gamma^{\rho}}{q} \cot [\beta \ln(1+\gamma)] + \frac{\gamma}{2q} \quad 5.1-4(b)$$

$$C_{AB} = C_{BA} = \frac{\gamma}{q \sqrt{1+\gamma}} \beta \csc[\beta \ln(1+\gamma)] - \frac{1}{q} \quad 5.1-5(b)$$

$$C_{BB} = \frac{1}{q} - \frac{\gamma^{\rho}}{q(1+\gamma)} \cot [\beta \ln(1+\gamma)] - \frac{\gamma}{2q(1+\gamma)} \quad 5.1-6(b)$$

where

$$\beta = \sqrt{\frac{q}{\gamma^2} - k} \quad 5.1-7(b)$$

If the member is prismatic ($\gamma = 0$), and there is no axial force imposed

$$C_{AA} = C_{BB} = \frac{1}{3} \quad 5.1-8$$

$$C_{AB} = C_{BA} = \frac{1}{6} \quad 5.1-9$$

Stiffness coefficients for tapered members are plotted in Figs. 5.3 to 5.6 as a function of $P/P_{c_{x_0}}$ and γ . Both compression and tension axial thrusts are presumed.

5.2 Side-Sway is Prevented

The frame illustrated in Fig. 5.1(a) is considered in this Section. Equations 5.1-1 and 5.1-2 can be applied to each member in the frame. The coefficients for the tapered columns are given by equations 5.1-4, -5, and -6 and for the prismatic beams by equations 5.1-8 and -9. From symmetric, geometric, and equilibrium conditions the eight slope-deflection equations reduce to two.

$$\begin{bmatrix} (C_{AA} + \frac{1}{2}R_B) & -C_{AD} \\ -C_{DA} & (C_{DD} + \frac{1}{2}R_T) \end{bmatrix} \begin{bmatrix} M_{AB} \\ M_{DA} \end{bmatrix} = \begin{bmatrix} 0 \\ 0 \end{bmatrix} \quad 5.2-1$$

where

$$R_B = \frac{b I_D}{l I_B}$$

$$R_T = \frac{b I_C}{l I_T}$$

Noting that the coefficients are a function of the applied load, and that the set is homogeneous, the critical load is determined by forcing the determinant of the coefficient matrix to equal zero. The complexities of the resulting equation require that the critical load be found by incrementing the applied load and testing for a zero solution. Once the critical load is found then the effective length factor can be calculated from

$$K_Y = \sqrt{\frac{\pi^2 EI_0}{P_{cr} L^2}} = \pi \sqrt{\frac{1}{q}}$$

5.2-2

since

$$P_{cr} = \frac{\pi^2 EI_0}{(K_Y L)^2}$$

The calculations for effective length were carried out for values of R_T and R_B ranging from zero to infinity. Figs. 5.7 to 5.15 contain graphs of the effective length factors for the case where "side-sway is prevented."

5.3 Side-Sway is Permitted

The stability of the frame illustrated in Fig. 5.1(h) is here considered. Proceeding in a similar way as in Section 5.2, the eight slope-deflection equations can be reduced to four equations involving the five unknowns: M_{AD} , M_{DA} , M_{BC} , M_{CB} , and Δ_{DA} . A fifth equation can be found by considering free body diagrams and shear equilibrium of the deflected frame. Thus the following system of equations is obtained.

Reproduced from best available copy.

$$\begin{bmatrix}
 (C_{AA} + \frac{1}{3}R_B) & & & & \\
 -C_{DA} & (C_{DD} + \frac{1}{3}R_T) & & & \\
 0 & -\frac{1}{6}R_T & (C_{CC} + \frac{1}{3}R_T) & & \\
 -\frac{1}{3}R_B & 0 & -C_{BC} & (C_{BB} + \frac{1}{3}R_B) & \\
 0 & 0 & 0 & 2q &
 \end{bmatrix}
 \begin{bmatrix}
 M_{AD} \\
 M_{DA} \\
 M_{CB} \\
 M_{BC} \\
 \frac{6DAEI_0}{L^2}
 \end{bmatrix}
 =
 \begin{bmatrix}
 0 \\
 0 \\
 0 \\
 0 \\
 0
 \end{bmatrix}
 \quad 5.3-1$$

Equation 5.3-1 is a set of homogeneous equations for which a non-trivial solution exists when the determinant of the coefficient matrix equals zero. Again, because of the numerical complexities involved, the critical load was obtained by incrementing the applied load and testing for a zero value of the determinant. Once the critical load is found, the effective length can be calculated from equations 5.2-2. Figs. 5.16 to 5.24 contain graphs of the effective length factors for the case where "side-sway is permitted."

5.4 Comments on the Use of Effective Lengths

In the preceding discussion, it was assumed that buckling occurred only about the strong axis of the tapered member. However, if buckling occurs about the weak axis, then the K_y values for prismatic columns ($\gamma = 0$) should be used -- the members being essentially prismatic in the weak direction.

Since the effective length of a tapered column is related to the length of a prismatic pin-ended column by K_y , the A.I.S.C. design formulas for F_c and F_c' can be used where K_y is determined from Fig. 5.7 to 5.24.

The solution for the effective length assumed that the tapered columns in the rigid frame are restrained at their ends by prismatic beams. If, however, these beams are also tapered, then an equivalent stiffness for these beams should be used; i.e. the tapered beams can be thought of as prismatic beams having the same end stiffness. The stiffness at A of a tapered beam whose end B is held rotationally and positionally fixed is given by

$$K_y = \frac{M_A}{\delta_A} = \frac{EI_0}{l} \left[\frac{C_{BB}}{C_{AA}C_{BB} - C_{AB}^2} \right]$$

Reproduced from best available copy.

where C_{AA} , C_{BB} and C_{AB} are defined by 5.1-4, -5 and -6. Equating equation 5.4-1 to the stiffness of a prismatic beam with the far end held fixed, $(4EI_{eq}/L)$, and solving for the equivalent moment of inertia gives

$$I_{eq} = \frac{I_o L}{4E} = \frac{I_o}{4} \left[\frac{C_{BB}}{C_{AA}C_{BB} - C_{AB}^2} \right] \quad 5.4-2$$

The moment of inertia I_{eq} is used in the expression R_T in place of I_2 if the tapered beam is on top and similarly for R_B when such a situation exists at the base of the structure. The stiffness factor f_V can be obtained also from Fig. 5.3 to 5.6.

Reproduced from
best available copy. 

6. SUMMARY AND DESIGN EXAMPLE

This report has tried to cover all major aspects of the design of tapered frames; from total frame analysis - to stress analysis of individual members - to the development of tapered design formulas, though not in that order. Since descriptions and methodology of frame and stress analysis for members of variable cross-section can be found elsewhere, the primary objective of the report was to present the rationale behind the development of the design formulas.

To facilitate presentation and understanding, the authors have reviewed and extended the background for the calculation of theoretical critical loads for these types of members. Many cases were examined, and using these calculated solutions modification factors were determined by normal curve fitting techniques which allow application of the current prismatic (A.I.S.C.) design formulas. The resulting modified design formulas were compared to experimental results, and found to be conservative to the same degree as the current A.I.S.C. design formulas for prismatic members.

It is to be understood that the design formulas developed describe the gross behavior of isolated members. That is, the normal underlying assumption that members are adequately proportioned against local buckling must be made. Until further research is performed on this topic, sound engineering judgement based on experience using prismatic members must be exercised to ensure adequacy of cross-sectional proportions.

In the interaction formula, the computed and allowable axial stress are based on the smaller end properties. Whereas, the computed and allowable bending stress are based on the larger end properties. This is a

consequence of non-dimensionalizing equation 3.2-3 which was used in determining the maximum stress.

The uses of the suggested formulas are perhaps best illustrated by means of an example. It should be recognized, however, that the case selected is only for demonstration purposes and does not, in and of itself, describe a range of suggested application. The structure chosen is a portal frame with an overhang on one side. (See Fig. 6.1). Moreover, it is specified at the outset that the overhang and both of the columns are to be tapered, built-up members whereas the main beam is to be a prismatic, wide-flange section. All members are to be of A-36 steel.

The frame was analyzed by the slope-deflection method making use of the stiffness and carry-over factors contained in Fig. 5.3 to 5.6. The first assumption made was that all members are prismatic and are of same size. (It should be recognized that for the purposes of this analysis the overhang can be replaced by a moment and a shear). The slope-deflection equations (assuming that side-sway is prevented) can be solved in terms of the required moment of inertia. A 30 WF 132 section satisfies the design.

Next the columns are assumed to have a taper ratio of, say, one (that is, $\gamma = 1.0$). The frame analysis is repeated and the design formulas checked. At this point the prevented side-sway case was again solved to obtain the moment diagram shown in Fig. 6.2. The use of the design formulas will be illustrated by checking the member AB. The section properties can be calculated from the dimensions listed in Fig. 6.3.

The axial stress at the smaller end: $f_{a0} = \frac{P_{AB}}{A_0} = \frac{87.5}{23.6} = 3.7 \text{ ksi}$

The bending stress at the larger end: $f_{b1} = \frac{M_{AB}}{S_{x1}} = \frac{3880}{354} = 15.3 \text{ ksi}$

The Allowable Axial Stress: F_{ay}

$$\gamma = \frac{d_t - d_o}{d_o} = 1.0$$

$$C_c = \sqrt{\frac{2\pi^2 E}{F_y}} = 126 \text{ in.}$$

weak axis (treat as prismatic) $r_{yo} = 3.06 \text{ in.}$

$$K = 0.70, \quad \frac{Kl}{r_{yo}} = 44.0$$

strong axis--side-sway allowed, $r_{xo} = 5.33 \text{ in.}$

$$R_T = \frac{bI_o}{Ll_T} = \frac{60 \times 671}{16 \times 4919} = 0.51$$

$$R_D = \frac{bI_o}{Ll_B} = \frac{60 \times 671}{16 \times 0} = \dots$$

From Fig. 5.15 $K_y = 1.5$, and $\frac{K_y l}{r_{xo}} = 54.0 \text{ in.}$

The allowable axial stress is therefore

$$F_{ay} = \frac{\left[1.0 - \frac{\left(\frac{K_y l}{r_{xo}} \right)^2}{C_c^2} \right]}{F.S.} = 17.99 \text{ ksi}$$

The Allowable Bending Stress: F_{by}

Based on the compression flange and 1/3 of the web, $r_{To} = 3.19 \text{ in.}$

The moment gradient is $\alpha = 0$, thus the moment gradient coefficient is

given by

$$C_{by} = \frac{1.0}{1.0 + 0.25\sqrt{7}} = 0.80$$

The division between elastic and inelastic bending behavior is determined

from the formula

$$C_r = \sqrt{\frac{510000 C_{tw}}{F_y}} = 106 \text{ in.}$$

The length modification factors for bending are

$$h_w = 1.0 + 0.00395 \sqrt{\ell/r_{To}} = 1.03$$

and

$$h_s = 1.0 + 0.0230 \sqrt{\ell d_o/A_f} = 1.32$$

Since $h_w \ell/r_{To} = 62 < C_r$

$$F_{b_y} = \frac{2}{3} \left[1.0 - \frac{(h_w \ell/r_{To})^2}{2 C_r^2} \right] F_y = 21.6 \text{ ksi}$$

or

$$F_{b_y} = \frac{12000 C_{by}}{h_s \ell d_o/A_f} = 27.8 \text{ ksi} > 0.6 F_y = 22 \text{ ksi}$$

therefore, $F_{by} = 22 \text{ ksi}$.

Combined Stress

From the previous calculations

$$\left(\frac{f_a}{F_{ay}}\right)_o = .21 \text{ and } \left(\frac{f_b}{F_{by}}\right)_t = 0.71$$

Since $\alpha = 0$

$$C_m = 1.0 - 0.9 \left(\frac{f_a}{F_{ay}}\right)_o + 0.6 \left(\frac{f_a}{F_{ay}}\right)_o^2 = 0.94$$

$$\text{where } F'_{ey} = \frac{12\pi^2 E}{23 \left(\frac{\ell}{r_{yo}}\right)^2} = 51.1 \text{ ksi}$$

Thus

$$\left(\frac{f_a}{F_{ay}}\right)_o + \frac{C_m}{1 - \left(\frac{f_a}{F_{ay}}\right)_o} \left(\frac{f_b}{F_{by}}\right)_t = 0.21 + \frac{.940}{1.0 - 0.07} (0.71) = 0.93 < 1.0$$

The tapered column selected (with $\lambda^* = 1$) is acceptable. Application of the design formulas to the other members yields the final design, as shown in Fig. 6.3.

It is noted that, if axial force effect is to be included in the analysis of frames consisting of tapered members, the slope-deflection equations described in Section 5 may be used in an iterative procedure by utilizing the stiffness and carry-over factors given in Figs 5.3-5.6. Again, the axial force in tapered columns should be estimated as a ratio in terms of the Euler's buckling load based on the smaller end geometry, $(P_{ex})_c$.

Reproduced from
best available copy.



7. ACKNOWLEDGMENTS

The results reported herein are based on research studies carried out at the State University of New York at Buffalo. These were financially supported jointly by the Naval Facilities Engineering Command, American Institute of Steel Construction, American Iron and Steel Institute, the Metal Building Manufacturer's Association, and the State University of New York at Buffalo. Technical guidance to the project was provided by the joint WRC-CRC subcommittee on Tapered Members of which Dr. A. Amirikian is Chairman. The subcommittee members are: Messrs. A. Amirikian, J. H. Adams, D. J. Butler, T. R. Higgins, R. L. Ketter, K. H. Koopman, W. A. Milek, L. W. Lu, G. C. Lee, N. W. Rimmer, A. Toprac, I. Viest. Messrs. Ronald Friend, H. H. Lee and Yasuo Tada, formerly graduate research assistants in the Department of Civil Engineering, State University of New York at Buffalo, made significant contributions to the investigation.

8. REFERENCES

1. Amirikian, A., "Wedge-Beam Framing," Trans. ASCE, Vol. 117, 1952, p. 596.
2. Lee, G. C. and Morrell, M. L., "Finite Element Analysis of Space Frames of Thin-Walled Members," Civil Engineering Research Report, SUNYAB, Oct. 1971.
3. Lee, L. H. N., "On the Lateral Buckling of Tapered Narrow Rectangular Beams," J. Appl. Mech. V. 26, Sept. 1959, pp. 457-458.
4. Boley, B. A., "On the Accuracy of the Bernoulli-Euler Theory for Beams of Variable Section," J. Appl. Mech. V. 30, Sept. 1963, pp. 373-378.
5. Lee, G. C. and Szabo, B. A., "Torsional Response of Tapered I-Girders," J. Struct. Div. ASCE, V. 93, No. ST 5, Oct. 1967, pp. 233-252.
6. Bleich, F., Buckling Strength of Metal Structures, McGraw-Hill, 1952.
7. Venkayya, V. B., "Lateral Stability of Non-Prismatic Continuous Beams," Dissertation Abstracts, V. XXIII:2, Ph.D. Thesis, Univ. of Ill. 1962, 98 pp., Univ. Microfilm Serv., No. 62-2986.
8. Lee G. C. and Ketter, R. L., "Residual Stresses in Welded Tapered Shapes," C.E. Research Report SUNYAB, Sept. 1971.
9. Krefeld, W. J., Butler, D. J., and Anderson, G. B., "Welded Cantilever Wedge Beams," Welding Journal Research Supplement, Vol. 38, No. 3, March 1959.
10. Butler, D. J. and Anderson, G. B., "The Elastic Buckling of Tapered Beam-Columns," Welding Journal Research Supplement, Vol. 42, No. 1, Jan. 1963.
11. Butler, D. J., "Elastic Buckling Tests on Laterally and Torsionally Braced Tapered I-Beams," Welding Journal Research Supplement, Vol. 45, No. 1, Jan. 1966.
12. Prawel, S. P., Morrell, M. L. and Lee, G. C., "Bending and Buckling Strength of Tapered Structural Members," paper to be published in Experimental Mechanics.
13. Lee, H. H., "Factor of Effective Length for Tapered Columns," Civil Engineering Project Report, SUNYAB, 1970.

ADDITIONAL LITERATURE

14. Abbassi, M. M., "Buckling of Struts of Variable Bending Rigidity," J. Appl. Mech., V. 25, Dec. 1958, pp. 537-540.
15. Abbassi, M. M., "The Second Approximation for Buckling Loads of Tapered Struts," J. Appl. Mech., V. 27, Mar. 1960, pp. 211-212.
16. Anonymous, "Useful Charts for Tapered Beams," Engineering, London, V. 186, No. 4871, Aug. 28, 1959, p. 108.
17. Appl, F. M. and Smith, J. O., "Buckling of Inelastic Tapered Pin-Ended Columns," Engineering Mechanics Div. J., V. 94, April 1968.
18. Bazant, Z. P., "Non-Uniform Torsion of Thin-Walled Bars of Variable Section," Publ's. Int. Assoc. for Bridge & Struct. Engng., V. 25, 1965, pp. 17-39.
19. Boley, B. A. and Zimnoch, V. P., "Lateral Buckling of Non-Uniform Beams," J. Aeronautical Sciences, Vol. 19, No. 8, Aug. 1952, p. 567.
20. Botizan, "The Generalization of Takabeya's Method for the Analysis of Multi-Story Frames with Members of Variable Section," Acier-Stahl-Steel, V. 33, No. 10, Oct. 1968, pp. 437-444.
21. Cram, A. A. and Hall, A. S., "Influence Lines for Non-Uniform Continuous Beams," Civil Engr. Trans., Australia, V. CR6, No. 1, Mar. 1964, pp. 25-28.
22. Cranch, E. T. and Adler, A. A., "Bending Vibration of Variable Section Beams," J. Appl. Mech., V. 23, March 1956, pp. 103-108.
23. Culver, C. G. and Preg, S. M. Jr., "Elastic Stability of Tapered Beam-Columns," J. Struct. Div. ASCE, V. 94, No. St2, Feb. 1968, pp. 455-470.
24. Cywinski, Z., "Theory of Torsion of Thin-Walled Bars with Variable Rigidity," Archiv. Inzynieru Ladovej, Vol. 10, No. 2, 1964, p. 161.
25. Desay, Prakash, "Determination of Buckling Load for Columns with Varying Section - An Approximate Easy Procedure for Certain Cases," The Structural Engineer, V. 45, No. 6, June 1967, pp. 205-209.
26. Diwa, A. F. S., "Three Moment Equation for Variable Depth Beams," J. Struct. Div. ASCE, V. 90, No. ST6, Dec. 1964, pp. 149-169.
27. Fleming, J. F., Podolny, W. Jr. and Rile, T. S., "Drift Study of Tapered Frameworks," Civil Eng. ASCE, Aug. 1967, pp. 38-41.

28. Fling, R. S., "Tapered Girders Cut Gym Cost," Eng. News-Record, New York, March 19, 1968, pp. 148-150.
29. Fogel, C. M. and Ketter, R. L., "Elastic Strength of Tapered Columns," J. Struct. Div. ASCE, V. 88, ST5, Oct. 1962, Proc. 3301, pp. 67-106.
30. Fok, T. D. Y. and Mosure, T. F., "Analysis of Non-Prismatic Continuous Structures," J. Struct. Div. ASCE, V. 92, No. ST1, Feb. 1966, pp. 1-10.
31. Fok, T. D. Y., "Formulas for Deflections of Cantilever Beam with Variable Section," Civil Engineering ASCE, V. 28, No. 10, Oct. 1958, p. 763.
32. Frisch-Fay R., "The Buckling of Struts with Varying Cross Sections," J. Inst. of Engrs., Australia, V. 31, March 1959, pp. 81-83.
33. Gaines, J. H. and Volterra, E., "Upper and Lower Frequencies of Tapered Beams," J. Engng. Mech. Div., ASCE, V. 94, No. EM2, April 1968, pp. 465-488.
34. Gatewood, B. E., "Buckling Loads for Beams of Variable Cross Section under Combined Loads," J. Aeronautical Sciences, Vol. 22, No. 4, April 1955, p. 281.
35. Gere, J. M., "Moment Distribution Factors for Tapered Beams," Civil Eng., ASCE, V. 28, No. 7, July 1958, pp. 597-598.
36. Gere, J. M. and Carter, W. O., "Critical Buckling Loads for Tapered Columns," J. Struct. Div. ASCE, V. 88, ST1, Feb. 1962, Proc. 3045, pp. 1-11.
37. Ghani, A. F. M. R. A., "Shakedown Analysis of Non-Prismatic Beams," Dissertation Abstracts, V. 27:6(B), Sc. D. Thesis, Washington Univ., 1966, Univ. Microfilm Serv. No. 66-11, 886, 133 pp.
38. Girijavallabhan, C. V., "Buckling Loads of Non-Uniform Columns," J. Struct. Div. ASCE, V. 95, No. ST11, Nov. 1969, pp. 2419-2431.
39. Gordon, A., "Deflections with Varying Moment of Inertia," Civil Eng. ASCE, V. 25, No. 2, Feb. 1955, pp. 98-100.
40. Hamzani, H. H., "Plastic Analysis of Non-Prismatic Members," Dissertation Abstracts, V. XVIII; 4, Ph.D. Thesis, Stanford Univ., 1958, 146 p., Univ. Microfilm Service No. 58-1290.

41. Hartmann, A. J., "Elastic Lateral Buckling of Continuous Beams," J. Structural Div. ASCE, Vol. 93, No. ST4, Aug. 1967, p. 11.
42. Harvey, J. W., "Buckling Loads for Stepped Columns," J. Struct. Div. ASCE, V. 90, No. ST2, April 1964, pp. 201-222.
43. Heidebrecht, A. C., "Vibration of Non-Uniform Simply-Supported Beams," J. Engng. Mech. Div. ASCE, V. 93, No. EM2, April 1967, pp. 1-15.
44. Hope-Jones, E. F., "Deflection of a Non-Uniform Beam," Proc. Inst. Civil Engr. London, V. 31, June 1965, pp. 154-158.
45. Housner, G. W. and Keightley, W. O., "Vibrations of Linearly Tapered Cantilever Beams," J. Engr. Mech. Div. ASCE, V. 88, No. EM2, April 1962, pp. 95-103.
46. Jenkins, W. M., "Influence Line Computation for Structures with Members of Varying Flexural Rigidity Using Electronic Digital Computer," Structural Engr. London, V. 39, No. 9, Sept. 1961, pp. 269-276.
47. Jones, G., "Using the Column Analogy to Determine Moment Distribution Factors for Non-Prismatic Members," Civ. Engr. & Publ. Works Rev., London, V. 60, No. 710, Sept. 1965, pp. 1303-1305.
48. Krishnaswamy, K. T., "Method for Determining Deflections in Beams of Variable Stiffness," J. Amer. Concrete Inst., V. 60, No. 1, Jan. 1963, pp. 157-160.
49. Krynicki, E. J. and Mazurkiewicz, E. Z., "Frames of Solid Bars of Varying Cross Section," J. Struct. Div. ASCE, V. 90, No. ST4, Aug. 1964, pp. 45-174.
50. Larnach, W. J., "The Analysis of Vierendeel Frames and Girders with Non-Prismatic Members," Civ. Engr. & Publ. Works Rev., London, V. 56, No. 661, Aug. 1961, pp. 1045-1048.
51. Lightfoot, E., "The Elastic Analysis of Open Frame Cantilevers and Girders of Variable Depth," Civil Engr. & Public Works Rev., London, V. 53, No. 629, Nov. 1958, pp. 1275-1277; V. 53, No. 630, Dec. 1958, pp. 1411-1412.
52. Lin, K. H., Rossow, E. C. and Lee, S. L., "Inelastic Stability of Tapered Web Columns," Publ's, Int'l. Assoc. for Bridge & Struct. Engng., V. 28-II, 1968, pp. 113-136.

53. Massey, P. C., "The Lateral Stability of a Non-Prismatic Beam," Building Science, Vol. 2, 1967, p. 273.
54. Ondra, O., "The Determination of Moment Distribution Constants of Members with a Variable Moment of Inertia," Dissertation Abstracts, V. XVI:2, Ph.D. Thesis, Lehigh Univ., 1955, 137 p., Univ. Microfilm Serv. No. 15,332.
55. Ormerod, A., "Moment Distribution Factors for Members with Change of Cross-Sections," Concrete & Constr. Engineering, V. 56, No. 4, April 1961, pp. 153-158.
56. Ormerod, A., "Calculation of Critical Loads for Struts of Non-Uniform Section," Civ. Engr. & Publ. Works Rev., London, V. 53, No. 630, Dec. 1958, pp. 1387-1388.
57. Ormerod, A., "Bending Moments in Pin-Ended Struts of Variable Section," Civ. Engr. & Publ. Works Rev., London, V. 54, No. 633, March 1959, pp. 333-334.
58. Otakar, Ondra, "Deflection and Slope of Beams with Varying I," J. Struct. Div. ASCE, V. 89, No. ST1, Feb. 1963, pp. 25-48.
59. Petcu, V., "A Method for Determining Deflections in Beams of Variable Stiffness," J. Amer. Concrete Inst., V. 61, No. 2, Feb. 1964, pp. 239-243.
60. Pei, M. L., "Matrix Solution of Beam with Variable Moments of Inertia," J. Struct. Div. ASCE, V. 85, ST8, Oct. 1959, Proc. 2218, pp. 1-14.
61. Pschunder, R. J., "Tapered Twoers with Variable Wall Thickness," J. Struct. Div. ASCE, V. 93, No. ST5, Oct. 1967, pp. 515-531.
62. Robertson, J. C., "The Lateral Stability of Beam of Non-Uniform Cross Section," Dissertation Abstracts, V. 24:3, Ph. D. Thesis, Stanford Univ. 1963, Univ. Microfilm Serv. No. 63-6444, 97 pp.
63. Rogers, B. G. and Munse, Jr., W. H., "Plastic Analysis and Design of Non-Prismatic Members," J. Struct. Div. ASCE, V. 90, No. ST5, Oct. 1965, pp. 299-324.
64. Sanko, F. and Willcock, B. K., "Computer Analysis of Bridge Having Varying Section Properties," The Structural Engineer, V. 45, No. 11, Nov. 1967, pp. 395-400.
65. Shou-ling, W., "Flexural Calculation of Non-Uniform Members," J. Struct. Div. ASCE, V. 89, No. ST6, Dec. 1963, pp. 271-295.

66. Smith, R. B., "Design Charts for Symmetrically Haunched Members," Civil Eng. ASCE, Aug. 1965, p. 72.
67. Strauss, M. W., "Design Constants for Beams of Variable Section," J. Amer. Concrete Inst., V. 27, No. 8, April 1956, pp. 839-849.
68. Srinivasan, A. V., "Buckling Load of Bars with Variable Stiffness: A Simple Numerical Method," J. Amer. Inst. Aeronautics & Astronautics, V. 2, No. 1, Jan. 1964, pp. 139-140.
69. Sami, S., "Continuous Girder Bridge with Variable Moment of Inertia," J. Struct. Div. ASCE, V. 86, ST1, Jan. 1960, Proc. 2346, pp. 19-39.
70. Kitipornchai, S. and Trahair, N. S., "Elastic Stability of Tapered I-Beams," C.E. Res. Rept. No. R166, Univ. of Sydney, March 1971.
71. Vickery, B. J., "The Behavior at Collapse of Simple Steel Frames with Tapered Members," Struct. Engr., London, V. 40, No. 11, Nov. 1962, pp. 365-376.
72. Wang, Shou-ling, "Flexibility of Axially-Loaded Non-Uniform Members," J. Struct. Div. ASCE, V. 92, No. ST2, April 1966, pp. 195-205.
73. Wilde, P., "The Torsion of Thin-Walled Bars with Variable Cross-Section," Archiwum Mechaniki Stosowanej, April 20, 1968, p. 431.
74. Wright, W., "Critical Loads for Non-Uniform Pin-Ended Columns," Civil Engr. & Publ. Works Rev., Feb. 1968, pp. 185-187.

FIGURE CAPTIONS

- Fig. 2.1 Wedge-Beam Framing Examples [1]
- 2.2 Channel Section with Linearly Tapered Web
- (a) Locus of Shear Centers
 - (b) Load Applied at the Smaller End Shear Center Parallel to the Web
 - (c) Load Applied at the Smaller End Shear Center Perpendicular to the Web
- 3.1 Tapered Beam Geometry Used for Analysis in Section 3
- 3.2 Loading Presumed for Analysis in Section 3
- 3.3 Functions which satisfy the Boundary Conditions for Use with Power Series Solutions
- 3.4(a) Section Properties at the Smaller End
- (b) Parameters Used to Examine Lateral Stability
 - (c) Limiting End-Moment Ratios "k"
- 3.5 Lateral Buckling Solutions for Section I, $\ell = 144$ and $\alpha = +k$
- (a) Pure Bending: $e = \infty$, $\lambda_{cr} = M_c / P e_y \cdot d_o$
 - (b) Bending plus Axial Thrust: $e = d_o$, $\lambda_{cr} = P / P e_y$
- 4.1 Definition of the Length Modification Factor "g" for Columns
- 4.2 Values of Length Modification Factors "g"
- 4.3 Comparison of "Exact" Strong-Axis Buckling Stress to Equation 4.1-3. Values greater than Unity are Conservative
- 4.4 Allowable Axial Compressive Stress
- 4.5 Definition of the Length Modification Factor "h" for Beams

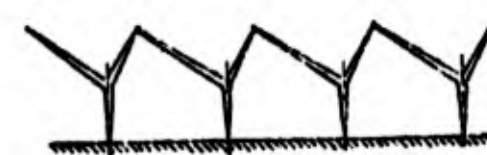
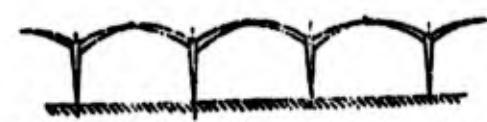
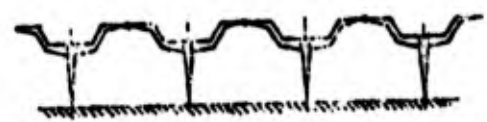
Reproduced from
best available copy.



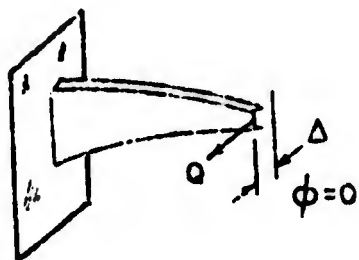
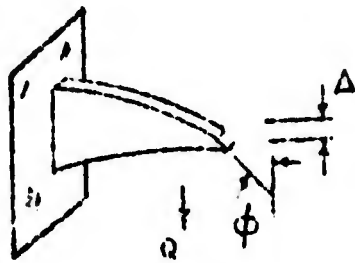
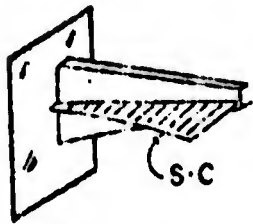
- 4.6 Critical Elastic Stresses Due to Bending
- 4.7 Comparison of Accuracy of Results for Lateral Buckling Stresses of Beams
- 4.8 Allowable Bending Stress for Thin, Deep Smaller End Cross Sections $C_{bY} = 1.0$
- 4.9 Allowable Bending Stress for Thick, Shallow Smaller End Cross Sections $C_{bY} = 1.0$
- 4.10 Values of Interaction Equation Term " C_2 "
- 4.11 Comparison of "Exact" $\left(\frac{M}{S_y}\right)l$ to $\left(\frac{M}{S_y}\right)l$ given by Eq. 4.3-1. Values Greater than Unity are Conservative
- 4.12 Comparison of Design Formulas to Columbia Test Results [10]
- 4.13 Comparison of Design Formulas to Buffalo Test Results [12]
- 5.1 Structural Models Used for the Determination of the Effective Length Factors of Tapered Columns in Frames
- 5.2 Sign System for the Slope-Deflection Equation of Tapered Members
- 5.3 Stiffness Factors: Small End Fixed
- 5.4 Stiffness Factors: Large End Fixed
- 5.5 Carry-Over Factors: Small End Fixed
- 5.6 Carry-Over Factors: Large End Fixed
- 5.7-5.15 Effective Length Factors for Tapered Columns: Side-Sway Prevented - $\gamma = 0, 0.5, 1.0, 1.5, 2.0, 3.0, 4.0, 5.0,$ and 6.0
- 5.16-5.24 Effective Length Factors for Tapered Columns: Side-Sway Permitted - $\gamma = 0, 0.5, 1.0, 1.5, 2.0, 3.0, 4.0, 5.0,$ and 6.0
- 6.1 Frame Example
- 6.2 Moment Diagram
- 6.3 Dimensions of Members for Final Design

Reproduced from
best available copy.

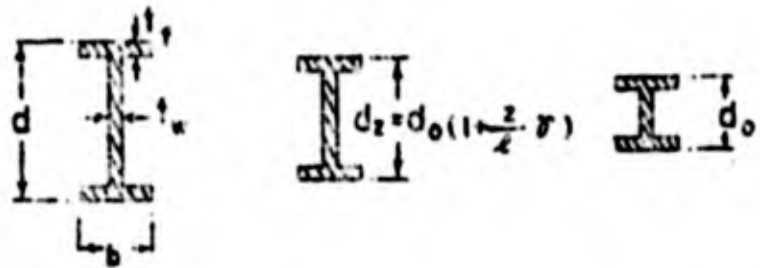
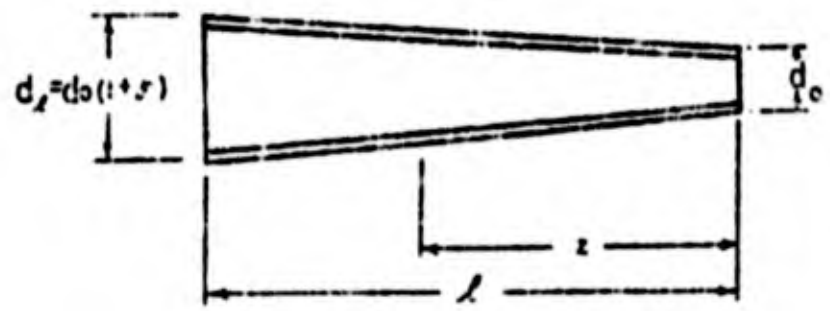


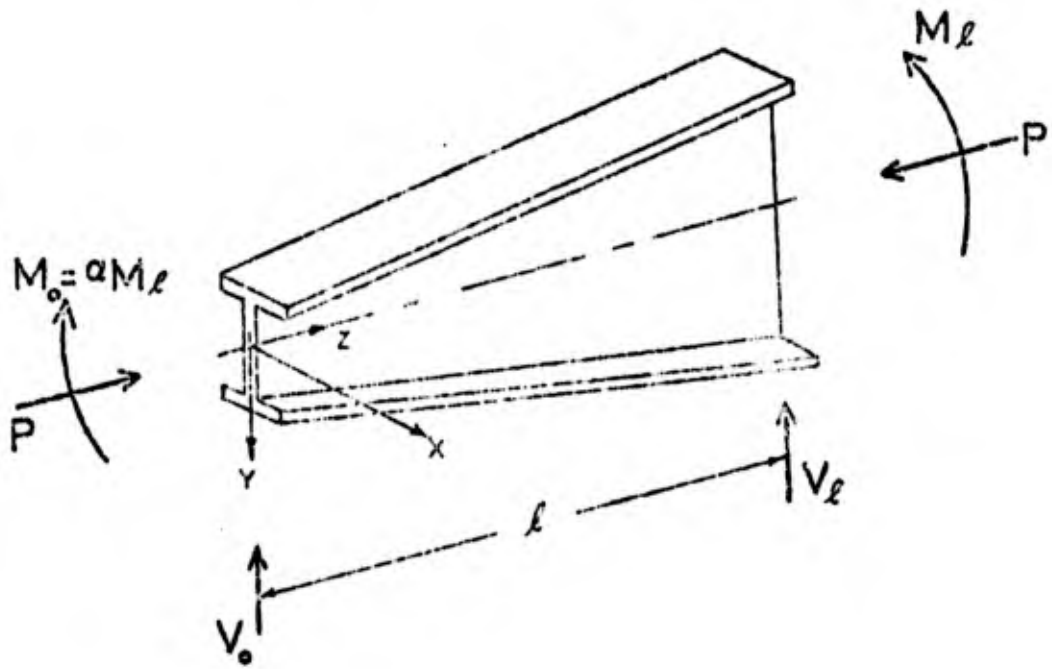


50



625




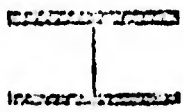

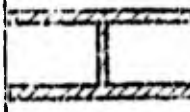



Boundary Conditions		$f(z), g(z), h(z)$
$z = 0$	$z = l$	
Clamped	Clamped	$z^2(z-l)^2$
Clamped	Simply Supported	$z^2(z-l)$
Simply Supported	Simply Supported	$z(z-l)$
Clamped	Free	z^2

Reproduced from
best available copy.



Fig. 3.3 - Functions which will satisfy the boundary conditions for use with power series solutions

	I	II	III	IV	V
					
d_o	6.00 in	6.00 in	6.00 in	6.00 in	12.00 in
b	4.00	12.00	4.00	12.00	6.00
t_f	0.25	0.25	0.75	0.75	0.25
t_w	0.10	0.10	0.25	0.25	0.10

l	96 in. ,	144 in. ,	192 in. ,	240 in.	
α	+1 ,	+k ,	0 ,	-k ,	-1
γ	0 ,	1.0 ,	1.5 ,	2.0 ,	3.0
$\frac{e}{d_o}$	0.5 ,	1.0 ,	2.0 ,	5.0 ,	∞

Fig. 3.4 (c) - Limiting end - moment ratios, "k"

γ	Section I	Section II	Section III	Section IV
0	1.000	1.000	1.000	1.000
1.0	0.460	0.485	0.468	0.488
1.5	0.354	0.382	0.363	0.386
2.0	0.284	0.314	0.293	0.318
3.0	0.196	0.229	0.208	0.233

Lateral-Torsional Buckling
 Section I, $L = 14\frac{1}{2}$ inches

VALUES OF λ

Pure Bending

γ	α	Number of Terms in Power Series					
		4	5	6	7	8	9
0	+1.0	0.8980	0.7866	0.7798	0.7760	0.7736	0.7720
	+0.5	1.0476	1.0261	1.0191	1.0152	1.0125	1.0108
	0	1.5799	1.3655	1.3604	1.3554	1.3517	1.3510
	-0.5	1.6967	1.6875	1.6812	1.6747	1.6719	1.6701
	-1.0	1.6022	1.5903	1.5754	1.5652	1.5606	1.5577
2.0	+1.0	1.1831	1.1557	1.1416	1.1337	1.1287	1.1253
	+0.5	1.7213	1.6831	1.6675	1.6580	1.6517	1.6474
	0	2.7797	2.7175	2.7058	2.6961	2.6896	2.6853
	-0.5	3.7147	3.5236	3.5005	3.4799	3.4695	3.4634
	-1.0	2.4694	2.2484	2.1953	2.1711	2.1587	2.1512

Bending Plus Axial Thrust $(e/d_o) = 1.0$

0	+1.0	0.5211	0.5061	0.5013	0.4986	0.4969	0.4958
	+0.5	0.6096	0.5934	0.5884	0.5854	0.5835	0.5823
	0	0.7110	0.6946	0.6894	0.6859	0.6833	0.6824
	-0.5	0.7954	0.7769	0.7706	0.7664	0.7640	0.7624
	-1.0	0.7826	0.7651	0.7563	0.7512	0.7485	0.7467
2.0	+1.0	0.6328	0.6151	0.6080	0.6040	0.6014	0.5997
	+0.5	0.7491	0.7286	0.7210	0.7166	0.7128	0.7118
	0	0.8900	0.8636	0.8554	0.8504	0.8473	0.8451
	-0.5	0.9858	0.9469	0.9364	0.9293	0.9265	0.9240
	-1.0	0.8952	0.8534	0.8407	0.8341	0.8300	0.8274

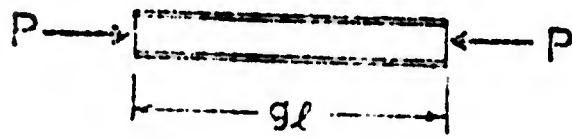
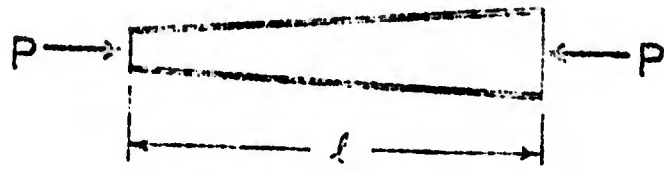


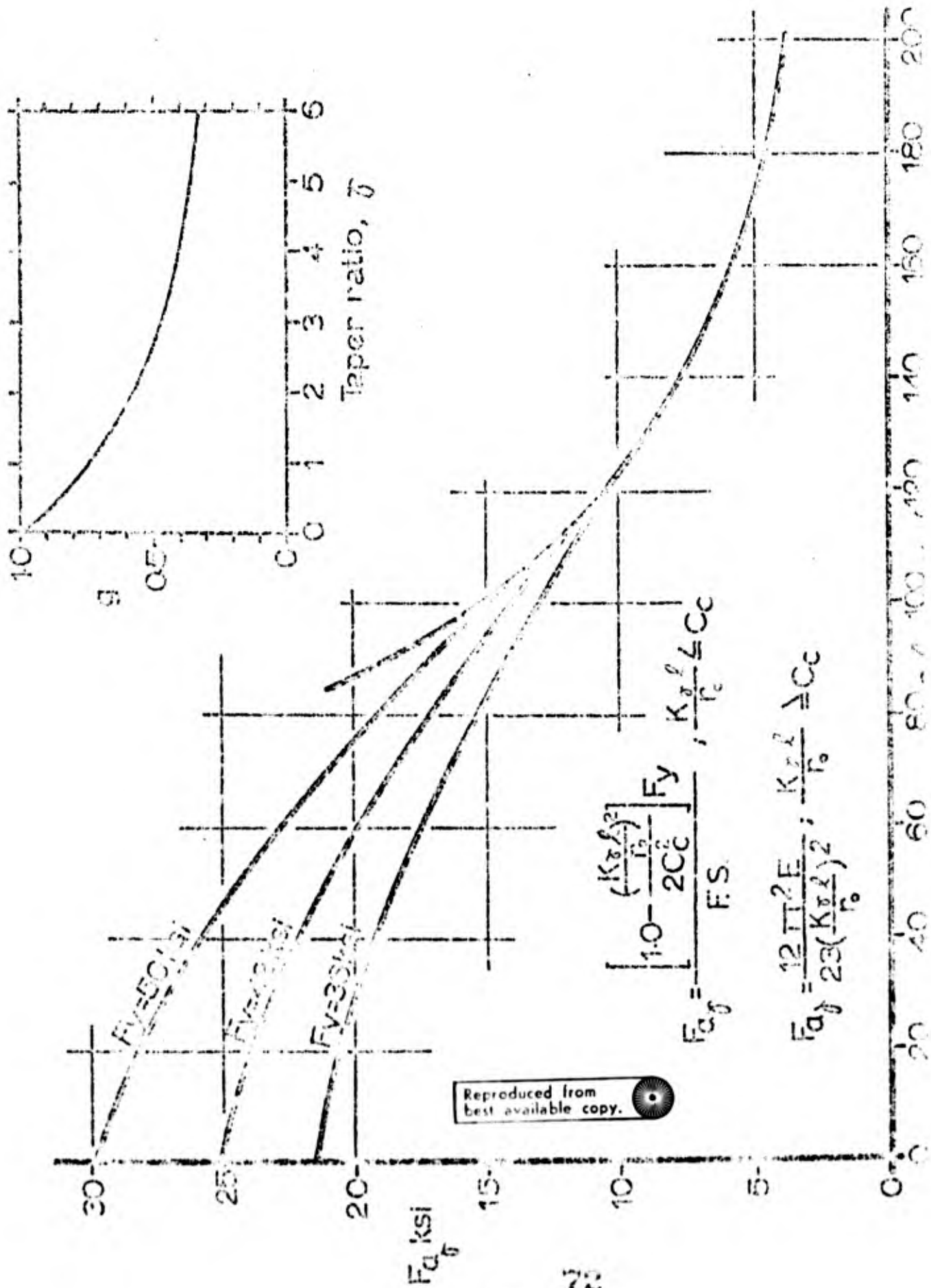
Fig. 4.2 - Values of length modification factors for strong-axis buckling, "g"

γ	ϵ	γ	ϵ
0	1.000	3.2	0.453
0.2	0.937	3.4	.447
0.4	.879	3.6	.436
0.6	.826	3.8	.427
0.8	.777	4.0	.418
1.0	.733	4.2	.410
1.2	.696	4.4	.402
1.4	.656	4.6	.394
1.6	.623	4.8	.386
1.8	.593	5.0	.377
2.0	.567	5.2	.368
2.2	.543	5.4	.359
2.4	.522	5.6	.347
2.6	.503	5.8	.334
2.8	.486	6.0	.320
3.0	.471		

γ	SECTIONS			
	I	II	III	IV
0	1.00	1.00	1.00	1.00
0.5	0.99	1.00	0.99	1.00
1.0	1.00	1.01	1.00	1.01
1.5	0.99	1.01	1.00	1.01
2.0	0.97	0.99	0.98	0.99
2.5	0.96	0.97	0.96	0.98
3.0	0.95	0.98	0.97	0.98

Reproduced from
best available copy.

Fig. 4.3 - Comparison of "exact" strength-to buckling stress to equation 4.1-3. Values greater than unity are conservative



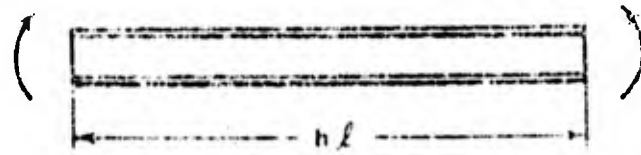
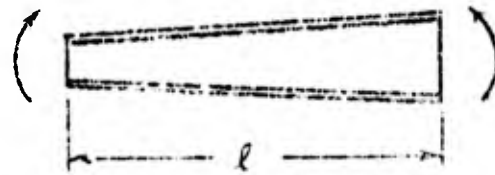


Fig. 4.6 - Critical elastic stresses due to bending

Section I $d_o = 6''$, $b = 4''$, $t_f = \frac{1}{8}''$, $t_w = 1/10''$

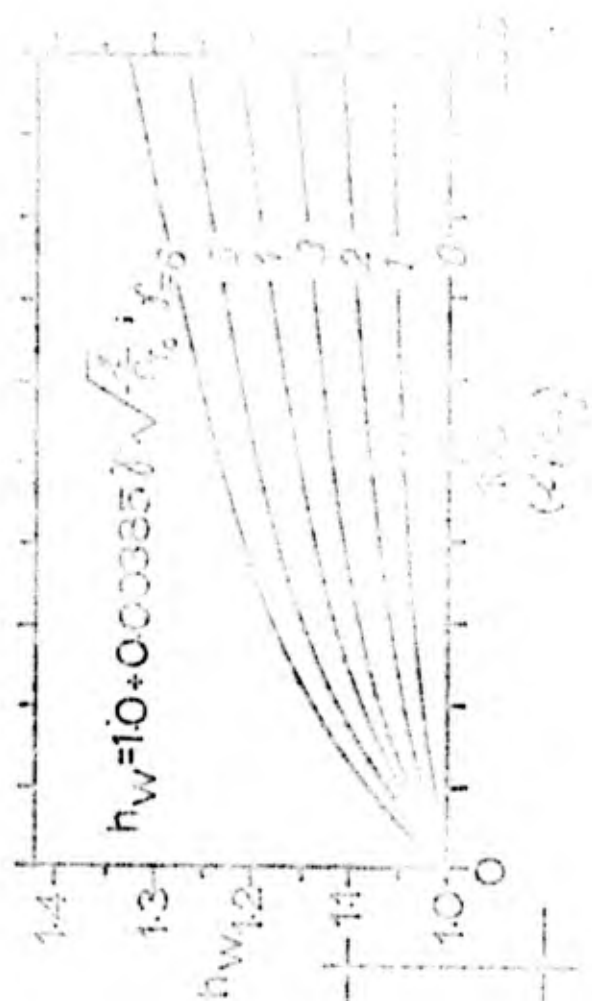
l	96"	144"	192"	240"	288"	336"	384"	432"
l/r_{T_o}	91	136	181	226	272	317	362	407
$\frac{ld_o}{\Delta f}$	576	865	1150	1440	1730	2016	2304	2592
0 ($k = 1.0$)	54.0	29.5	20.1	15.3	12.4	10.4	8.9	7.9
1 ($k = .460$)	47.2	23.8	15.3	11.2	8.7	7.2	6.1	5.3
2 ($k = .284$)	45.2	21.9	13.5	9.5	7.2	5.8	4.8	4.1
3 ($k = .198$)	44.5	21.0	12.6	8.6	6.4	5.0	4.1	3.4

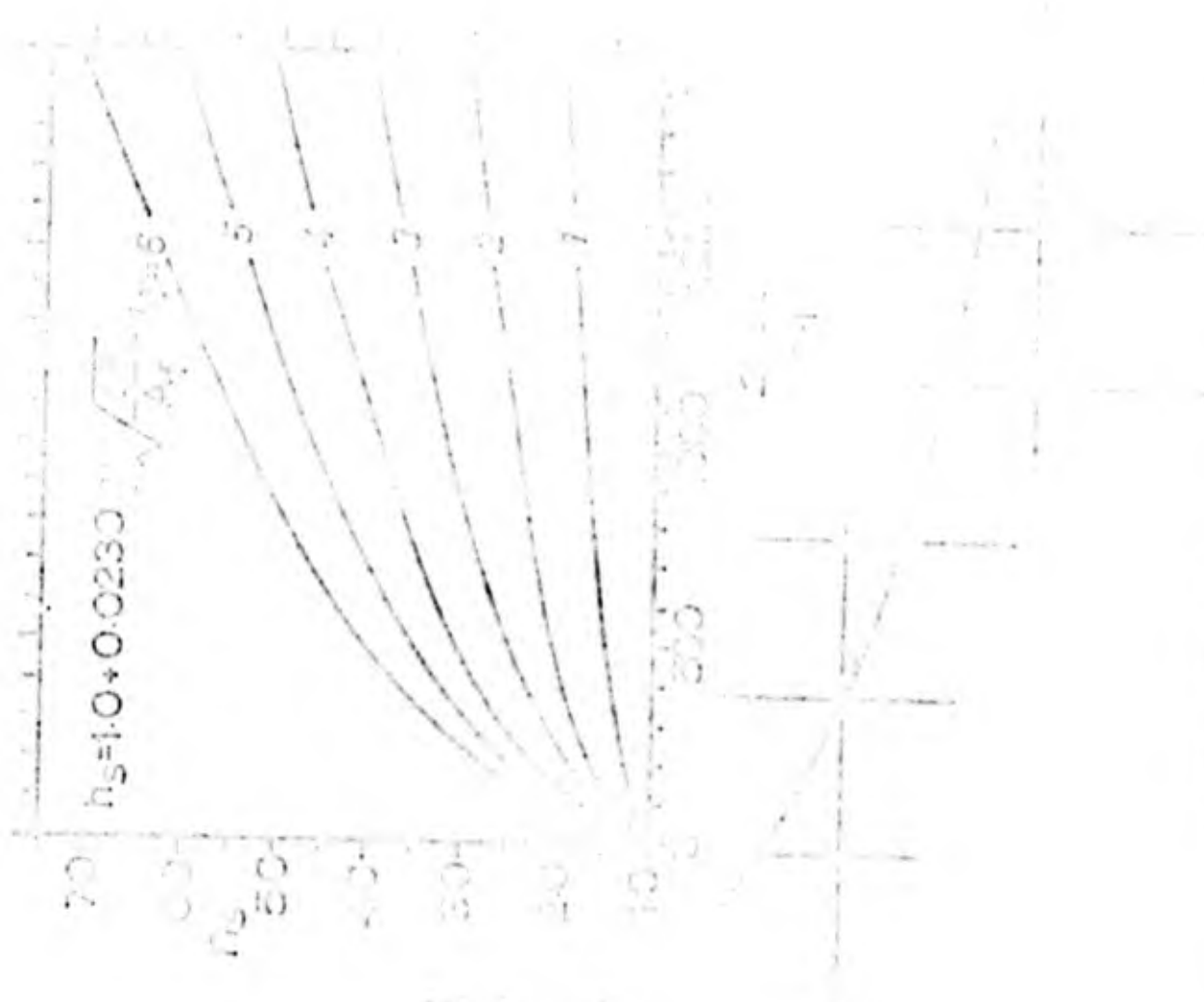
Section III $d_o = 6''$, $b = 4''$, $t_f = 3/4''$, $t_w = \frac{1}{8}''$

l	96"	144"	192"	240"	288"	336"	384"	432"
l/r_{T_o}	89	134	179	223	268	312	357	401
$\frac{ld_o}{\Delta f}$	192	288	384	480	576	672	768	864
0 ($k = 1.0$)	133.0	86.0	63.5	50.5	41.9	35.8	31.4	27.8
1 ($k = .468$)	94.0	57.0	41.0	32.2	26.4	22.4	19.5	17.3
2 ($k = .294$)	77.5	44.0	30.6	23.3	18.9	15.9	13.7	12.1
3 ($k = .208$)	68.5	37.2	24.9	18.6	14.8	12.3	10.5	9.2

Section V $d_o = 12''$, $b = 6''$, $t_f = \frac{1}{2}''$, $t_w = 1/10''$

l	96"	144"	192"	240"	288"	336"	384"	432"
l/r_{T_o}	62	93	124	155	186	216	248	278
$\frac{ld_o}{\Delta f}$	768	1150	1540	1920	2300	2690	3070	3450
0 ($k = 1.0$)	92.6	42.9	25.4	17.3	12.8	10.0	8.2	6.8
1 ($k = .448$)	87.6	39.8	23.0	15.3	11.0	8.4	6.7	5.5
2 ($k = .271$)	86.6	39.1	22.3	14.6	10.4	7.8	6.2	5.0
3 ($k = .186$)	86.1	38.6	21.9	14.2	10.0	7.5	5.8	4.7





$\frac{P}{(P_{x_0})_E}$	0	0.1	0.2	0.3	0.4	0.5	0.6	0.7	0.8	0.9	1.0
+1.0	1.000	1.126	1.290	1.510	1.813	2.250	2.920	4.037	6.360	13.330	*
+0.9	1.000	1.111	1.258	1.459	1.739	2.145	2.773	3.844	6.024	12.637	*
+0.8	1.000	1.097	1.229	1.410	1.667	2.054	2.631	3.633	5.694	11.951	*
+0.7	1.000	1.084	1.201	1.365	1.600	1.945	2.494	3.438	5.372	11.274	*
+0.6	1.000	1.072	1.174	1.322	1.556	1.856	2.363	3.244	5.058	10.605	*
+0.5	1.000	1.060	1.156	1.281	1.475	1.760	2.238	3.056	4.750	9.944	*
+0.4	1.000	1.050	1.127	1.244	1.418	1.686	2.117	2.875	4.450	9.291	*
+0.3	1.000	1.041	1.107	1.209	1.365	1.603	2.002	2.700	4.156	8.646	*
+0.2	1.000	1.032	1.088	1.176	1.315	1.534	1.893	2.532	3.870	8.003	*
+0.1	1.000	1.025	1.070	1.147	1.265	1.465	1.789	2.369	3.592	7.381	*
0	1.000	1.018	1.055	1.120	1.227	1.400	1.690	2.213	3.320	6.760	*
-0.1	1.000	1.012	1.041	1.096	1.183	1.340	1.597	2.084	3.056	6.148	*
-0.2	1.000	1.007	1.030	1.074	1.153	1.284	1.509	1.920	2.798	5.543	*
-0.3	1.000	1.003	1.020	1.055	1.121	1.233	1.426	1.783	2.546	4.947	*
-0.4	1.000	1.000	1.011	1.040	1.093	1.186	1.349	1.652	2.306	4.359	*
-0.5	1.000	1.000	1.005	1.024	1.063	1.144	1.278	1.528	2.070	3.779	*
-0.6	1.000	1.000	1.003	1.016	1.048	1.105	1.211	1.410	1.842	3.207	*
-0.7	1.000	1.000	1.000	1.008	1.020	1.073	1.150	1.298	1.620	2.643	*
-0.8	1.000	1.000	1.000	1.003	1.017	1.054	1.095	1.192	1.406	2.037	*
-0.9	1.000	1.000	1.000	1.000	1.007	1.020	1.045	1.093	1.200	1.540	*
-1.0	1.000	1.000	1.000	1.000	1.000	1.000	1.000	1.000	1.000	1.000	*

Fig. 4.10 - Values of interaction equation magnification term " C_E "

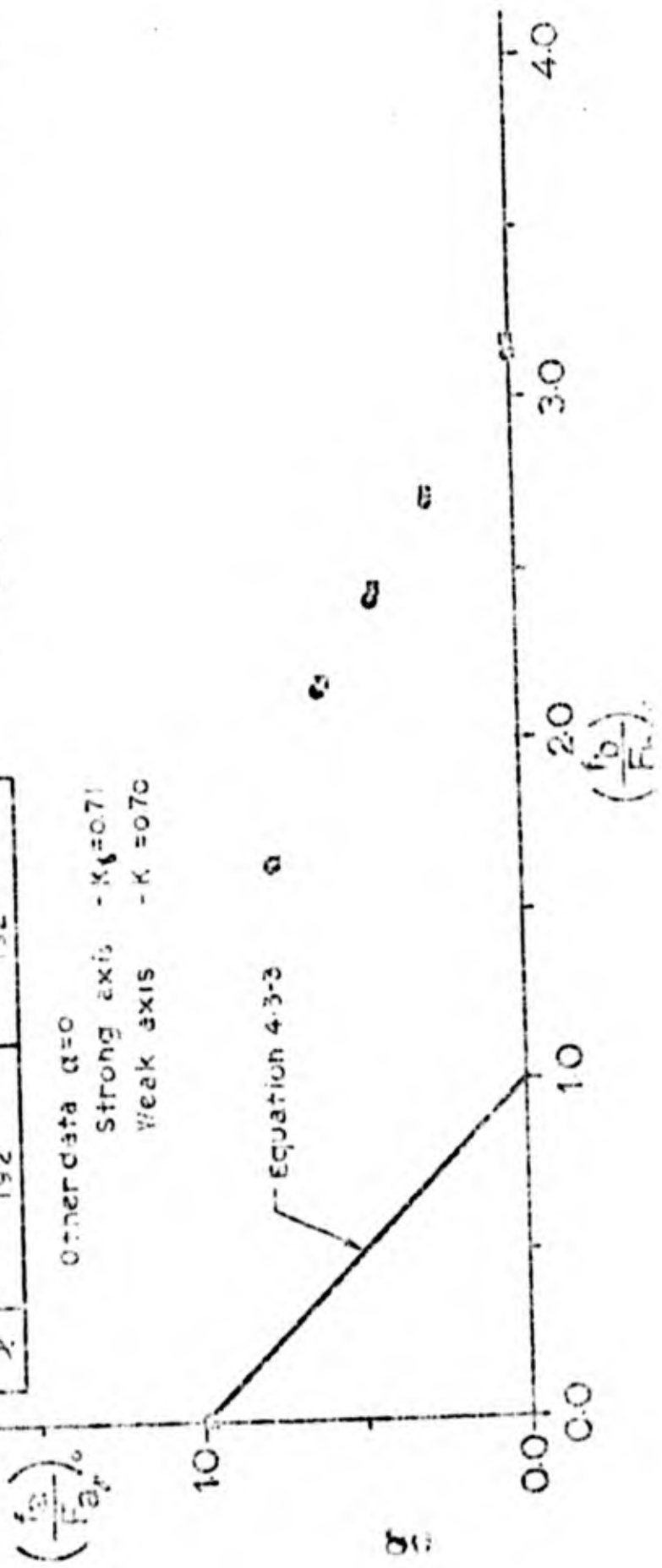
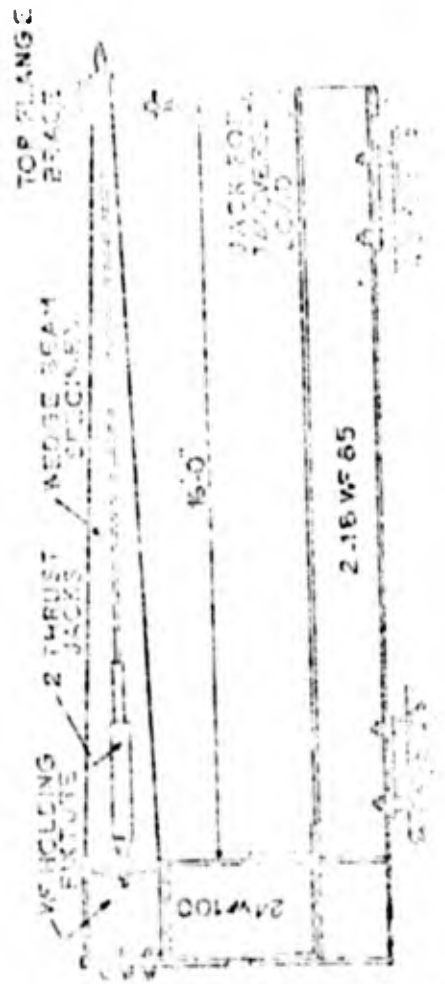
Reproduced from
best available copy.

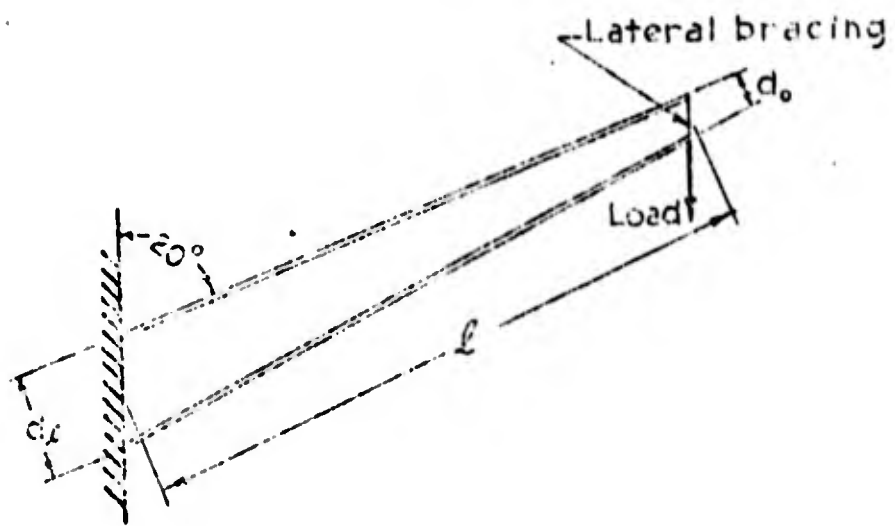
Section I	Section II					Section III					Section IV									
	$(\sqrt{1/2})_c$					$(\sqrt{1/2})_c$					$(\sqrt{1/2})_c$					$(\sqrt{1/2})_c$				
	0	0.5	1.0	1.5	2.0	0	0.5	1.0	1.5	2.0	0	0.5	1.0	1.5	2.0	0	0.5	1.0	1.5	2.0
0	0.00	0.00	0.00	0.00	0.00	0.00	0.00	0.00	0.00	0.00	0.00	0.00	0.00	0.00	0.00	0.00	0.00	0.00	0.00	0.00
0.1	0.00	0.00	0.00	0.00	0.00	0.00	0.00	0.00	0.00	0.00	0.00	0.00	0.00	0.00	0.00	0.00	0.00	0.00	0.00	0.00
0.2	0.00	0.00	0.00	0.00	0.00	0.00	0.00	0.00	0.00	0.00	0.00	0.00	0.00	0.00	0.00	0.00	0.00	0.00	0.00	0.00
0.3	0.00	0.00	0.00	0.00	0.00	0.00	0.00	0.00	0.00	0.00	0.00	0.00	0.00	0.00	0.00	0.00	0.00	0.00	0.00	0.00
0.4	0.00	0.00	0.00	0.00	0.00	0.00	0.00	0.00	0.00	0.00	0.00	0.00	0.00	0.00	0.00	0.00	0.00	0.00	0.00	0.00
0.5	0.00	0.00	0.00	0.00	0.00	0.00	0.00	0.00	0.00	0.00	0.00	0.00	0.00	0.00	0.00	0.00	0.00	0.00	0.00	0.00
0.6	0.00	0.00	0.00	0.00	0.00	0.00	0.00	0.00	0.00	0.00	0.00	0.00	0.00	0.00	0.00	0.00	0.00	0.00	0.00	0.00
0.7	0.00	0.00	0.00	0.00	0.00	0.00	0.00	0.00	0.00	0.00	0.00	0.00	0.00	0.00	0.00	0.00	0.00	0.00	0.00	0.00
0.8	0.00	0.00	0.00	0.00	0.00	0.00	0.00	0.00	0.00	0.00	0.00	0.00	0.00	0.00	0.00	0.00	0.00	0.00	0.00	0.00
0.9	0.00	0.00	0.00	0.00	0.00	0.00	0.00	0.00	0.00	0.00	0.00	0.00	0.00	0.00	0.00	0.00	0.00	0.00	0.00	0.00
1.0	0.00	0.00	0.00	0.00	0.00	0.00	0.00	0.00	0.00	0.00	0.00	0.00	0.00	0.00	0.00	0.00	0.00	0.00	0.00	0.00

Reproduced from
best available copy.

C-Specimen No.	a-Specimen No 6
d.	4"
d _r	20"
b	4"
t _w	1/4"
t _f	5/16"
λ	192

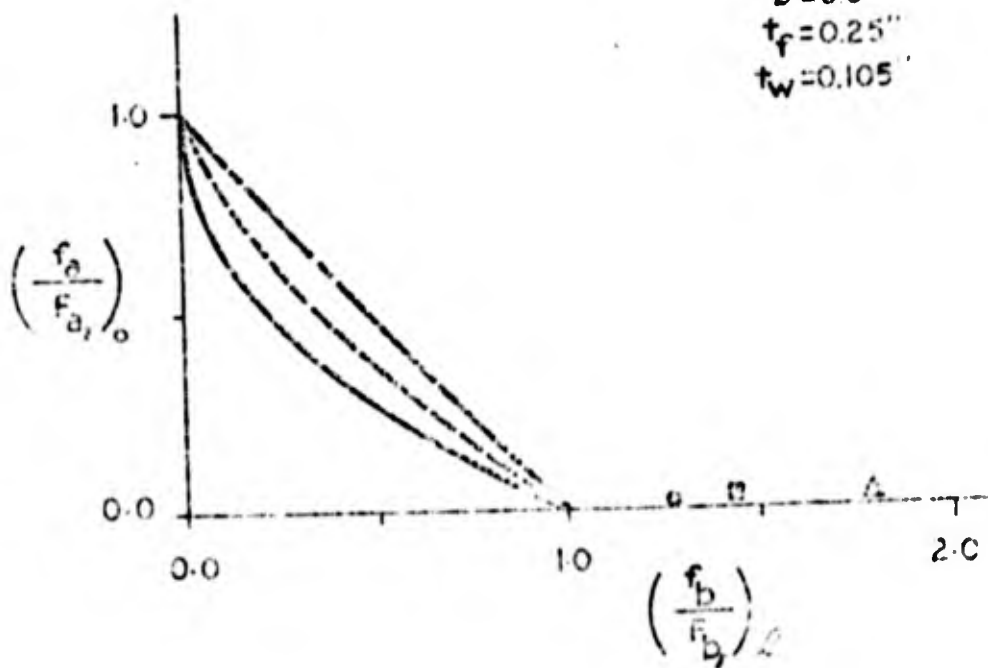
Other data α=0
 Strong axis - K_y=0.71
 Weak axis - K = 0.70

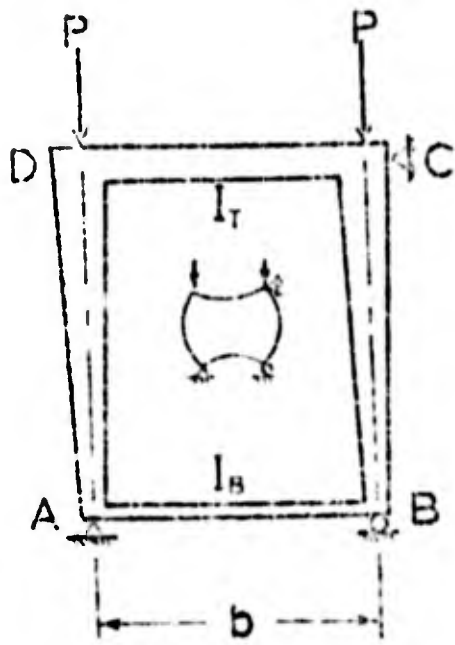




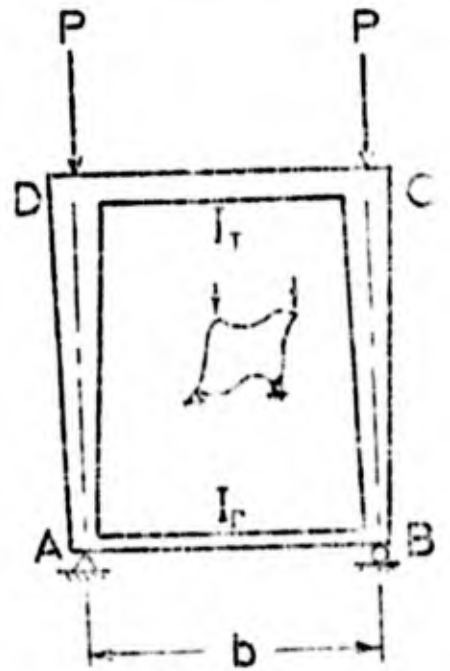
Specimen No.	Test point	Eq. 4.3-3	d_o	d_f	l
LB-C-7	●	-----	6.0"	6.0'	116.5"
LB-C-9	■	-----	6.1"	11.8"	115.4"
LB-C-10	▲	-----	6.1'	175"	114.0"

Other data: $\alpha = 0$
 $b = 6.0$
 $t_f = 0.25$
 $t_w = 0.105$



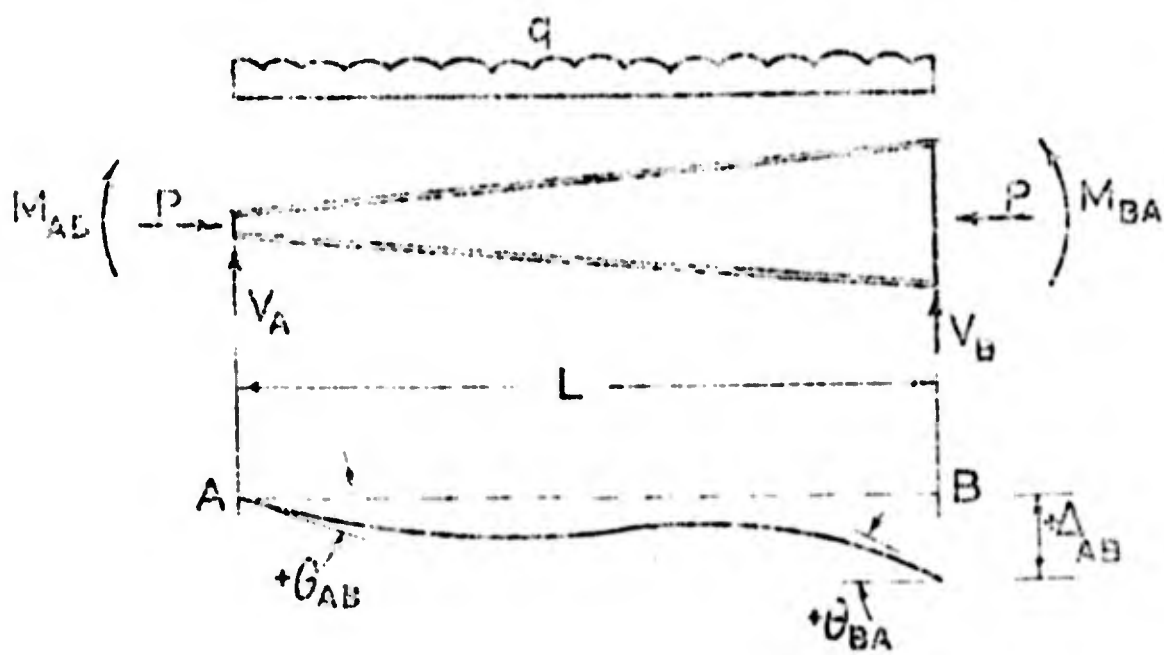


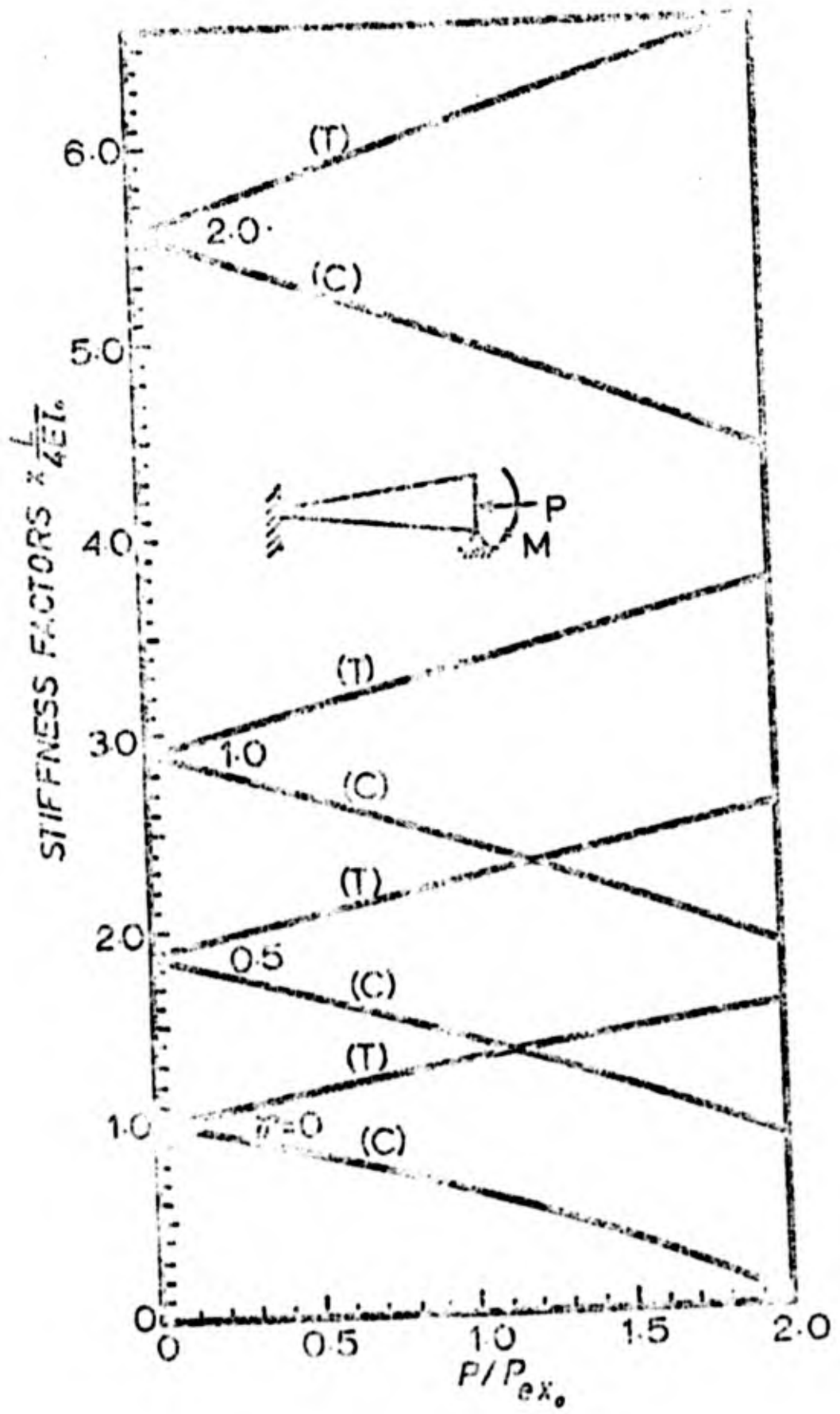
(a) No sidesway

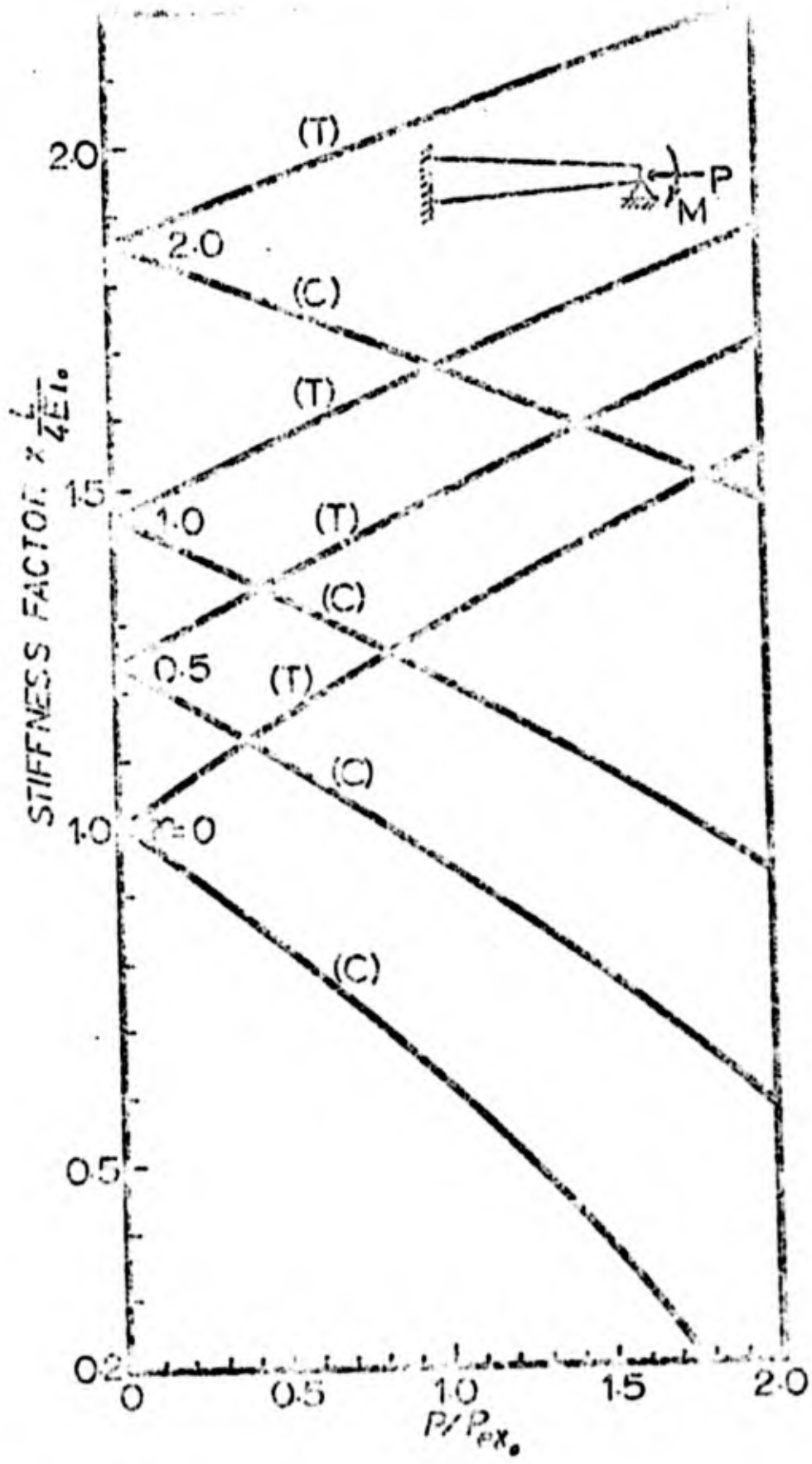


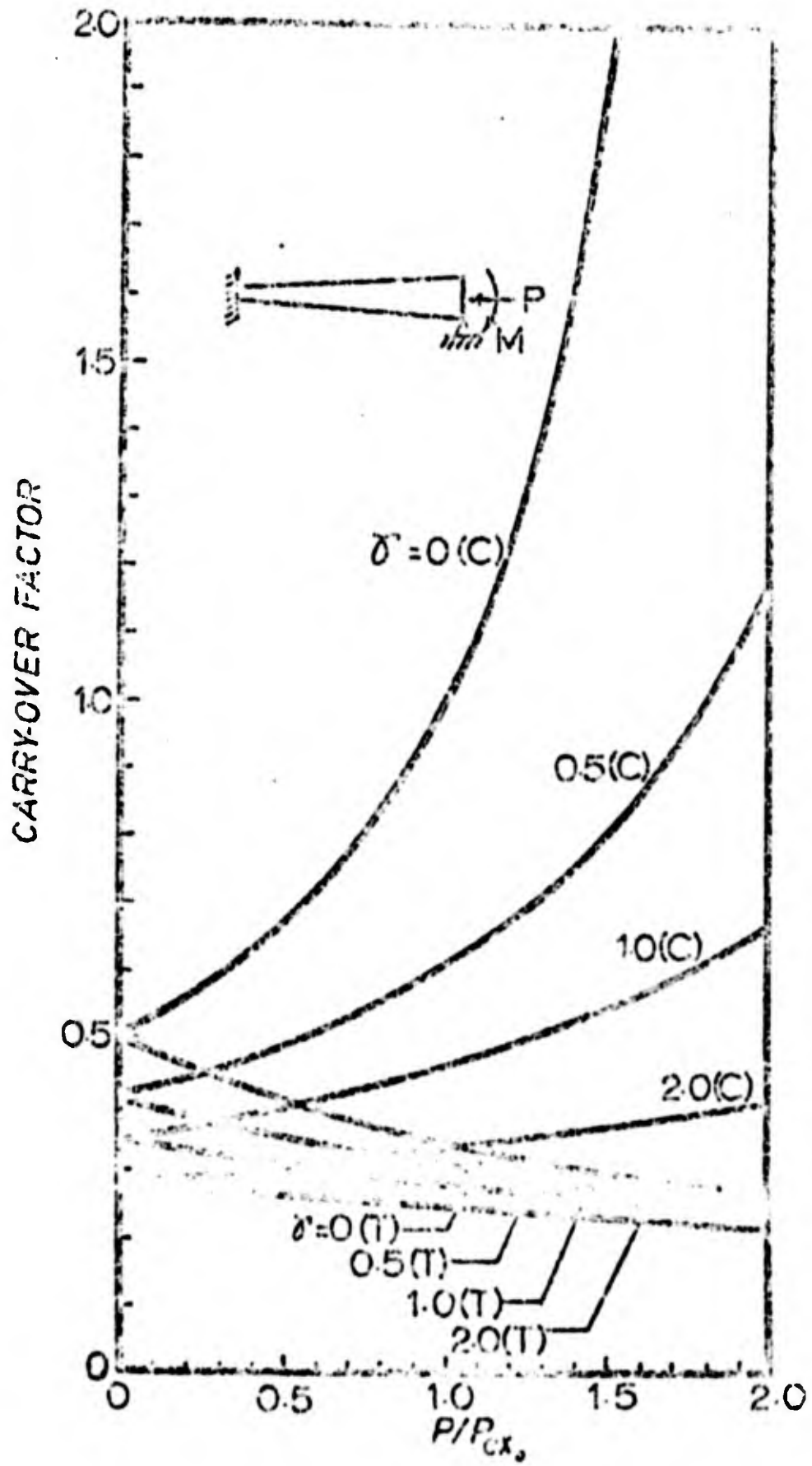
(b) With sidesway

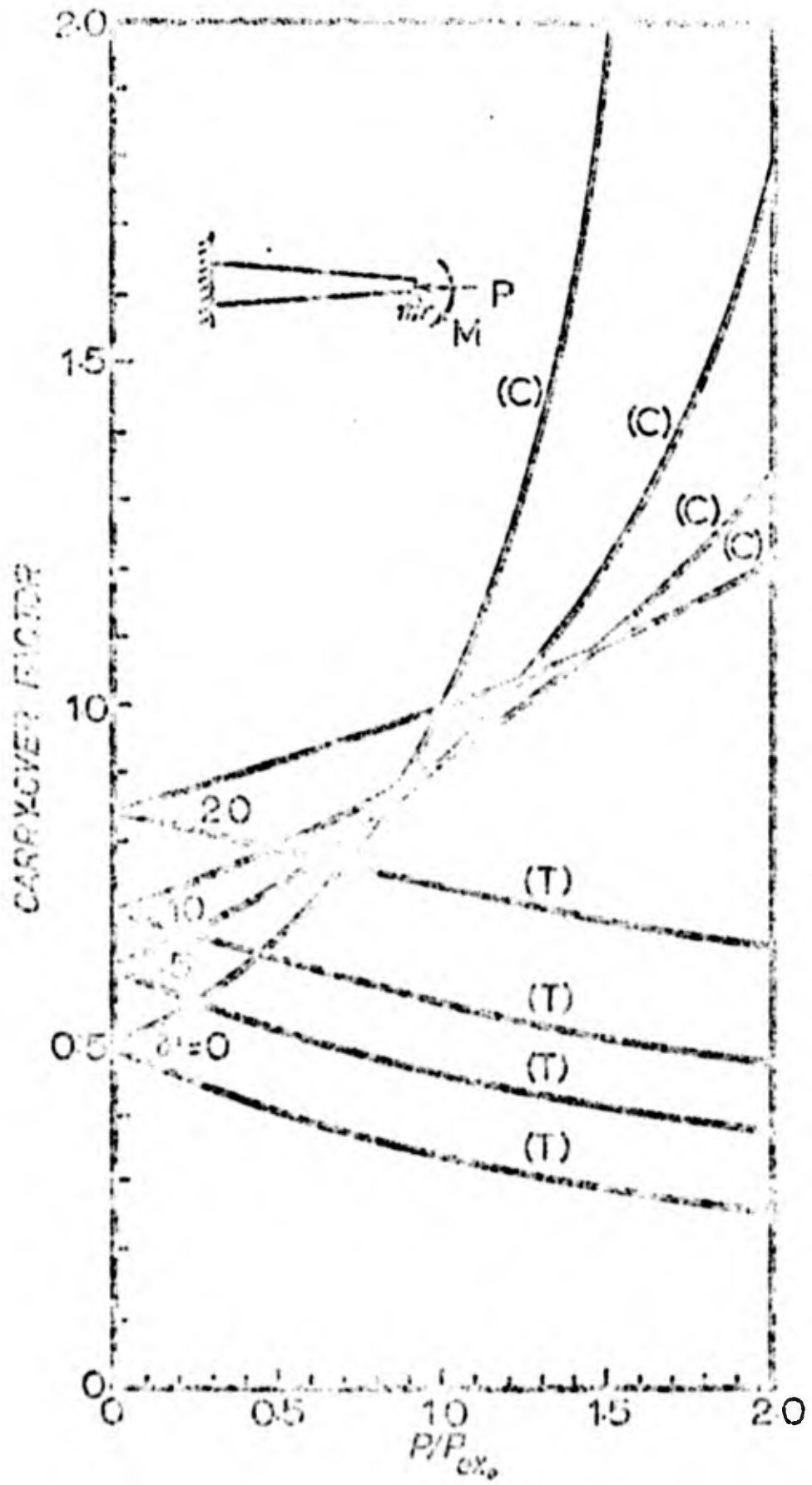
80

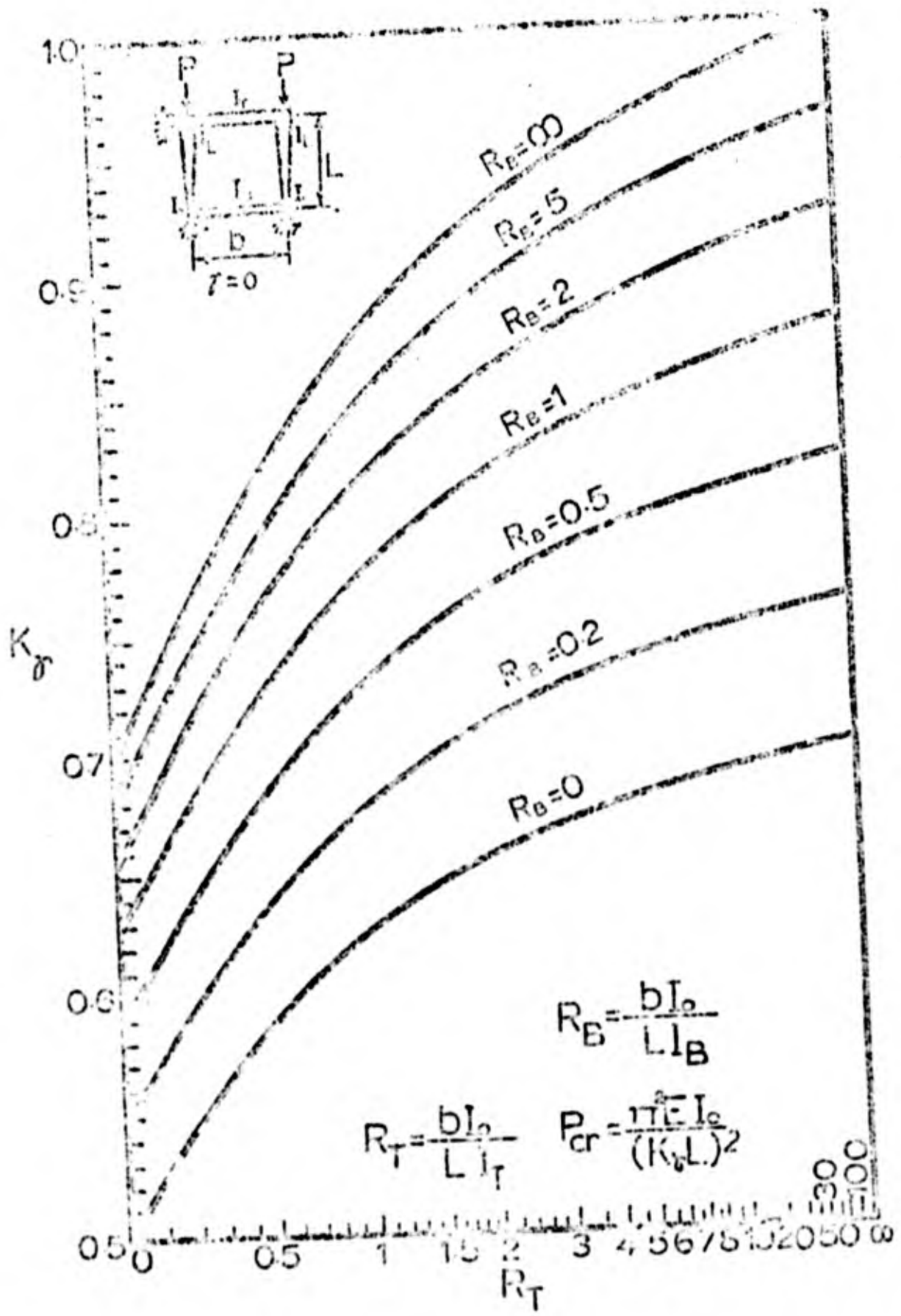


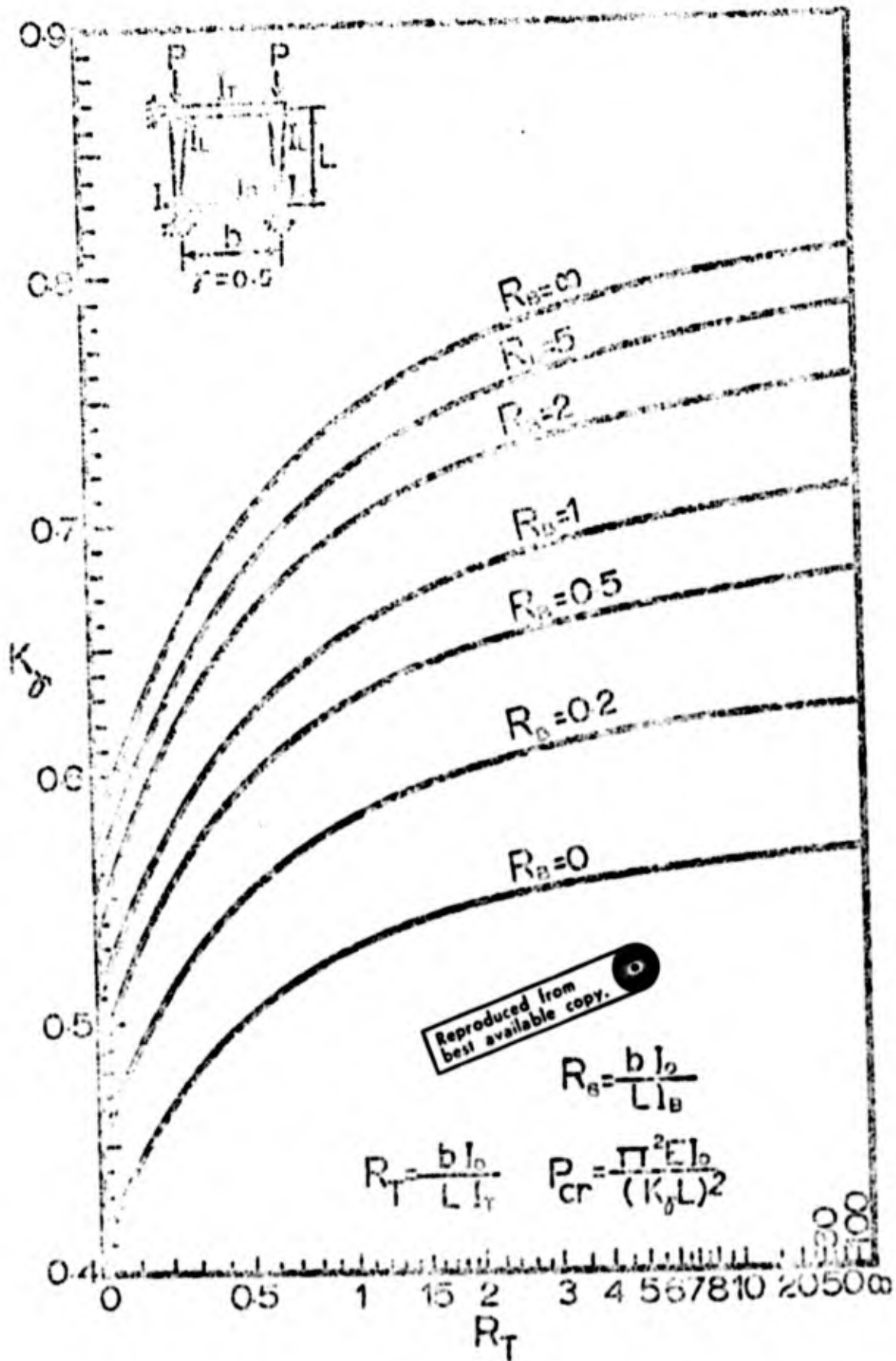


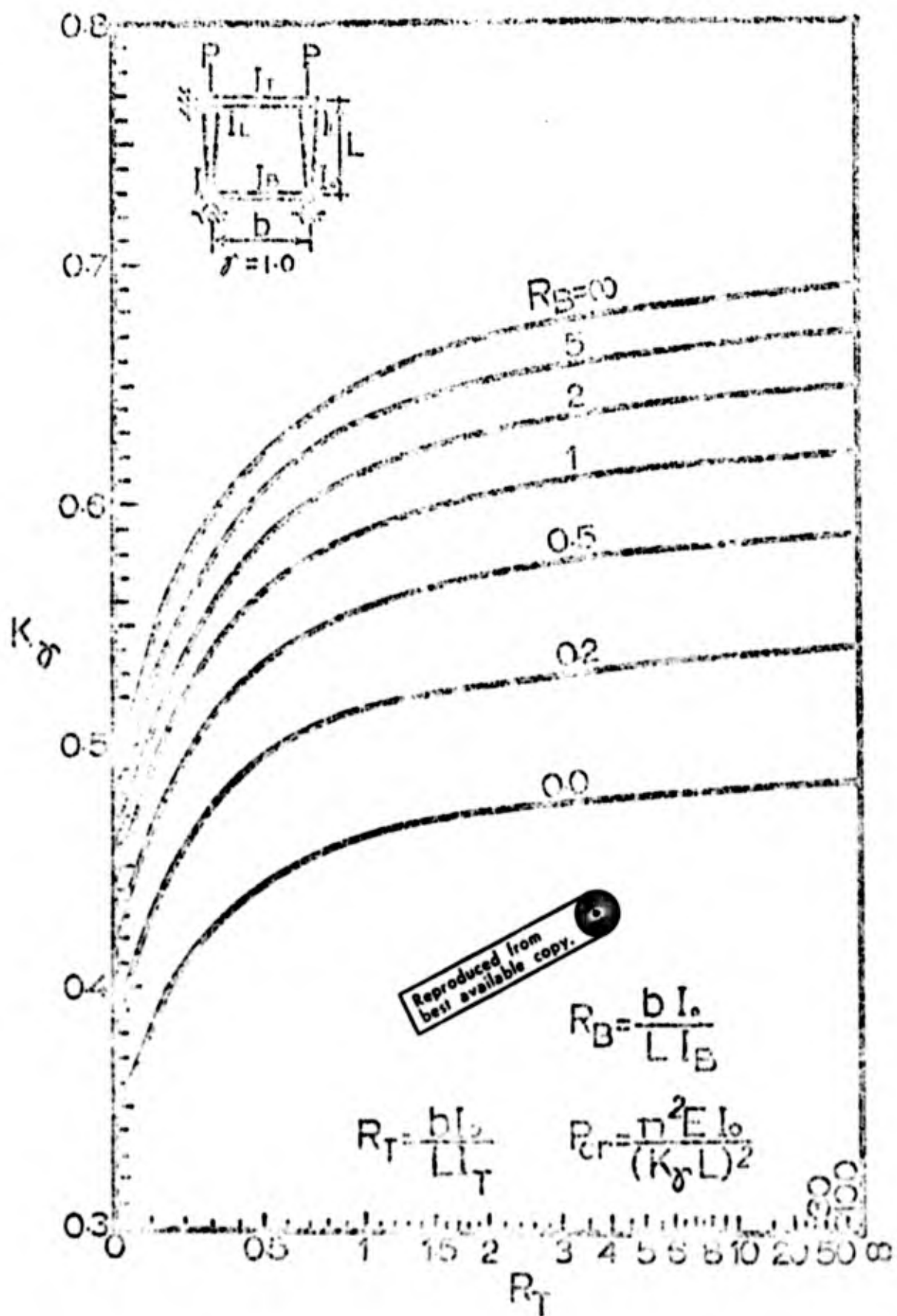


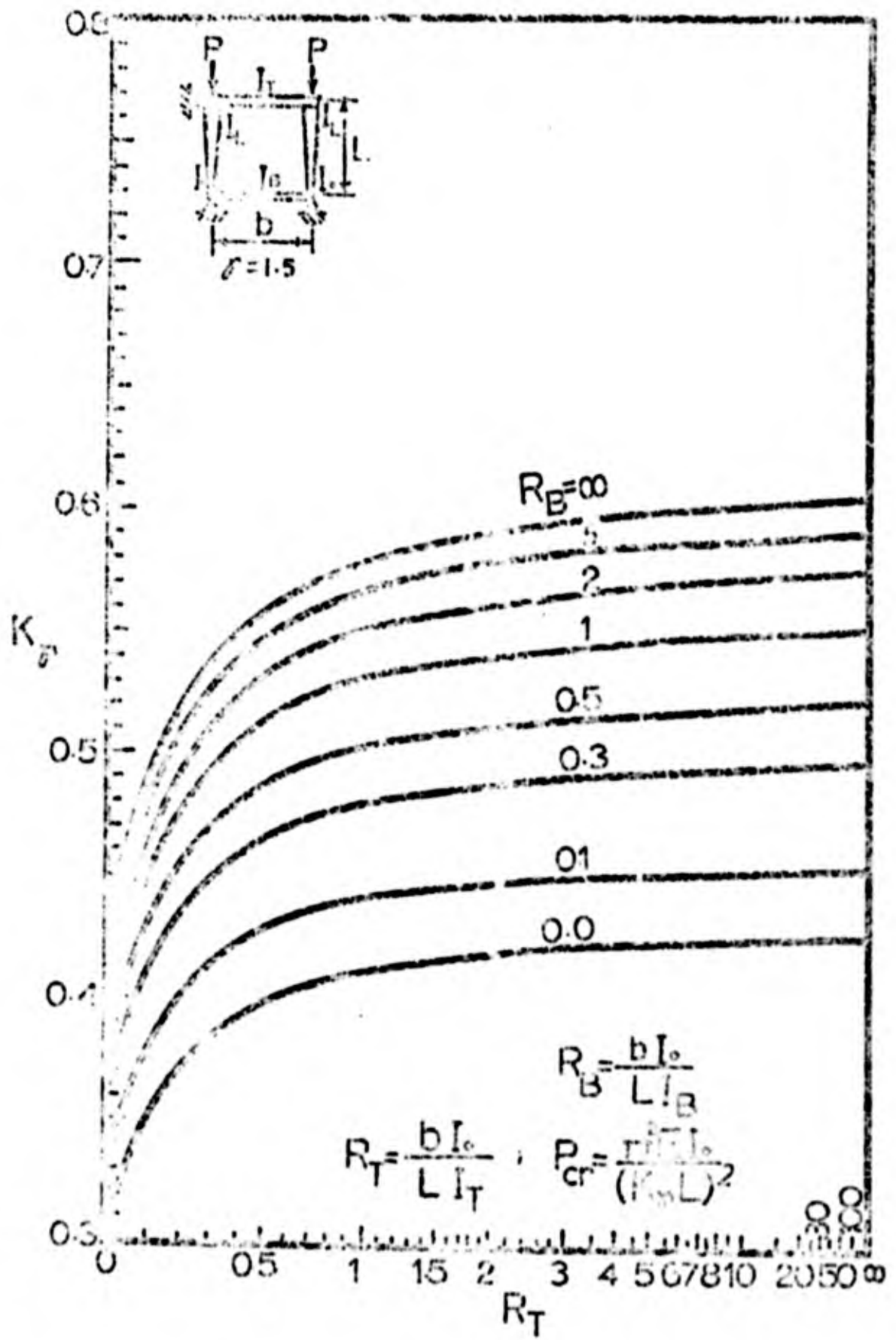


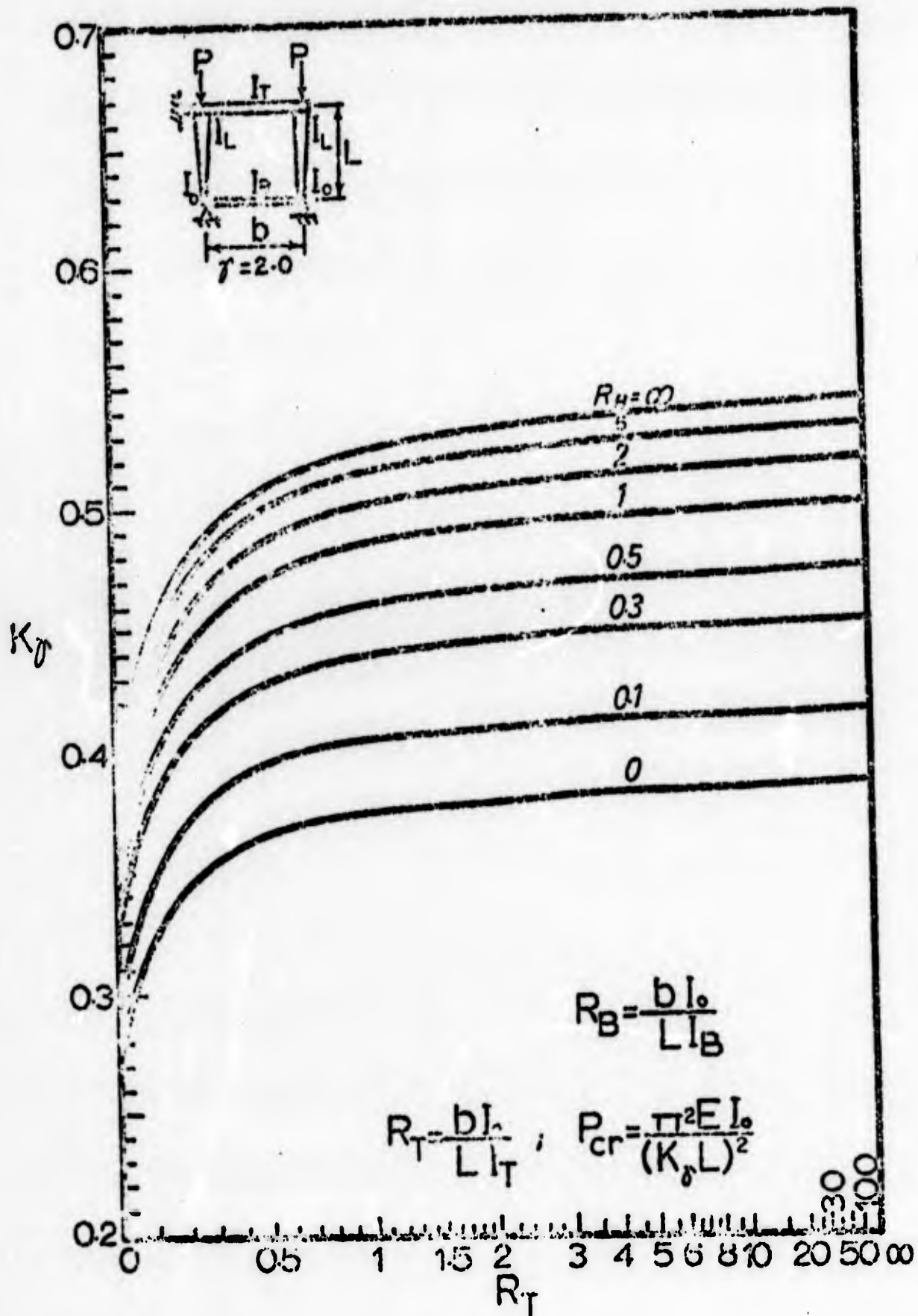


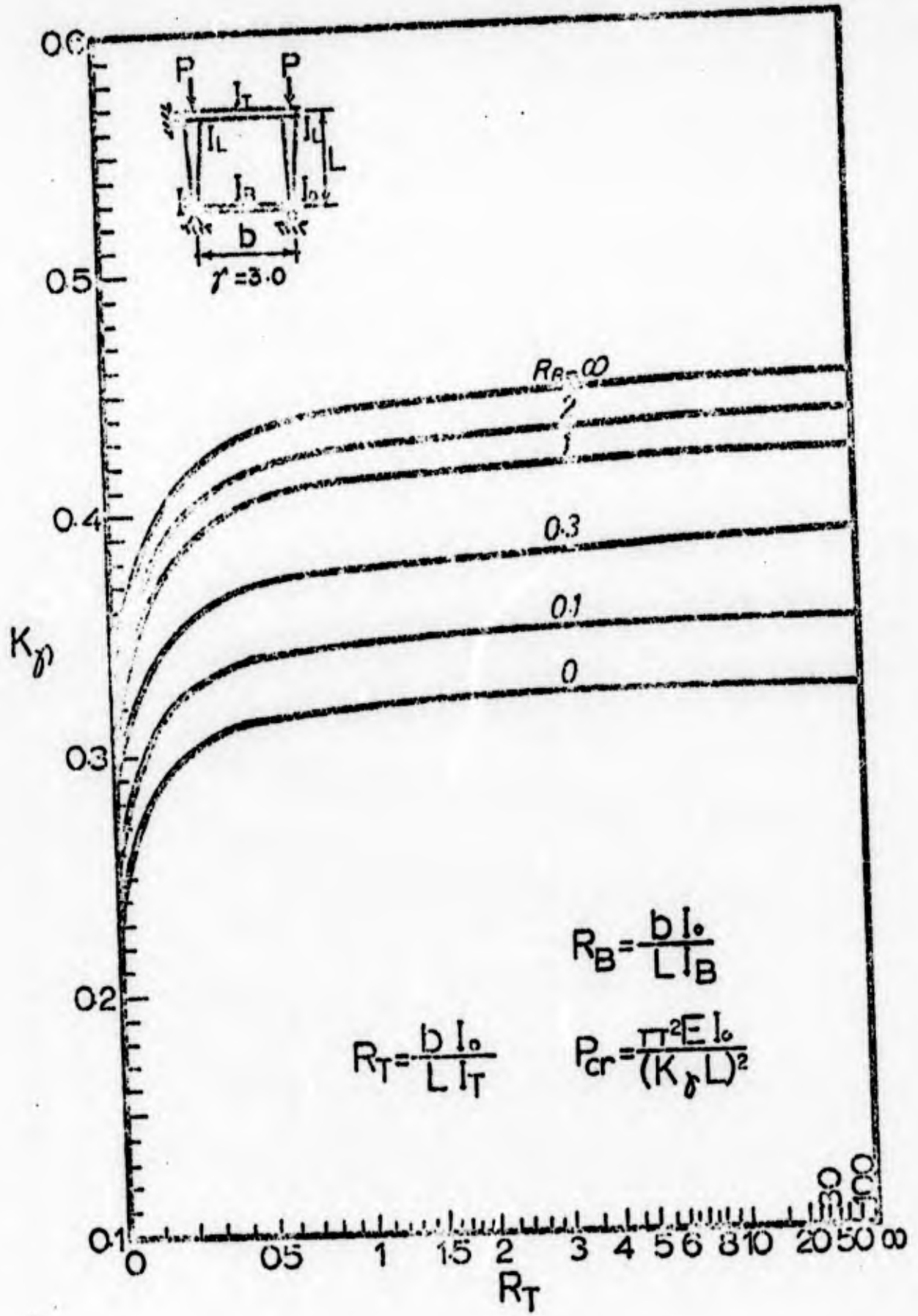


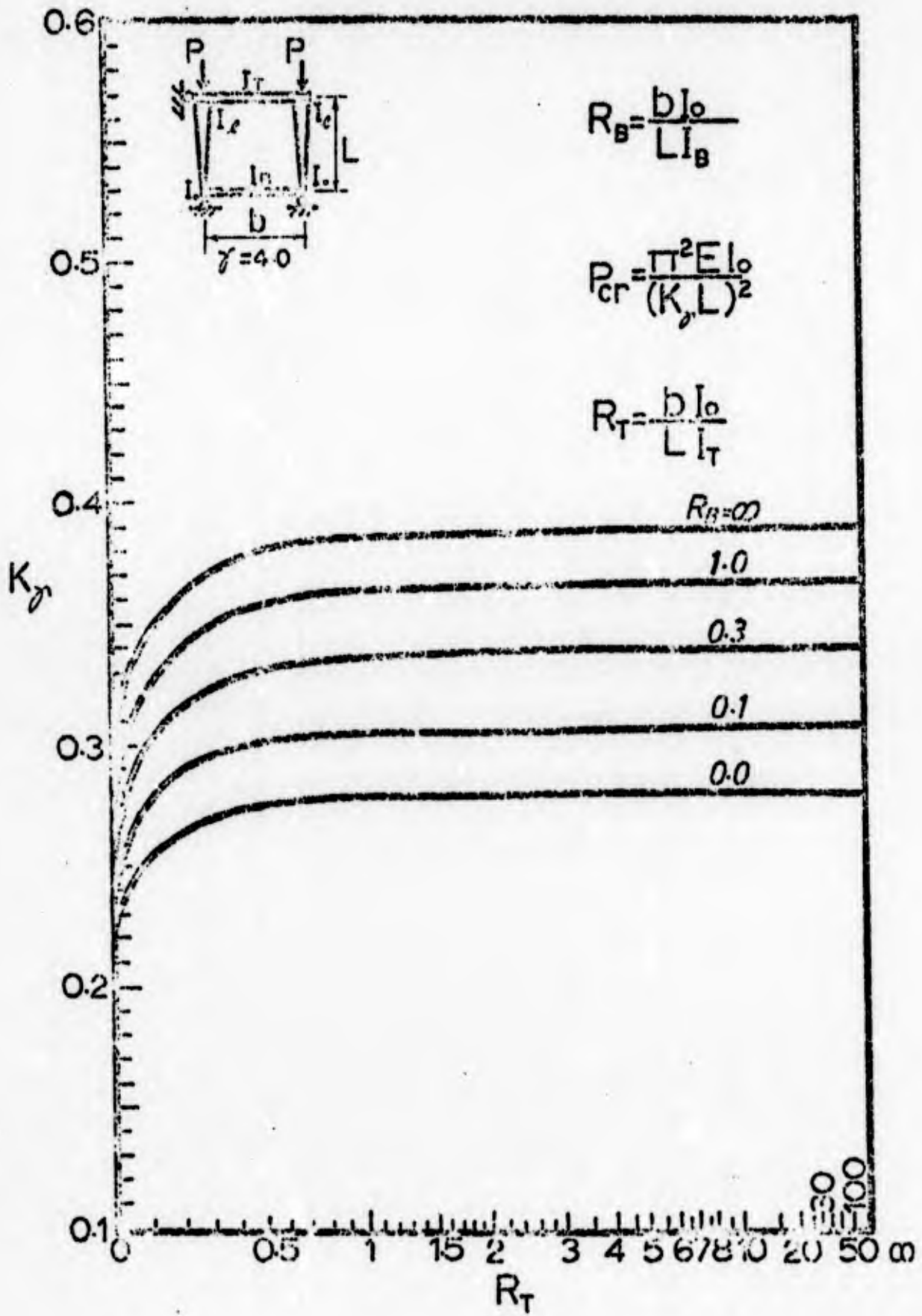


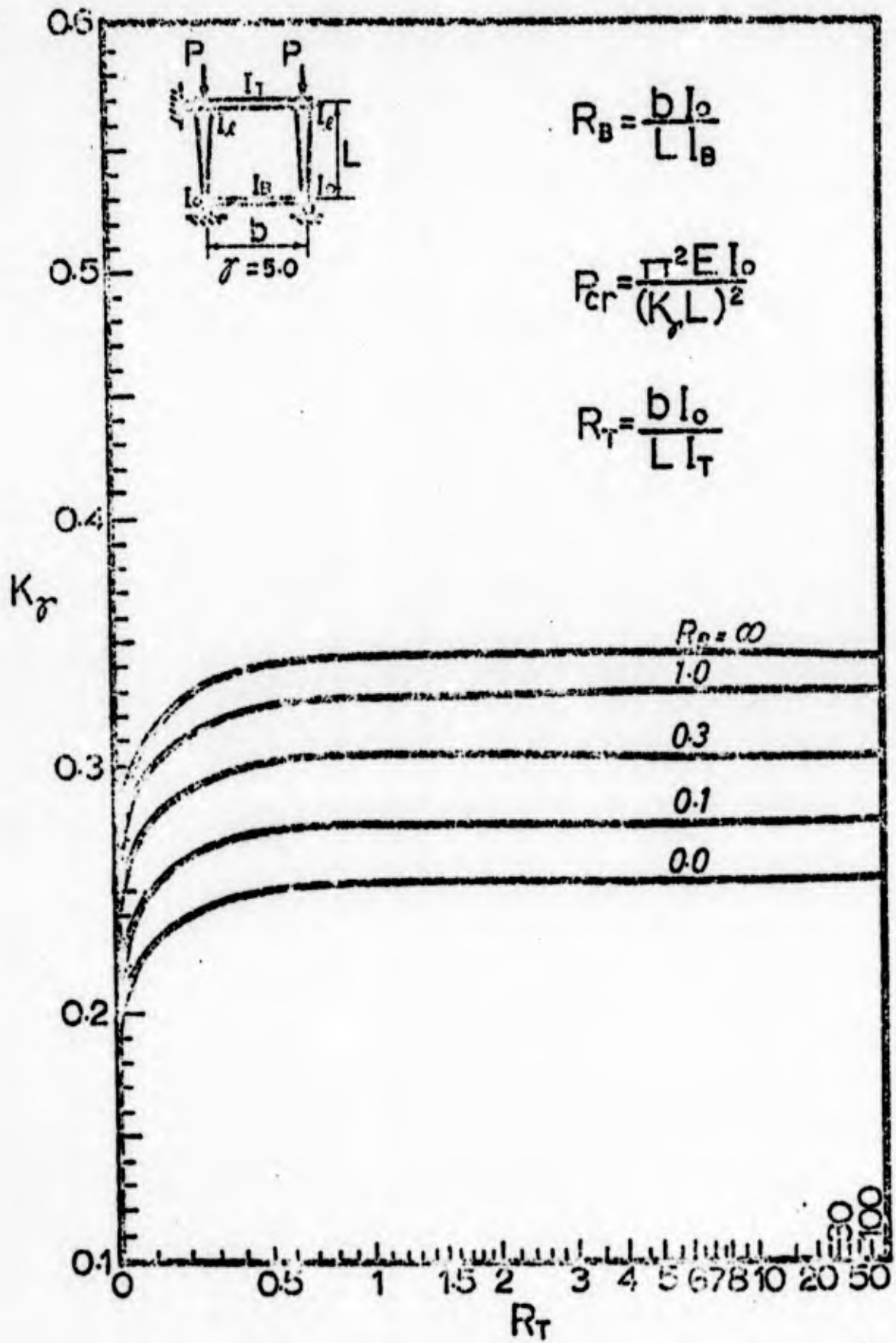


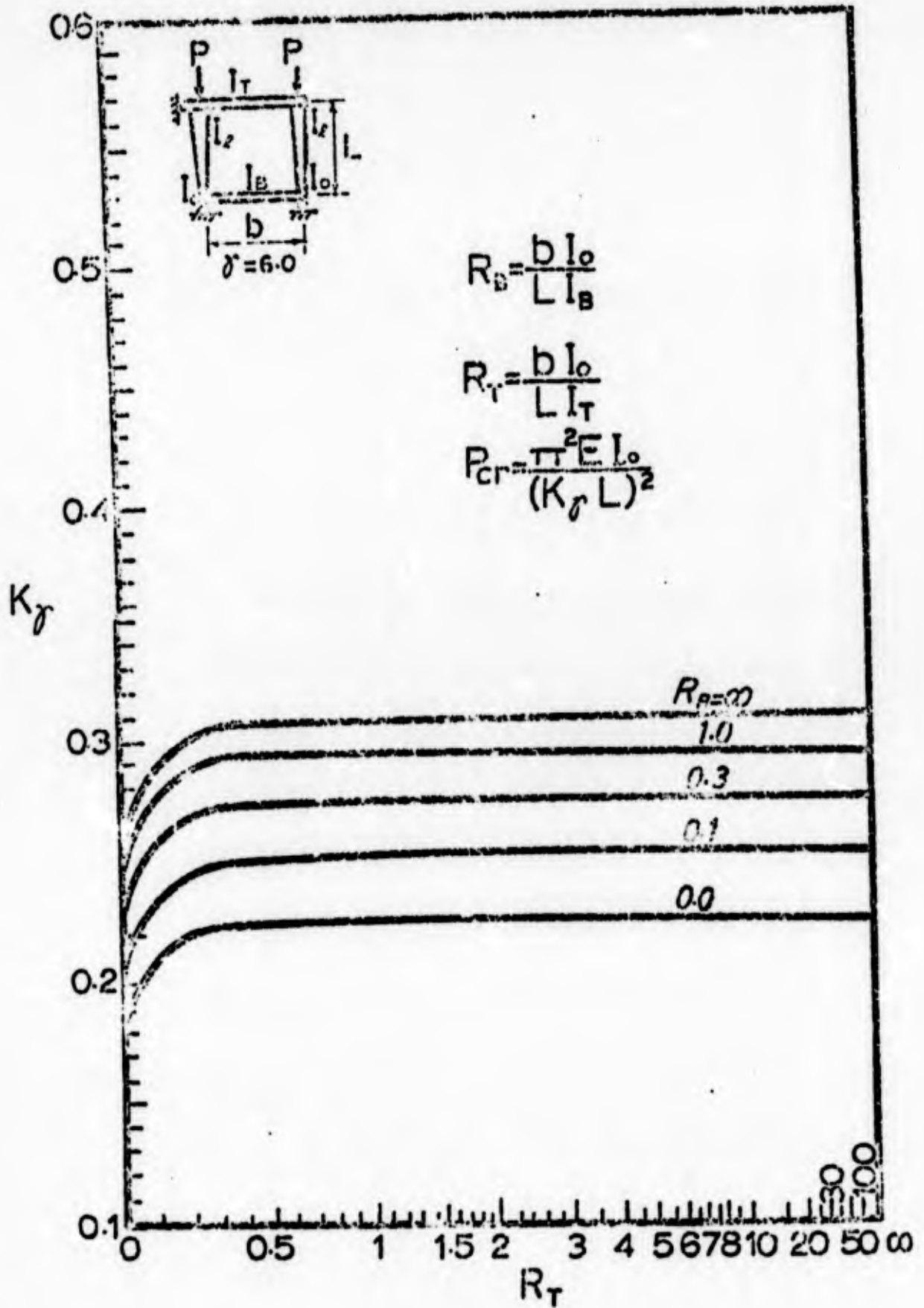


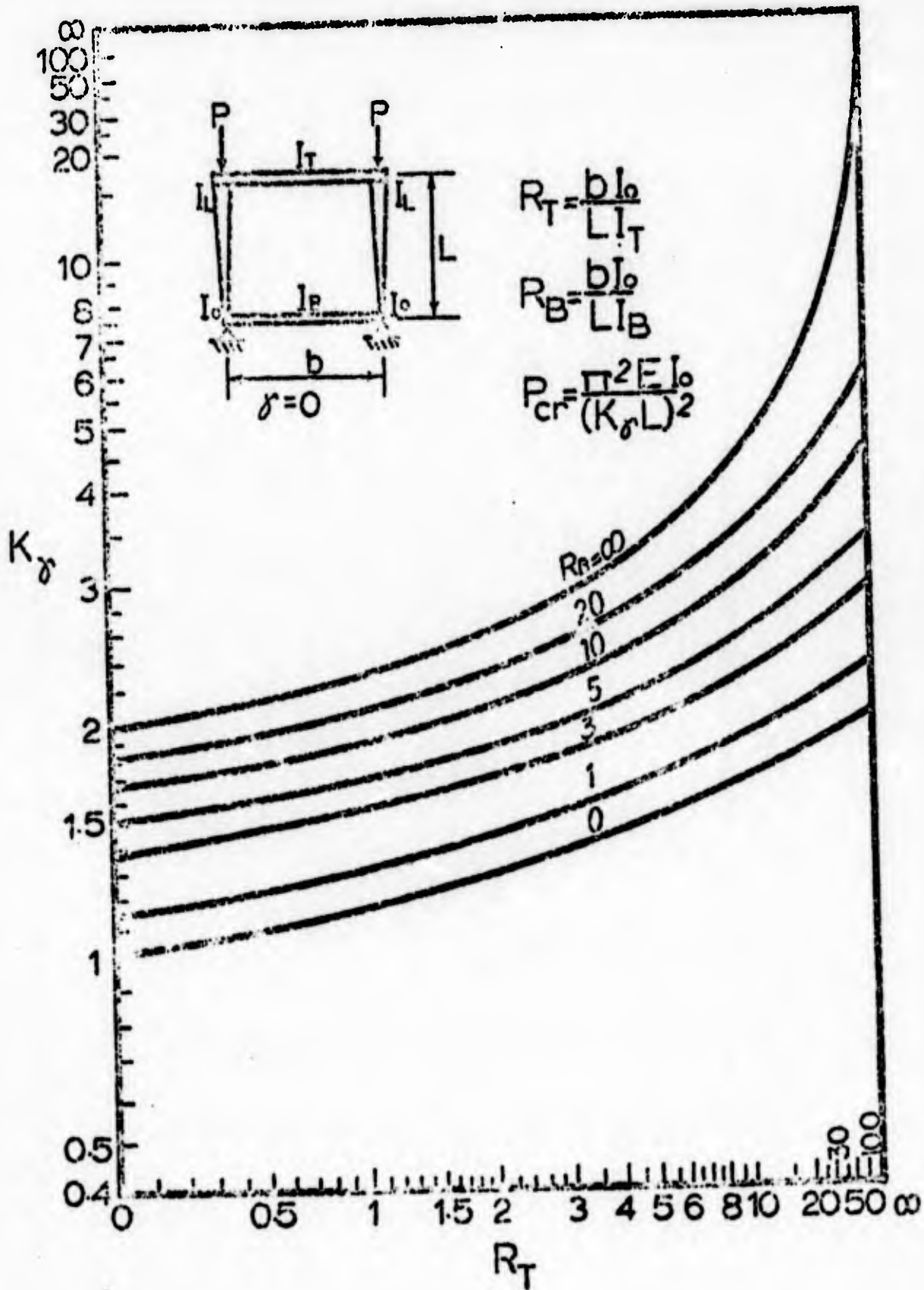


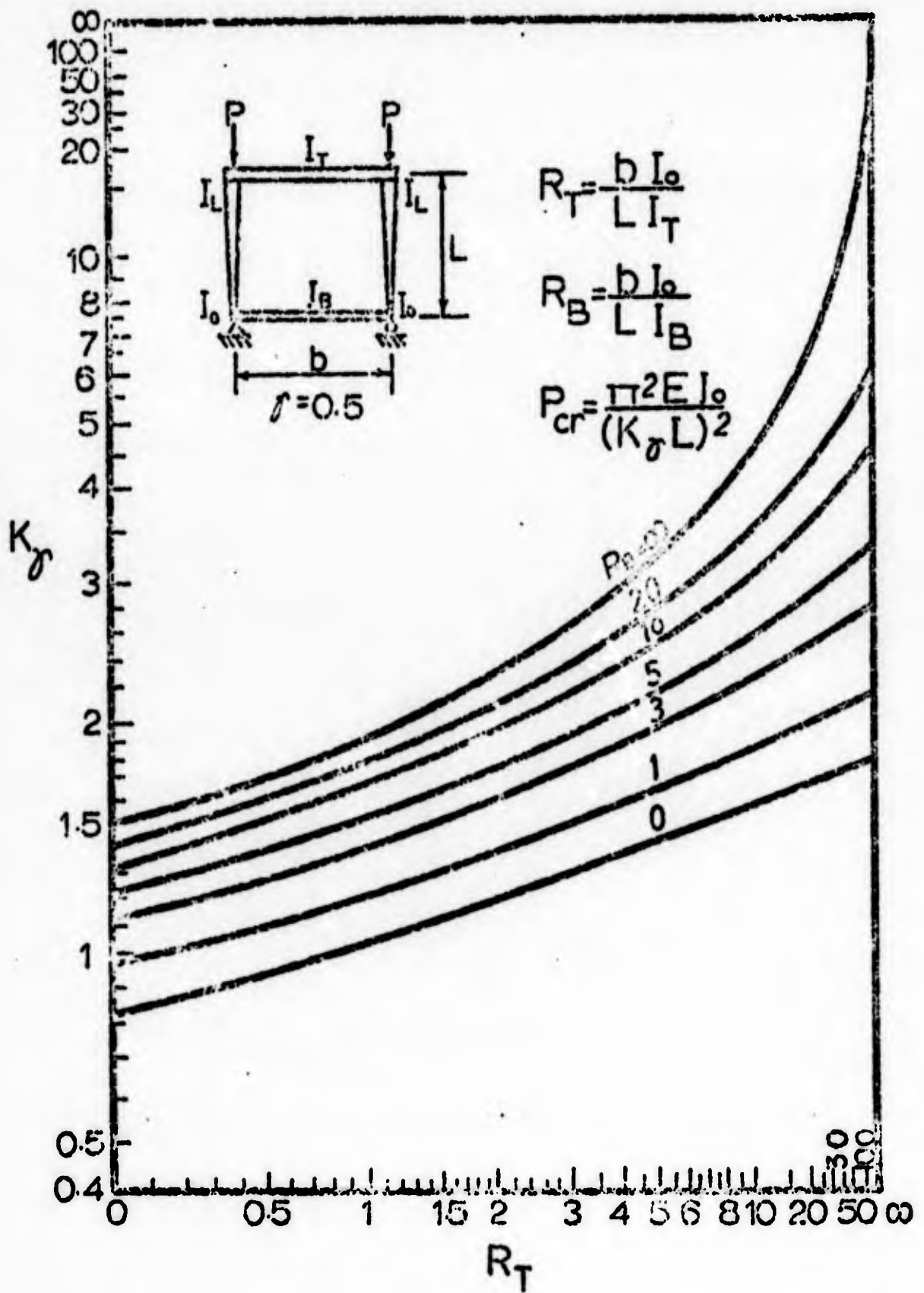


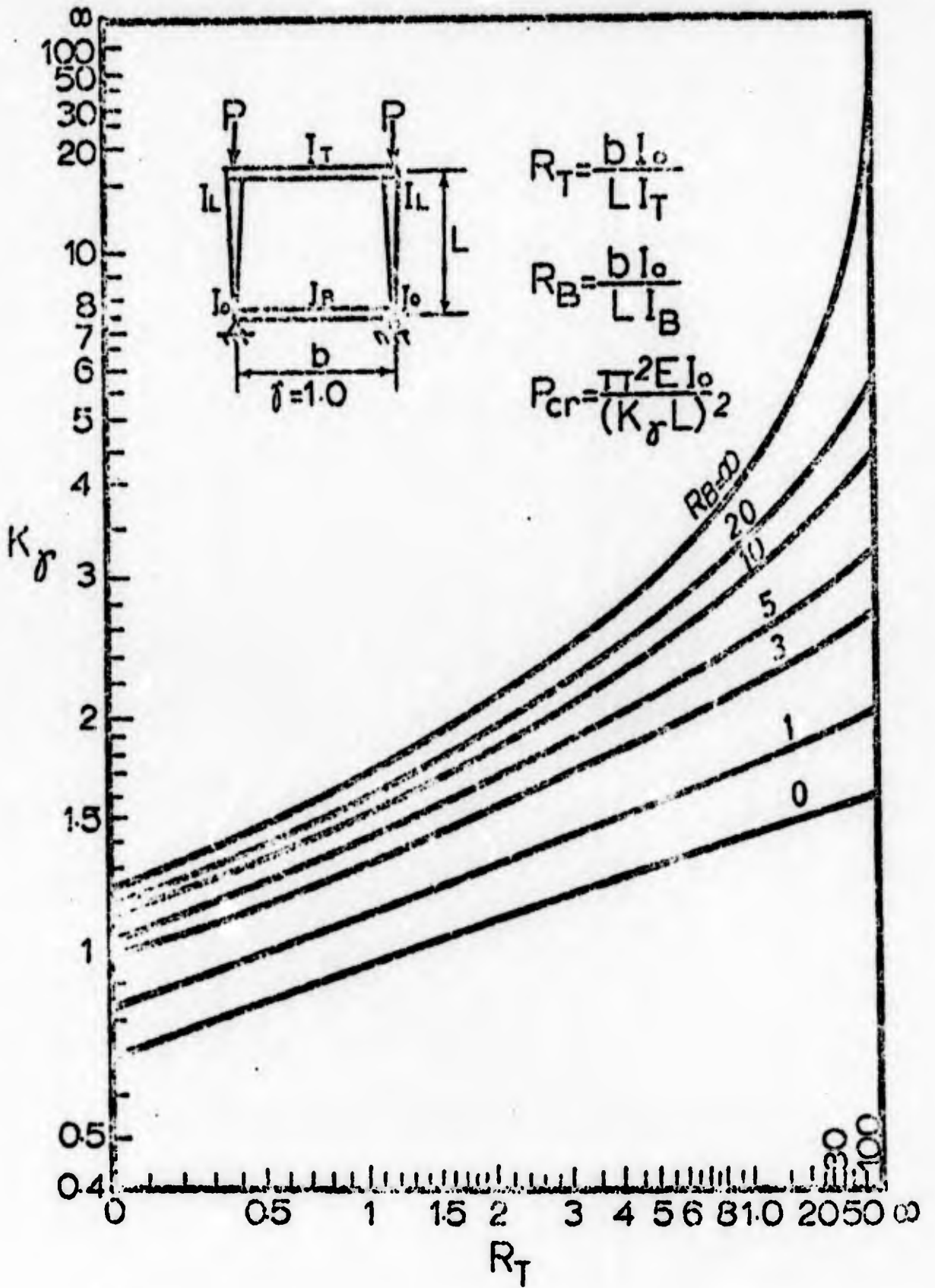


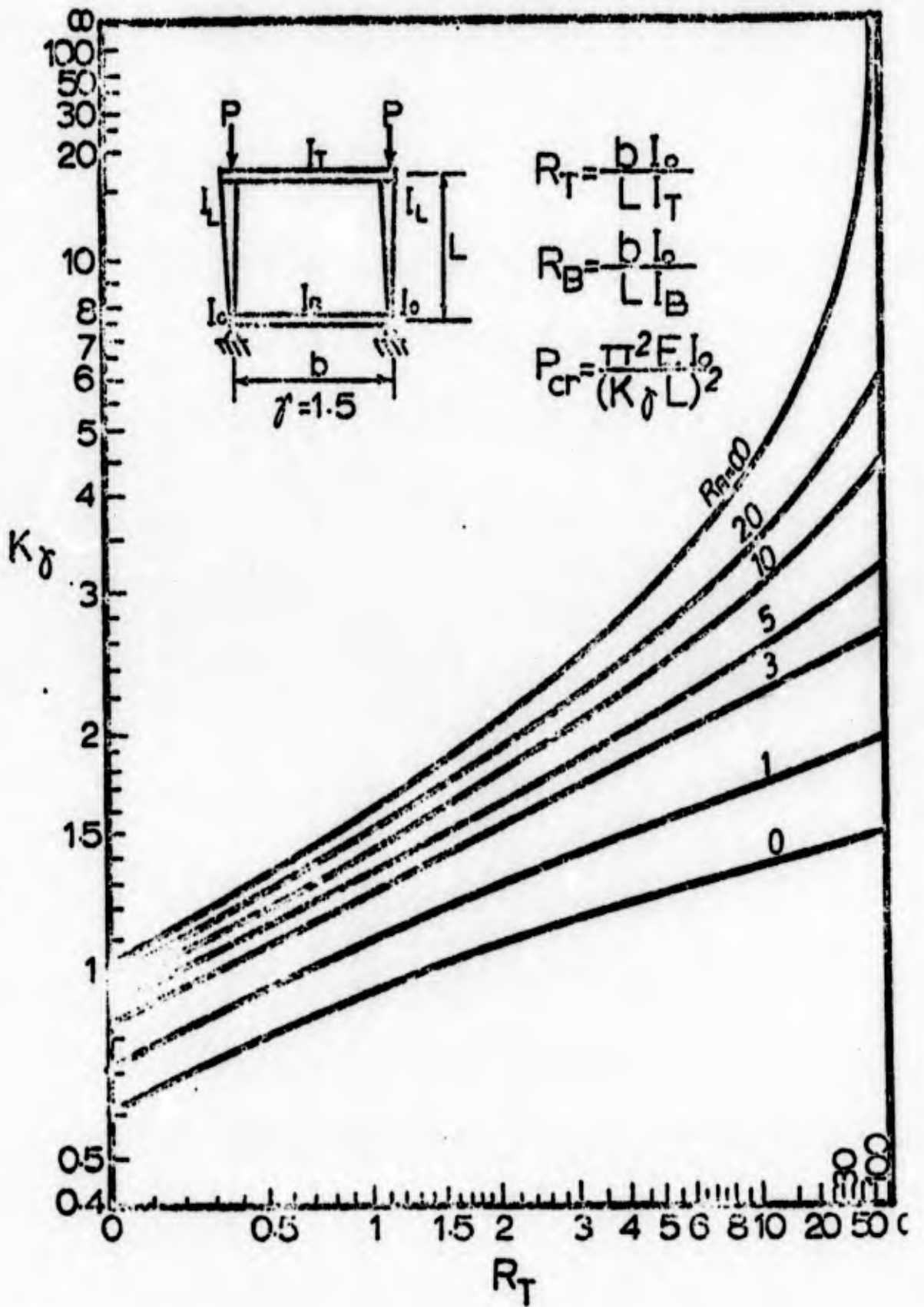


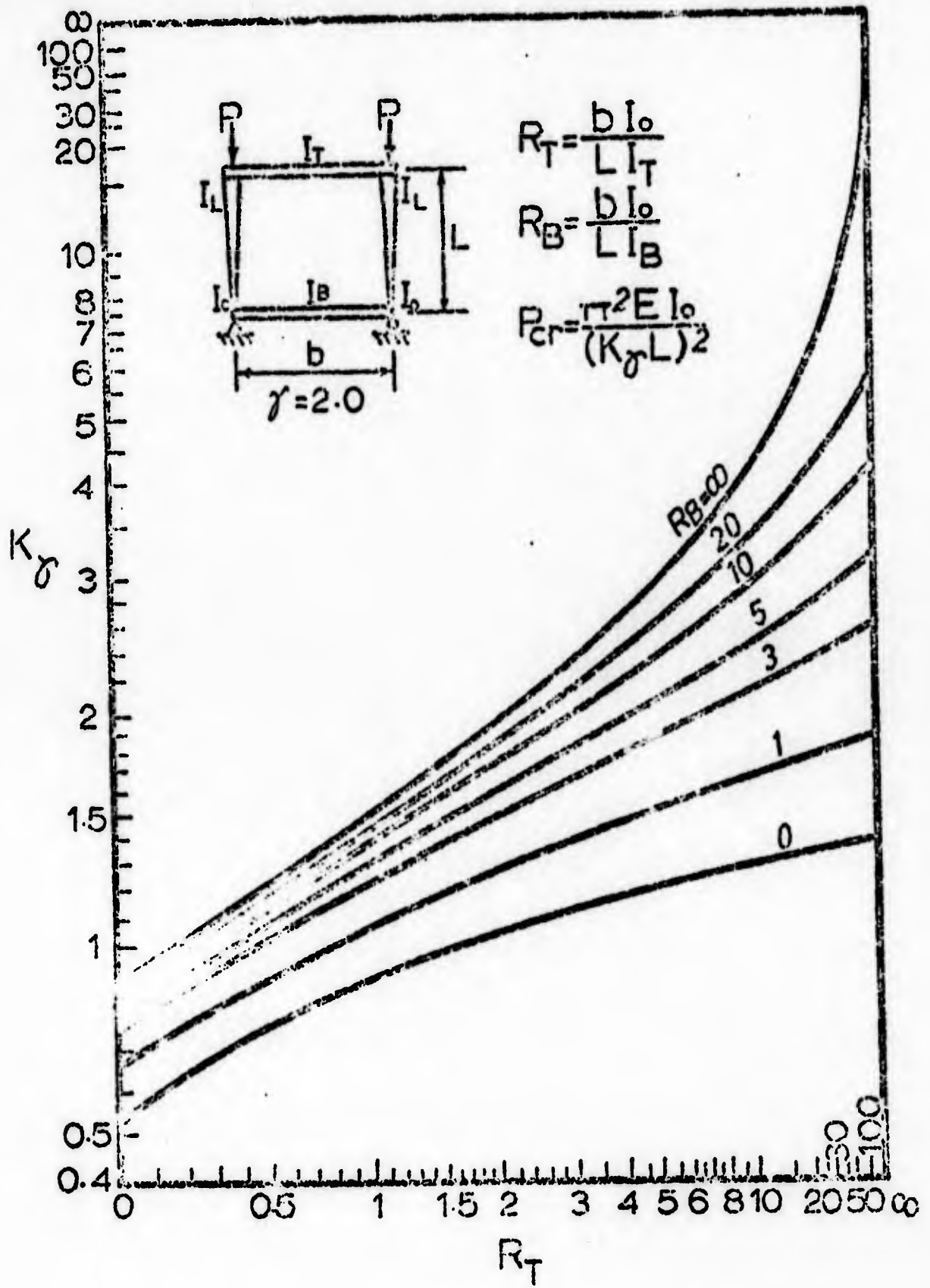


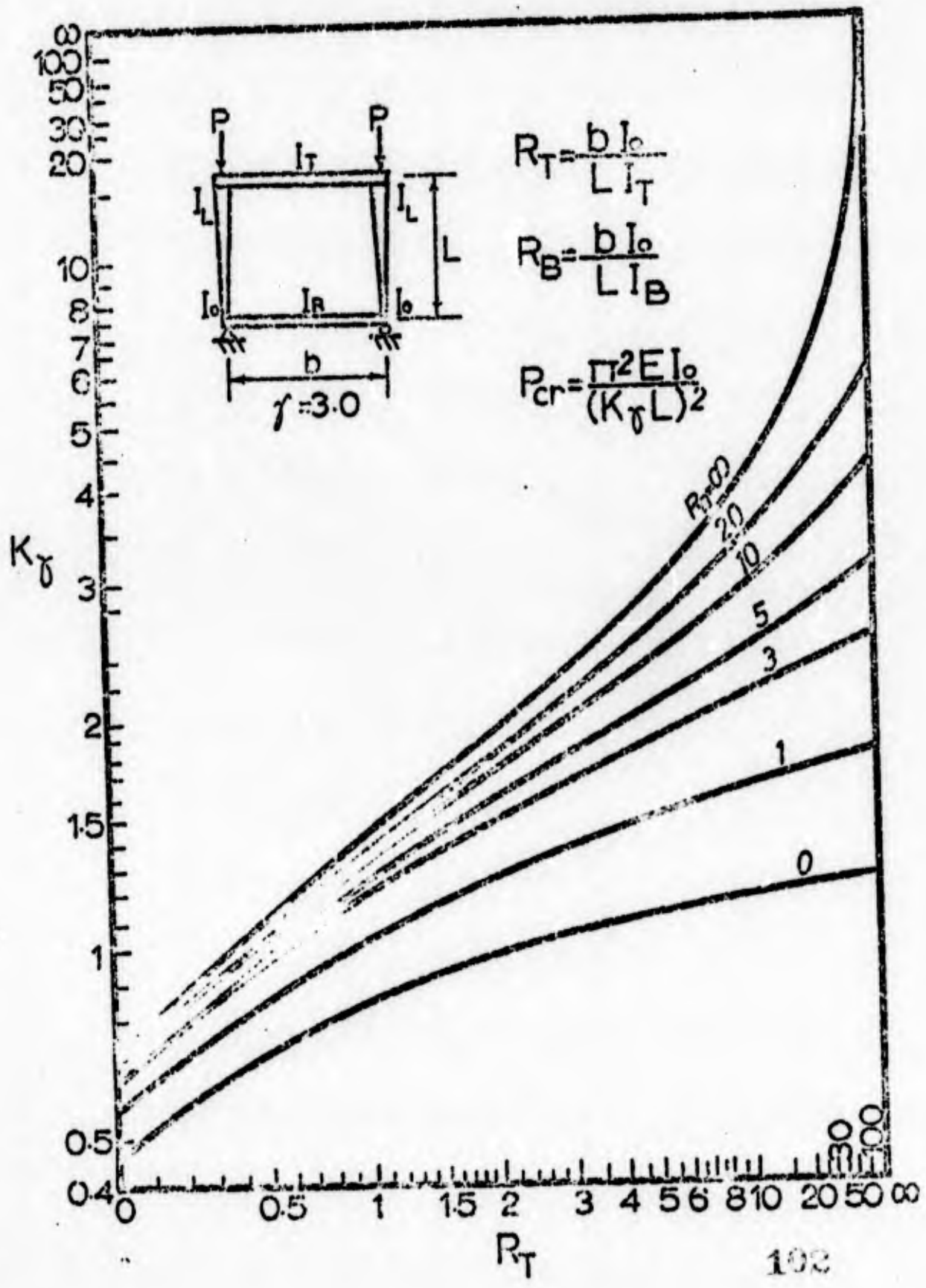


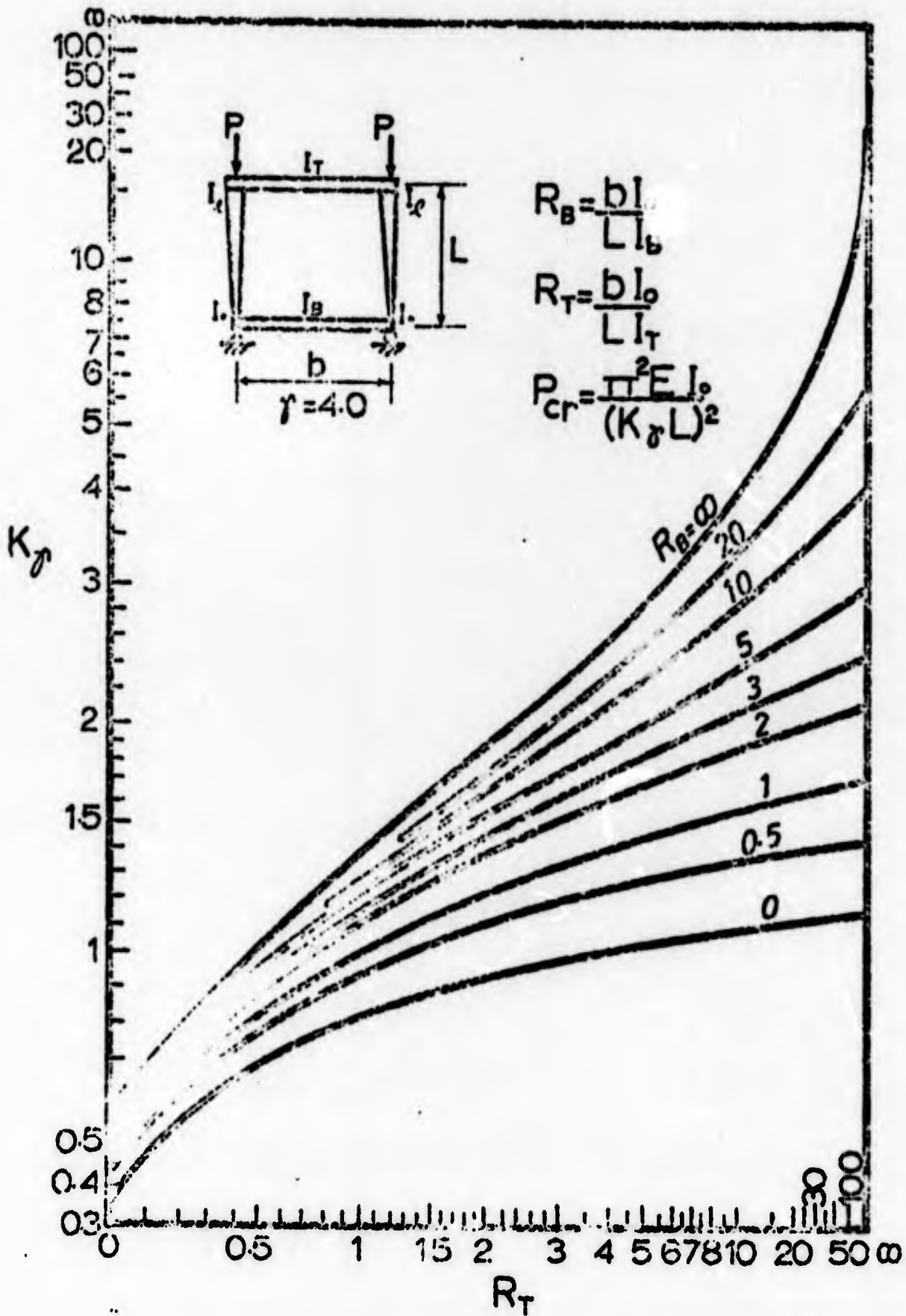


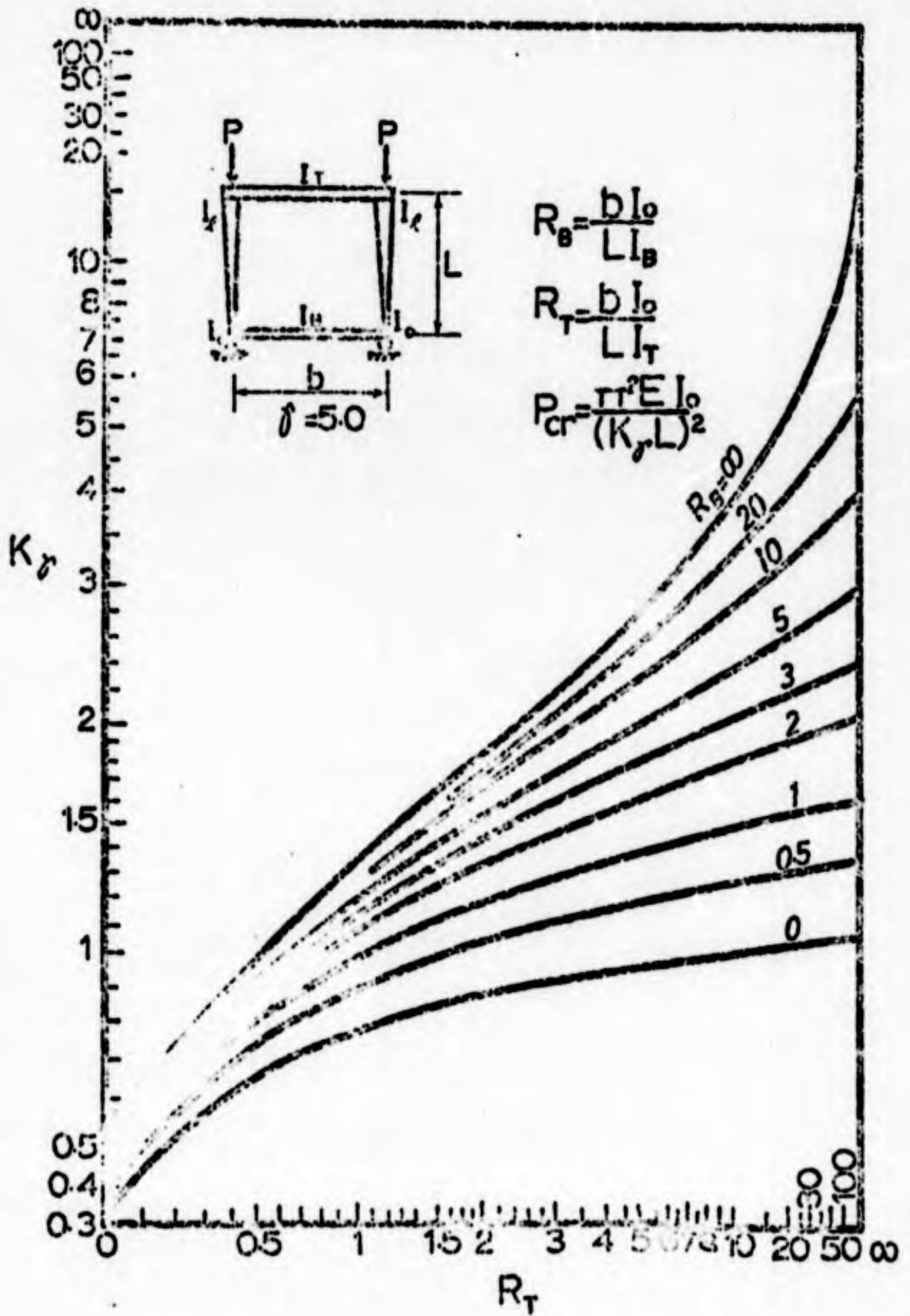


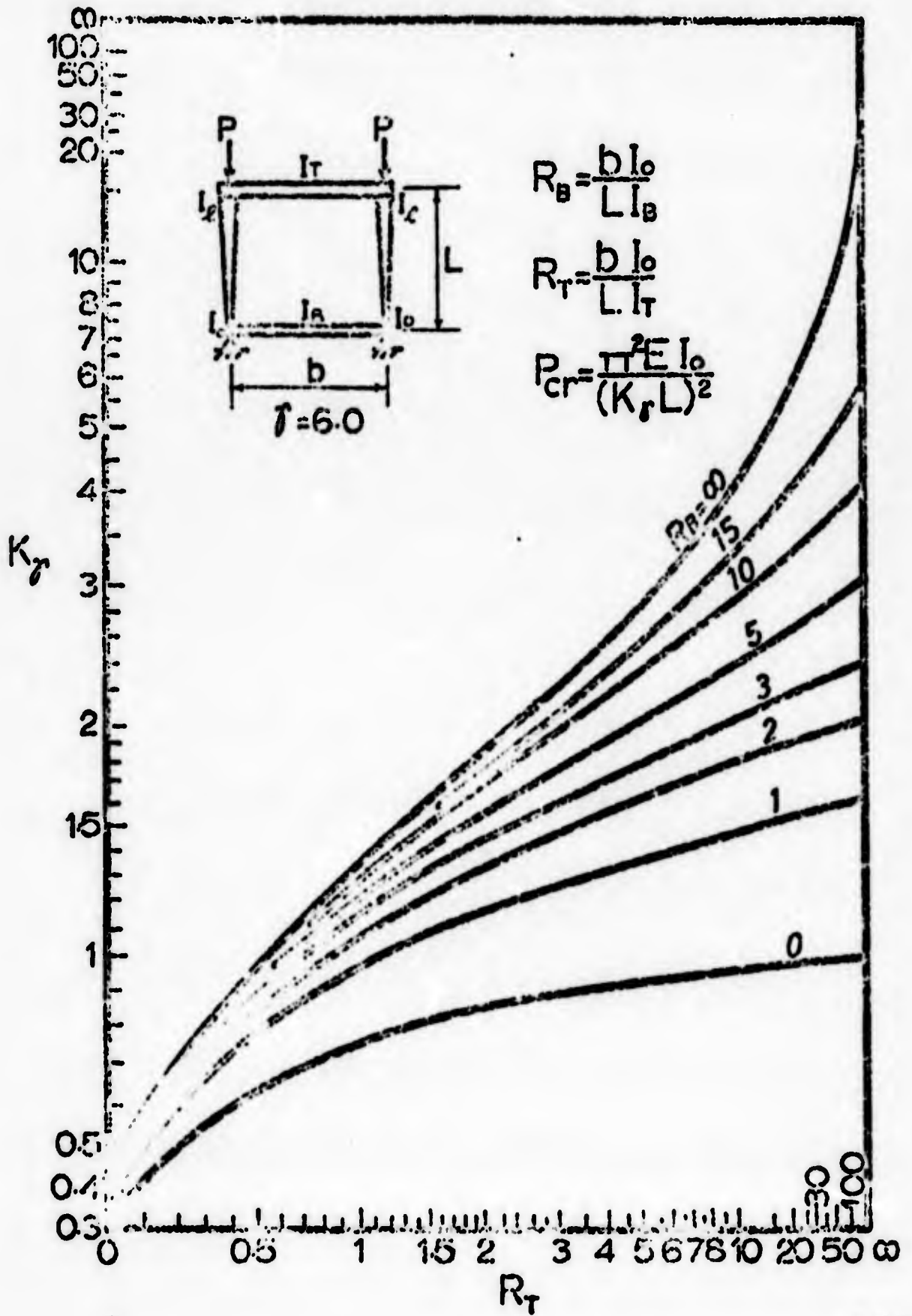












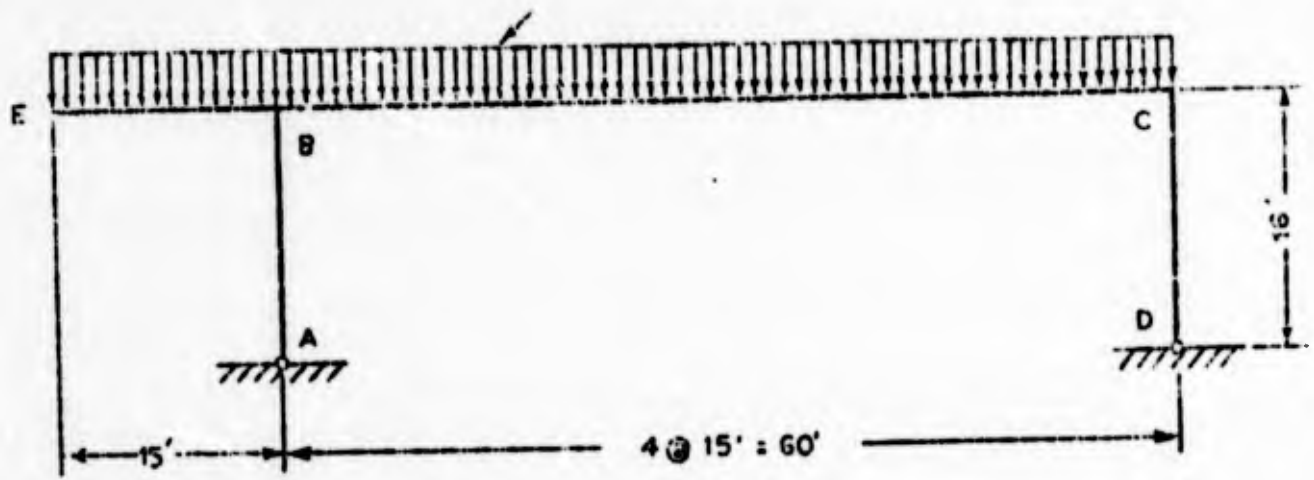


Fig. 6.1 - Frame example .

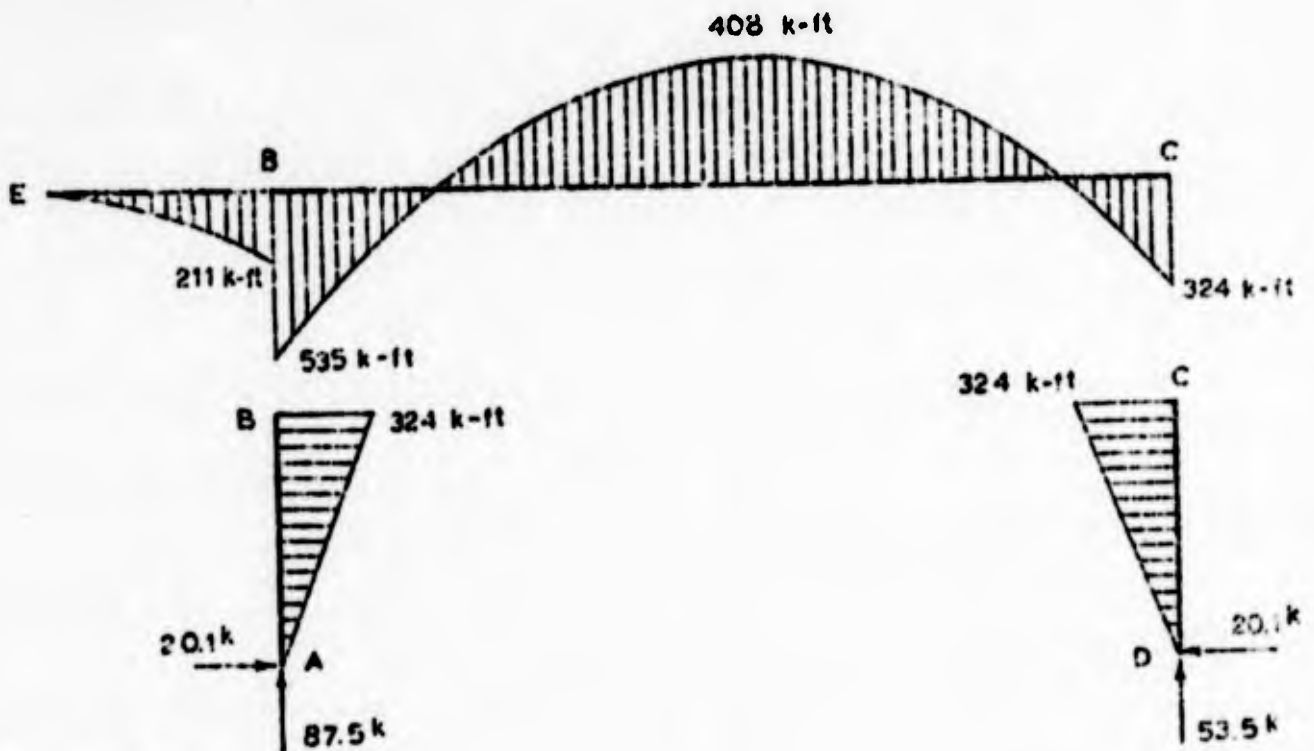


Fig. 6.2 - Moment diagram

Member	d_o	d_e	t_w	b	t_f
AB	12.4	24.8	0.50	12.1	0.75
BC	----- 30 WF 116 -----				
CD	12.4	24.8	0.50	12.1	0.75
EB	8.0	24.0	0.42	7.0	0.60

Fig. 6.3 - Dimensions of members for final design

APPENDIX

This appendix has been included to provide the designer with a quick reference to the proposed tapered-beam design formulas. Since the development of the formulas closely follows that of prismatic beams, this section paraphrases the appropriate A.I.S.C. provisions.

The following is a working definition of a tapered member that is within the scope of the proposed formulas:

A tapered member is a member possessing at least one axis of symmetry, e.g., I-shapes and [-shapes, which axis of symmetry corresponds to the flexural axis if moments are present, where the flanges are of equal and constant area, and where only the depth of the member varies in a linear fashion according to the equation

$$d(z) = d_0 \left(1 + \gamma \frac{z}{L} \right)$$

where γ is the tapering ratio and is equal to $(d_L - d_0)/d_0$.

Section 1.5 ALLOWABLE STRESS

1.5.1.3 Compression

1.5.1.3.1 On the gross section of axially loaded tapered compression members when $K\sqrt{L}/r_0$, the largest effective slenderness ratio of any unbraced segment, is less than C_c

$$F_{ay} = \frac{\left[1.0 - \frac{\left(\frac{K_y l}{r_o} \right)^2}{2C_c^2} \right] F_y}{\text{F.S.}} \quad (1.5-1)$$

where F.S. = factor of safety = $\frac{5}{3} + \frac{3(K_y l / r_o)}{8C_c} - \frac{(K_y l / r_o)^2}{8C_c^2}$

and

$$C_c = \sqrt{\frac{2\pi^2 E}{F_y}}$$

1.5.1.3.2 On the gross section of axially loaded tapered columns

when $K_y l / r_o$ exceed C_c

$$F_{ay} = \frac{12\pi^2 E}{23 (K_y l / r_o)^2} \quad (1.5-2)$$

(The allowable axial stresses are tabulated for $F_y = 36, 42, 50, 65,$ and 100 ksi in tables A1. The effective length factor K_y can be determined from Figs. 5.7-5.24).

1.5.1.4. Bending

1.5.1.4.6a Compression on extreme fibers of tapered flexural members, having an axis of symmetry in, and loaded in, the plane of their web: the larger value computed by formulas (1.5-6a) or (1.5-6b) and (1.5-7) as applicable, but not more than $0.60 F_y$.

When $h_w l / r_{T_o} \leq C_r$

$$F_{by} = \frac{2}{3} \left[1.0 - \frac{(h_w l / r_{T_o})^2}{2C_r^2} \right] F_y \quad (1.5-6a)$$

When $h_w l / r_{T_o} \geq C_r$

$$F_{by} = \frac{170,000 C_{by}}{(h_w l / r_{T_o})^2} \quad (1.5-6b)$$

Or, when the compression flange is solid and approximately rectangular in cross-section and its area is not less than that of the tension flange

$$F_{b_y} = \frac{12000 C_{b_y}}{h_w l d_o / A_f} \quad (1.5-7)$$

In the foregoing,

l = distance between cross-sections braced against twist or lateral displacement of the compression flange

r_{T_o} = radius of gyration of the smaller end cross-section comprising the compression flange plus one-third of the compression web area, taken about an axis in the plane of the web

A_f = area of the compression flange

$$C_{b_y} = \begin{cases} 1.0 & \text{for } \alpha = +k \\ \frac{1.75}{1.0 + 0.25 \sqrt{y}} & \text{for } \alpha = 0 \end{cases}$$

where $\alpha = M_b / M_c$ and k is defined in equation 3.1.18

$$h_w = 1.0 + 0.00385 y \sqrt{l / r_{T_o}}$$

$$h_s = 1.0 + 0.0230 y \sqrt{l d_o / A_f}$$

$$C_r = \sqrt{\frac{510,000 C_{b_y}}{F_y}}$$

(The allowable bending stresses are tabulated for $F_y = 36, 42, 50, 65,$ and 100 ksi and for $\alpha = 0$ and $+k$ in tables A5 through A13. Tables A2, A3, and A4 contain values for functions $h_w, h_s,$ and C_{b_y} respectively. The heavy solid line in tables A5, A7-A13 indicates the division between formulas (1.5-6a) and (1.5-6b). Thus the values below this line, i.e., formula (1.5-6b), can be converted to the $\alpha = 0$ case by simple multiplications by C_{b_y} . The same conversion applies to table A6, formulas (1.5-7).

This simple conversion cannot be applied to values above the heavy line, thus tables A7-A11 have been provided.

Section 1.6 COMBINED STRESSES

1.6.1 Axial Compression and Bending

Tapered members subjected to both axial compression and bending stresses shall be proportioned to satisfy the following requirements:

$$\left(\frac{f_a}{F_{ay}}\right)_o + \frac{C_m}{\left(1 - \frac{f_a}{F_{ay}}\right)} \left(\frac{f_b}{F_{by}}\right)_L \leq 1.0 \quad (1.6-1a)$$

and

$$\frac{f_{an}}{0.6F_y} + \left(\frac{f_b}{F_{by}}\right)_L \leq 1.0 \quad (1.6-1b)$$

When $(F_y / F_{ay})_o \leq 0.15$, formulas (1.6-2) may be used in lieu of formulas (1.6-1a) and (1.6-1b)

$$\left(\frac{f_a}{F_{ay}}\right)_o + \left(\frac{f_b}{F_{by}}\right)_L \leq 1.0 \quad (1.6-2)$$

where

f_{ay} = axial stress at the smaller end that would be permitted if axial force alone existed

f_{by} = compressive bending stress at the larger end that would be permitted if bending moment alone existed

C_m = $\frac{12EI}{23(K_1^2/b^2/r_{yo}^2)}$ where L_b is the actual unbraced length in the plane of bending and r_{yo} is the corresponding smaller end radius of gyration.

f_{an} = computed smaller end axial stress

f_{bl} = computed larger end bending stress

Reproduced from
best available copy.

and

$$C_m = \begin{cases} 1.0 + 0.1 \left(\frac{f_{a_0}}{F'_{ey}} \right) + 0.3 \left(\frac{f_{a_0}}{F'_{ey}} \right)^2; & \text{for } \alpha = +k \\ 1.0 - 0.9 \left(\frac{f_{a_0}}{F'_{ey}} \right) + 0.6 \left(\frac{f_{a_0}}{F'_{ey}} \right)^2; & \text{for } \alpha = 0 \end{cases}$$

where $\alpha = N_b/M$ and k is defined in equation 3.1.18.

(Table 2 of the Manual of Steel Construction, A.I.S.C., 7th edition, can be used for F'_{ey} if $F_y b/t_b$ is substituted for $F_y d/t_b$.)

Table A1
 Allowable Axial Stress, F_a (ksi)

$\frac{K_1 L}{r_c}$ / F_y	36 ksi.	42 ksi.	50 ksi.	65 ksi.	100 ksi.
0	126.1	116.7	107.0	93.8	15.7
1	126.1	116.7	107.0	93.8	15.7
2	126.1	116.7	107.0	93.8	15.7
3	126.1	116.7	107.0	93.8	15.7
4	126.1	116.7	107.0	93.8	15.7
5	126.1	116.7	107.0	93.8	15.7
6	126.1	116.7	107.0	93.8	15.7
7	126.1	116.7	107.0	93.8	15.7
8	126.1	116.7	107.0	93.8	15.7
9	126.1	116.7	107.0	93.8	15.7
10	126.1	116.7	107.0	93.8	15.7
11	126.1	116.7	107.0	93.8	15.7
12	126.1	116.7	107.0	93.8	15.7
13	126.1	116.7	107.0	93.8	15.7
14	126.1	116.7	107.0	93.8	15.7
15	126.1	116.7	107.0	93.8	15.7
16	126.1	116.7	107.0	93.8	15.7
17	126.1	116.7	107.0	93.8	15.7
18	126.1	116.7	107.0	93.8	15.7
19	126.1	116.7	107.0	93.8	15.7
20	126.1	116.7	107.0	93.8	15.7
21	126.1	116.7	107.0	93.8	15.7
22	126.1	116.7	107.0	93.8	15.7
23	126.1	116.7	107.0	93.8	15.7
24	126.1	116.7	107.0	93.8	15.7
25	126.1	116.7	107.0	93.8	15.7
26	126.1	116.7	107.0	93.8	15.7
27	126.1	116.7	107.0	93.8	15.7
28	126.1	116.7	107.0	93.8	15.7
29	126.1	116.7	107.0	93.8	15.7
30	126.1	116.7	107.0	93.8	15.7
31	126.1	116.7	107.0	93.8	15.7
32	126.1	116.7	107.0	93.8	15.7
33	126.1	116.7	107.0	93.8	15.7
34	126.1	116.7	107.0	93.8	15.7
35	126.1	116.7	107.0	93.8	15.7
36	126.1	116.7	107.0	93.8	15.7
37	126.1	116.7	107.0	93.8	15.7
38	126.1	116.7	107.0	93.8	15.7
39	126.1	116.7	107.0	93.8	15.7
40	126.1	116.7	107.0	93.8	15.7
41	126.1	116.7	107.0	93.8	15.7
42	126.1	116.7	107.0	93.8	15.7
43	126.1	116.7	107.0	93.8	15.7
44	126.1	116.7	107.0	93.8	15.7
45	126.1	116.7	107.0	93.8	15.7
46	126.1	116.7	107.0	93.8	15.7
47	126.1	116.7	107.0	93.8	15.7
48	126.1	116.7	107.0	93.8	15.7
49	126.1	116.7	107.0	93.8	15.7
50	126.1	116.7	107.0	93.8	15.7

Reproduced from
 best available copy.

Table A4
 Moment Gradient Coefficient, C_{br}

δ'	C_{br}	δ'	C_{br}	δ'	C_{br}
0.0	1.000	0.0	1.000	0.0	1.000
0.1	1.000	0.1	1.000	0.1	1.000
0.2	1.000	0.2	1.000	0.2	1.000
0.3	1.000	0.3	1.000	0.3	1.000
0.4	1.000	0.4	1.000	0.4	1.000
0.5	1.000	0.5	1.000	0.5	1.000
0.6	1.000	0.6	1.000	0.6	1.000
0.7	1.000	0.7	1.000	0.7	1.000
0.8	1.000	0.8	1.000	0.8	1.000
0.9	1.000	0.9	1.000	0.9	1.000
1.0	1.000	1.0	1.000	1.0	1.000
1.1	1.000	1.1	1.000	1.1	1.000
1.2	1.000	1.2	1.000	1.2	1.000
1.3	1.000	1.3	1.000	1.3	1.000
1.4	1.000	1.4	1.000	1.4	1.000
1.5	1.000	1.5	1.000	1.5	1.000
1.6	1.000	1.6	1.000	1.6	1.000
1.7	1.000	1.7	1.000	1.7	1.000
1.8	1.000	1.8	1.000	1.8	1.000
1.9	1.000	1.9	1.000	1.9	1.000
2.0	1.000	2.0	1.000	2.0	1.000

Reproduced from
 best available copy.

Table 25

Allowable bending stress, $P_b(ksi)$ as computed from Formulas (1.5-6a) and (1.5-6b) for $a = 4k$

$\frac{L}{D}$ \ $\frac{L}{k}$	36 ksi.	42 ksi.	50 ksi.	60 ksi.	100 ksi.
1.0	137.0	115.8	101.0	88.6	71.9
1.2	136.5	115.3	100.5	88.1	71.4
1.4	136.0	114.8	100.0	87.6	70.9
1.6	135.5	114.3	99.5	87.1	70.4
1.8	135.0	113.8	99.0	86.6	69.9
2.0	134.5	113.3	98.5	86.1	69.4
2.2	134.0	112.8	98.0	85.6	68.9
2.4	133.5	112.3	97.5	85.1	68.4
2.6	133.0	111.8	97.0	84.6	67.9
2.8	132.5	111.3	96.5	84.1	67.4
3.0	132.0	110.8	96.0	83.6	66.9
3.2	131.5	110.3	95.5	83.1	66.4
3.4	131.0	109.8	95.0	82.6	65.9
3.6	130.5	109.3	94.5	82.1	65.4
3.8	130.0	108.8	94.0	81.6	64.9
4.0	129.5	108.3	93.5	81.1	64.4
4.2	129.0	107.8	93.0	80.6	63.9
4.4	128.5	107.3	92.5	80.1	63.4
4.6	128.0	106.8	92.0	79.6	62.9
4.8	127.5	106.3	91.5	79.1	62.4
5.0	127.0	105.8	91.0	78.6	61.9
5.2	126.5	105.3	90.5	78.1	61.4
5.4	126.0	104.8	90.0	77.6	60.9
5.6	125.5	104.3	89.5	77.1	60.4
5.8	125.0	103.8	89.0	76.6	59.9
6.0	124.5	103.3	88.5	76.1	59.4
6.2	124.0	102.8	88.0	75.6	58.9
6.4	123.5	102.3	87.5	75.1	58.4
6.6	123.0	101.8	87.0	74.6	57.9
6.8	122.5	101.3	86.5	74.1	57.4
7.0	122.0	100.8	86.0	73.6	56.9
7.2	121.5	100.3	85.5	73.1	56.4
7.4	121.0	99.8	85.0	72.6	55.9
7.6	120.5	99.3	84.5	72.1	55.4
7.8	120.0	98.8	84.0	71.6	54.9
8.0	119.5	98.3	83.5	71.1	54.4
8.2	119.0	97.8	83.0	70.6	53.9
8.4	118.5	97.3	82.5	70.1	53.4
8.6	118.0	96.8	82.0	69.6	52.9
8.8	117.5	96.3	81.5	69.1	52.4
9.0	117.0	95.8	81.0	68.6	51.9
9.2	116.5	95.3	80.5	68.1	51.4
9.4	116.0	94.8	80.0	67.6	50.9
9.6	115.5	94.3	79.5	67.1	50.4
9.8	115.0	93.8	79.0	66.6	49.9
10.0	114.5	93.3	78.5	66.1	49.4

Reproduced from best available copy.

Table A

Monthly Double Rates of Interest computed from Formula (1.2-7) for
 $n = 12$

$\frac{m}{100}$	i_1	$\frac{m}{100}$	i_2
50	240.00	2000	5.65
100	120.00	2100	5.71
150	80.00	2200	5.80
200	60.00	2300	5.90
250	48.00	2400	6.00
300	40.00	2500	6.11
350	35.29	2600	6.22
400	30.00	2700	6.34
450	26.67	2800	6.46
500	23.00	2900	6.58
550	21.00	3000	6.71
600	19.00	3100	6.84
650	18.46	3200	6.97
700	17.14	3300	7.10
750	16.00	3400	7.23
800	15.00	3500	7.36
850	14.12	3600	7.49
900	13.33	3700	7.62
950	12.65	3800	7.75
1000	12.00	3900	7.88
1050	11.43	4000	8.01
1100	10.91	4100	8.14
1150	10.43	4200	8.27
1200	10.00	4300	8.40
1250	9.60	4400	8.53
1300	9.23	4500	8.66
1350	8.89	4600	8.79
1400	8.57	4700	8.92
1450	8.28	4800	9.05
1500	8.00	4900	9.18
1550	7.75	5000	9.31
1600	7.50	5100	9.44
1650	7.27	5200	9.57
1700	7.06	5300	9.70
1750	6.86	5400	9.83
1800	6.67	5500	9.96
1850	6.49	5600	10.09
1900	6.33	5700	10.22
1950	6.18	5800	10.35
2000	6.00	5900	10.48
		6000	10.61

Table 17

Algebraic Building Structure \mathcal{L}_n (1.3-1) as Computed from Formulas (1.3-6a) and (1.3-6b) for $n = 0$ and $n = 1$

n	\mathcal{L}_n	\mathcal{L}_n	\mathcal{L}_n	\mathcal{L}_n	\mathcal{L}_n
0	1	1	1	1	1
1	1	1	1	1	1
2	1	1	1	1	1
3	1	1	1	1	1
4	1	1	1	1	1
5	1	1	1	1	1
6	1	1	1	1	1
7	1	1	1	1	1
8	1	1	1	1	1
9	1	1	1	1	1
10	1	1	1	1	1
11	1	1	1	1	1
12	1	1	1	1	1
13	1	1	1	1	1
14	1	1	1	1	1
15	1	1	1	1	1
16	1	1	1	1	1
17	1	1	1	1	1
18	1	1	1	1	1
19	1	1	1	1	1
20	1	1	1	1	1
21	1	1	1	1	1
22	1	1	1	1	1
23	1	1	1	1	1
24	1	1	1	1	1
25	1	1	1	1	1
26	1	1	1	1	1
27	1	1	1	1	1
28	1	1	1	1	1
29	1	1	1	1	1
30	1	1	1	1	1
31	1	1	1	1	1
32	1	1	1	1	1
33	1	1	1	1	1
34	1	1	1	1	1
35	1	1	1	1	1
36	1	1	1	1	1
37	1	1	1	1	1
38	1	1	1	1	1
39	1	1	1	1	1
40	1	1	1	1	1
41	1	1	1	1	1
42	1	1	1	1	1
43	1	1	1	1	1
44	1	1	1	1	1
45	1	1	1	1	1
46	1	1	1	1	1
47	1	1	1	1	1
48	1	1	1	1	1
49	1	1	1	1	1
50	1	1	1	1	1

Reproduced from best available copy.

Table 42

Allowable Tensile Stress, f_t (ksi) as Computed from Formula (1.5-5a)
 for (1.5-6b) $\sigma_{cr} = 0$ and $\sigma = 1$

λ	f_t (ksi)				
	1000	1200	1400	1500	1600
0.0	1000	1200	1400	1500	1600
0.1	998	1198	1398	1498	1598
0.2	992	1192	1392	1492	1592
0.3	982	1182	1382	1482	1582
0.4	968	1168	1368	1468	1568
0.5	950	1150	1350	1450	1550
0.6	928	1128	1328	1428	1528
0.7	902	1102	1302	1402	1502
0.8	872	1072	1272	1372	1472
0.9	838	1038	1238	1338	1438
1.0	800	1000	1200	1300	1400
1.1	758	958	1158	1258	1358
1.2	712	912	1112	1212	1312
1.3	662	862	1062	1162	1262
1.4	608	808	1008	1108	1208
1.5	550	750	950	1050	1150
1.6	488	688	888	988	1088
1.7	422	622	822	922	1022
1.8	352	552	752	852	952
1.9	278	478	678	778	878
2.0	200	400	600	700	800
2.1	118	318	518	618	718
2.2	32	232	432	532	632
2.3	-42	142	342	442	542
2.4	-132	52	252	352	452
2.5	-242	-38	162	262	362
2.6	-362	-128	72	172	272
2.7	-482	-238	-18	82	182
2.8	-602	-312	-108	-12	92
2.9	-722	-352	-182	-62	2
3.0	-842	-358	-212	-102	12
3.1	-962	-322	-192	-132	22
3.2	-1082	-242	-122	-152	32
3.3	-1202	-118	-12	-152	42
3.4	-1322	32	78	-152	52
3.5	-1442	142	178	-152	62
3.6	-1562	252	278	-152	72
3.7	-1682	362	378	-152	82
3.8	-1802	472	478	-152	92
3.9	-1922	582	578	-152	102
4.0	-2042	692	678	-152	112
4.1	-2162	802	778	-152	122
4.2	-2282	912	878	-152	132
4.3	-2402	1022	978	-152	142
4.4	-2522	1132	1078	-152	152
4.5	-2642	1242	1178	-152	162
4.6	-2762	1352	1278	-152	172
4.7	-2882	1462	1378	-152	182
4.8	-3002	1572	1478	-152	192
4.9	-3122	1682	1578	-152	202
5.0	-3242	1792	1678	-152	212

Reproduced from
 best available copy. ©

State of New York
County of ...

No.	Name	Age	Sex	Color	Profession
1
2
3
4
5
6
7
8
9
10
11
12
13
14
15
16
17
18
19
20
21
22
23
24
25
26
27
28
29
30
31
32
33
34
35
36
37
38
39
40
41
42
43
44
45
46
47
48
49
50

Reproduced from
best available copy.

